Electronic Theses and Dissertations

5-2010

Ribosome maturation in yeast models of Diamond-Blackfan anemia and Shwachman-Diamond syndrome.

Joseph Brady Moore 1981-
University of Louisville

Follow this and additional works at: https://ir.library.louisville.edu/etd

Recommended Citation

RIBOSOME MATURATION IN YEAST MODELS OF DIAMOND-BLACKFAN
ANEMIA AND SHWACHMAN-DIAMOND SYNDROME

By

Joseph Brady Moore IV
B.S., University of Louisville, 2005
M.S., University of Louisville, 2009

A Dissertation
Submitted to the Faculty of the
Graduate School of the University of Louisville
in Partial Fulfillment of the Requirements
for the Degree of

Doctor of Philosophy

Department of Biochemistry and Molecular Biology
University of Louisville
Louisville, Kentucky

May 2010

RIBOSOME MATURATION IN YEAST MODELS OF DIAMOND-BLACKFAN
ANEMIA AND SHWACHMAN-DIAMOND SYNDROME

By

Joseph Brady Moore IV
B.S., University of Louisville, 2005
M.S., University of Loiusville, 2009

A Dissertation Approved on

April 12, 2010

by the following Dissertation Committee:

_____
Dissertation Director: Dr. Steve Ellis

_____
Dr. Nancy Martin

_____
Dr. Johnson Liu

_____
Dr. Yong Li

_____
Dr. Tom Geoghegan

DEDICATION

This dissertation is dedicated to my father

Mr. Joseph Brady Moore III

who provided me with the determination, the courage, and the opportunities to become

the person I am today. Sine labore nihil.

ACKNOWLEDGEMENTS

Lastly, I would like to thank the Biochemistry Department, for affording me the opportunity to pursue this degree, and to all of its faculty members, as each contributed in some way to my growth as a scientist. Thank you all!

ABSTRACT

RIBOSOME MATURATION IN YEAST MODELS OF DIAMOND-BLACKFAN
ANEMIA AND SHWACHMAN-DIAMOND SYNDROME

Joseph B. Moore IV

April 12, 2010

The inherited bone marrow failure syndromes (IBMFS) encompass a
heterogeneous collection of rare disorders characterized by hematological abnormalities,
generalized growth delays, and an increased incidence of malignant transformation.
These disorders include: Diamond-Blackfan anemia (DBA), Shwachman-Diamond
syndrome (SDS), cartilage-hair hypoplasia (CHH), and dyskeratosis congenita (DC).
Despite sharing overarching similarities, each of these disorders manifests distinct
clinical phenotypes. Similar to their clinical features, the molecular underpinnings of the
IBMFS have characteristics that are both shared and distinctive. Aberrations in ribosome
synthesis have been associated with each of the IBMFS providing a common molecular
target for pathogenic mutations in disease related genes. In some cases, the ribosome
appears to be the major target of pathogenic lesions, whereas in others, effects on
ribosome synthesis are secondary and appear to have a modifying influence on disease
presentation. For example, the primary target of pathogenic lesions in dyskeratosis
congenita is telomerase which distinguishes it from other IBMFS. The X-linked form of
dyskeratosis congenita, however, affects both telomerase function and ribosome synthesis
and is considerably more severe than the somatic forms of the disease that only affect

telomerase. Thus, differences in primary targets of pathogenic lesions can account for the distinct clinical presentations of certain IBMFS. In other cases, where ribosome synthesis appears to be the major target of disease causing mutations, the basis for diverse clinical manifestations remains unknown.

The body of work presented in this dissertation is focused on Shwachman-Diamond syndrome and Diamond-Blackfan anemia, two IBMFS where defects in ribosome synthesis appear to underlie disease pathophysiology. The approach was to use yeast models of both diseases to explore mechanisms by which ribosome synthesis was affected using the 60S ribosomal subunit as a common molecular target. My studies revealed that 60S subunit biogenesis was affected by distinct mechanisms in the two disease models and that these differences may provide the molecular underpinnings for the distinct clinical presentations observed in DBA and SDS patients. Further studies on the mechanism by which 60S subunit biogenesis was affected in the SDS model have clear implications for the treatment of this disorder.

TABLE OF CONTENTS

LIST OF FIGURES

PAGE

FIGURE

CHAPTER I

FROM RIBOSOMES TO MARROW FAILURE

General Introduction

Ribosomal Defects as a Causative Agent in Marrow Failure

Diamond-Blackfan anemia (DBA), Shwachman-Diamond syndrome (SDS), cartilage-hair hypoplasia (CHH), and dyskeratosis congenita (DC) are members of a rare group of disorders recognized as the inherited bone marrow failure syndromes (IBMFS) (Liu and Ellis 2006). The members of this group are characterized by defective hematopoiesis, enhanced cancer susceptibility, and a variable assortment of congenital aberrations. While the IBMFS have these overarching similarities, each presents with characteristic physical stigmata giving rise to distinct clinical presentations (Liu and Ellis 2006; Shimamura 2006; Ganapathi and Shimamura 2008). Faulty ribosome synthesis has been observed in each of the IBMFS suggesting a common target, which initially proffered explanation for their general overarching features. While having a common molecular target could explain some of the universal characteristics of the IBMFS, it does not account for their unique features. Studies on molecular etiology led to the discovery that the target genes affected in some of the IBMFS were multifunctional and that they had secondary effects on ribosome synthesis. Thus, the primary process affected by the pathogenic lesion could account for distinct clinical phenotypes in a number of these

disorders. However, two of the IBMFS, DBA and SDS, both appear to have ribosome synthesis as their primary molecular target raising the question of how defects in a common molecular process can give rise to unique clinical manifestations.

The Cell's Translational Machinery

Ribosomes: Structure and Function

Ribosomes are responsible for the translation of genome encoded messenger RNAs (mRNA) into protein. The structure and function of ribosomes, as well as the fundamental pathway of rRNA synthesis, look to be significantly conserved among all kingdoms (Hage and Tollervey 2004). Translationally competent ribosomes require the union of both a small ribosomal subunit (bacterial 30S or eukaryotic 40S) and a large ribosomal subunit (bacterial 50S or eukaryotic 60S). The small subunit is primarily responsible for mRNA binding and the identification of initiation codons. Once an initiation codon is identified as part of a 48S initiation complex, the large ribosomal subunit joins and further steps in the translational process can commence (Hage and Tollervey 2004). Structurally, these ribonucleoprotein (RNP) complexes are composed of intricately arranged RNAs possessing numerous interactions with a network of ribosomal proteins with approximately 60% of their composition being rRNA and the other 40% ribosomal proteins (Moore 1997). A large majority of ribosomal proteins (RPs) are rich in basic amino acids (i.e. lysine and arginine) and therefore are highly positively charged. This property of RPs facilitates the stability of an otherwise sterically unfavorable compact mass of rRNA by interacting and reducing the repulsive forces imposed by the highly negatively charged rRNAs.

Much of what is now understood concerning ribosome structure and catalytic function has been elucidated from high resolution x-ray crystallographic structures of bacterial and archaeal ribosomes (Steitz 2008). Atomic structures of the small and large ribosomal subunits from eubacterium *Thermus thermophilus* (Schluenzen, Tocilj et al. 2000) and archaeon *Haloarcula marismortui* (Ban, Nissen et al. 2000), respectively, have been elucidated. These crystallographic-based studies revealed that RPs primarily reside at the ribosome's exterior. These proteins frequently possess distinctively folded extensions that project into the subunit's interior where they interact with RNA to stabilize and interlock numerous rRNA domains (Ban, Nissen et al. 2000; Schluenzen, Tocilj et al. 2000). These studies suggested ribosomal proteins to have a minimal role in protein synthesis, a theory inferred previously from evolutionary consideration, as RPs were shown to be largely deficient from both the subunit interface and the peptidyl-transferase active site, major functional areas consisting of only RNA constituents (Ban, Nissen et al. 2000; Schluenzen, Tocilj et al. 2000). Consistent with this view, "naked" 23S rRNA depleted of ribosomal proteins from *Escherichia coli* was shown to be capable of catalyzing peptide bond formation *in vitro*, this further illustrating the notion that RP's are not an absolute requirement for certain critical activities of the ribosome (Nitta, Ueda et al. 1998; Khaitovich, Tenson et al. 1999). The perception that the ribosome is a ribozyme, or rather that its catalytic function is exclusively dependent upon its rRNA, was finally confirmed by studying atomic structures of the large ribosomal subunit (from *Haloarcula marismortui*) in complex with substrate analogs (Nissen, Hansen et al. 2000). Steitz and colleagues demonstrated these substrate analogs interact with conserved rRNA elements at the peptidyl-transferase active site and that ribosomal protein side-chain

moieties were fairly distant, no closer than 18 angstroms, to the forming peptide bond at the presumed peptidyl-transferase active site (Nissen, Hansen et al. 2000). Based on these studies, it is now generally accepted that ribosomal proteins principally function in maintaining the three-dimensional organization of the rRNA in forming the active sites necessary for the myriad of activities involved in protein synthesis (Ban, Nissen et al. 2000; Nissen, Hansen et al. 2000; Schluenzen, Tocilj et al. 2000).

The Fundamentals of Ribosome Assembly

Despite sharing many general characteristics, the eukaryotic ribosome is structurally and functionally more complex than its bacterial counterpart (Dinman 2009). The fact that bacterial ribosomes have been successfully reconstituted *in vitro* from their purified protein and rRNA components whereas eukaryotic ribosomes have not, further illustrates this concept (Traub and Nomura 1968; Culver 2003). Despite these distinctions, the pathway of rRNA synthesis appears to be significantly conserved among the two kingdoms, as does the structure and polarity of the rDNA operons from which mature rRNAs are derived (Hage and Tollervey 2004). For example, in both kingdoms the small and large subunit rRNAs are cotranscribed with the small subunit rRNA being positioned upstream of the large subunit rRNAs. The mature rRNA species are then liberated from their primary pre-rRNA transcript by a coordinated series of endo- and exonucleolytic cleavage reactions. Despite these similarities, however, the intricacies of ribosome assembly appear to be quite distinct among bacteria and eukaryotes.

In bacteria, a single RNA polymerase is responsible for synthesizing the cell's rRNA, whereas in eukaryotes, RNA polymerases I and III are responsible for the

transcription of the 35S pre-rRNA and 5S rRNA, respectively. In the bacterium

Escherichia coli, numerous rRNA processing and modifying enzymes, as well as a small

number of non-ribosomal factors (i.e. putative helicases, GTPases, putative RNA

chaperones, and protein chaperones), have been identified to participate in the ribosome

assembly process (Srivastava and Schlessinger 1990; Nierhaus 1991; Culver 2003).

Intriguingly, all of these non-ribosomal factors have been shown to be dispensable for

ribosome assembly, suggesting that they simply facilitate a spontaneous process (Dinman

2009). The bacterial ribosome is thought to assemble via an "assembly gradient," where

ribosomal protein interactions are coupled to rRNA folding and maturation, in a process

that is largely co-transcriptional (Figure 1, top panel) (Lewicki, Margus et al. 1993). In

contrast, eukaryotic pre-rRNA processing and modifications are largely post-

transcriptional and require a substantial number of non-structural or trans-acting factors

(Figure 1, bottom panel). For example, the proper assembly of the ~80 ribosomal

proteins with four rRNAs (18S, 5.8S, 25S, and 5S) to form yeast ribosomes requires over

240 trans-acting factors, which include approximately 170 non-ribosomal proteins and

over 70 small nucleolar rRNAs (snoRNAs). Moreover, the majority of these trans-acting

factors are essential for ribosome assembly and function (Venema and Tollervey 1999).

In addition to an already inherently complex ribosome assembly program, eukaryotes

have the added issue of subcellular compartmentalization, a challenge the prokaryotic cell

does not contend with. In yeast and other eukaryotes, rRNA transcription occurs in the

nucleolus, as do the initial steps of ribosome synthesis and rRNA modification. The

resultant pre-ribosomes are eventually transported to the nucleoplasm, where they

undergo additional steps of maturation, and subsequently to the cytoplasm where the

process is completed (Fromont-Racine, Senger et al. 2003).
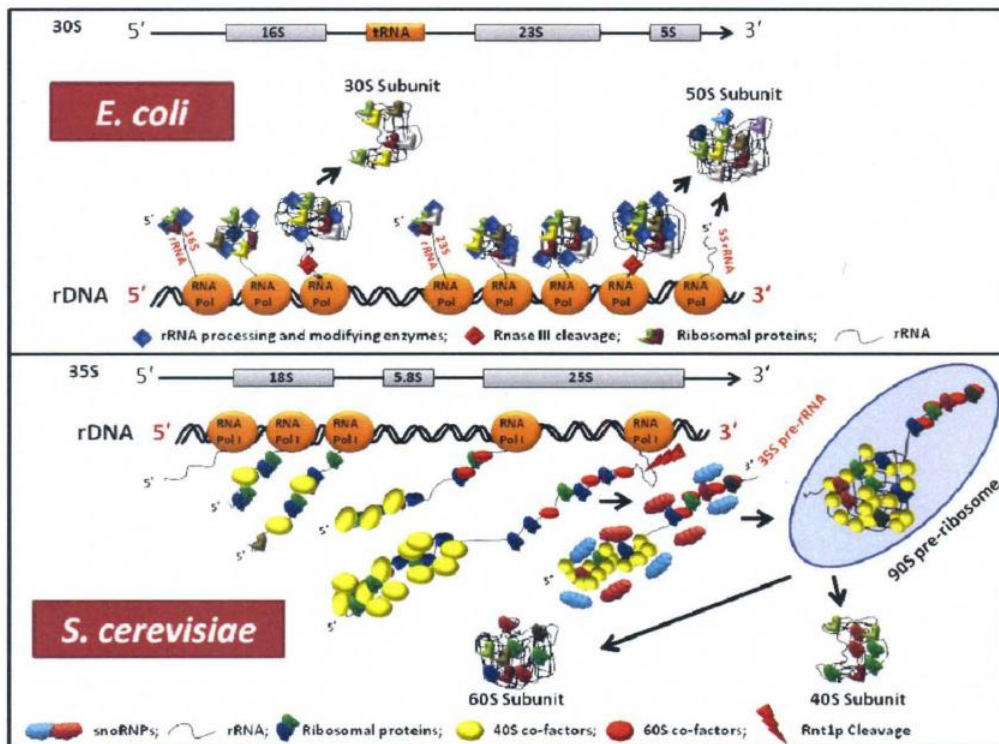
<u>Figure 1.</u> **Ribosome maturation in *E. coli* and *S. cerevisiae*.** Top panel, *E. coli*

ribosome maturation is largely a co-transcriptional process whereas the binding of

ribosomal proteins is coupled to rRNA folding and maturation. The mature 16S and 23S

rRNAs are cleaved from the nascent transcript by RNase III. Bottom panel, in yeast the

35S pre-rRNA nascent transcript systematically interacts with ribosomal proteins and

assembly factors, starting with small subunit proteins and related processing factors that

assist with rRNA folding. The nascent 35S pre-rRNA is cleaved by RNase III (Rnt1p)

and is post-transcriptionally modified by numerous snoRNPs. The "earliest detectable"

90S pre-ribosome particle consists of 35S pre-rRNA, small ribosomal subunit proteins,

non-ribosomal assembly factors, and the U3 snoRNP. With the addition of large subunit

RPs, the 90S particle is further processed leading to the formation of 66S and 43S

particles, which give rise to mature 60S and 40S ribosomal subunits, respectively. Figure

adapted from Hage and Tollervey 2004.

Yeast: A Model Organism for the Study of Eukaryotic Ribosome Biogenesis

Ribosome assembly has been extensively studied and is best characterized in the budding yeast *Saccharomyces cerevisiae* (Venema and Tollervey 1999; Fatica and Tollervey 2002; Fromont-Racine, Senger et al. 2003; Dinman 2009). As previously noted, this process begins with RNA polymerase I mediated transcription of the 35S pre-rRNA transcript and rapid snoRNA guided, site-specific modifications. These modifications include box C/D snoRNA-mediated 2'-hydroxyl ribose methylation (the most prevalent of the modifications) and box H/ACA snoRNA-mediated isomerization of uridine to pseudouridine (ψ). Early yeast labeling experiments suggested that methylation events did not occur co-transcriptionally, but instead occurred immediately following transcription (Udem and Warner 1972). These nucleotide modifications appear to be clustered in functional rRNA regions and tend to be vacant from regions where ribosomal proteins bind (Decatur and Fournier 2002). Their biological purposes are not clear, but these modifications have been proposed to be involved in rRNA stabilization by acting as a "molecular mortar" to secure structural domains, and to play a role in enhancing the ribosome's translational activity by fine-tuning its function (Kowalak, Bruenger et al. 1995; Green and Noller 1996; Nissen, Hansen et al. 2000). The 35S pre-rRNA is located within a 90S pre-ribosome particle inside the nucleolus, which contains the U3 small nucleolar ribonucleoprotein complex, an extensive number of small ribosomal subunit proteins, and non-ribosomal factors, all of which are assembled co-transcriptionally. Recent evidence suggests that 5S rRNA, together with other large ribosomal subunit proteins, is also recruited and integrated into the 90S pre-ribosomal particle early in the assembly program (Zhang, Harnpicharnchai et al. 2007). From this

juncture, the 35S transcript subsequently undergoes a series of nucleolytic cleavage events which commence near the 5' end of the pre-rRNA (outlined in Figure 2).

The initial steps in this process involve the sequential endonucleolytic cleavage of sites A_0 and A_1 within the 5' external transcribed sequence (5' ETS), which leads to the formation of 33S and 32S pre-rRNA species, respectively. The next step is an endonucleolytic cleavage at site A_2 which results in the division of the 90S particle into 43S and 66S pre-ribosomal particles containing 20S and 27S A_2 pre-rRNAs, respectively. The 43S precursor is ultimately transported to the cytoplasm where it matures, via endonucleolytic cleavage of site D, to a functionally competent 40S ribosomal subunit containing mature 18S rRNA. The 27S A_2 pre-rRNA proceeds via two alternative processing pathways that generate mature 5.8S and 25S rRNAs, components of the 60S ribosomal subunit. Approximately 85% of the 27S A_2 pre-rRNA species are cleaved at site A_3 via RNase MRP followed by 5' to 3' exonucleolytic digestion (by Rat1p exonuclease) to site B_{1S}, while the other 15% of the 27S A_2 pre-rRNA species are cleaved at site B_{1L}; both precursors are eventually subjected to endonucleolytic cleavage of site B_2. From these reactions two 27S B pre-rRNA species are formed, 27S B_S (short) and 27S B_L (long), the significance of which is currently unknown. Both of these pre-rRNA species undergo further processing at sites C_1 and C_2, as well as exosome mediated 3' to 5' exonucleolytic digestion to site E, finally generating the mature 5.8S (long and short species) and 25S rRNA constituents of the 60S ribosomal subunit.
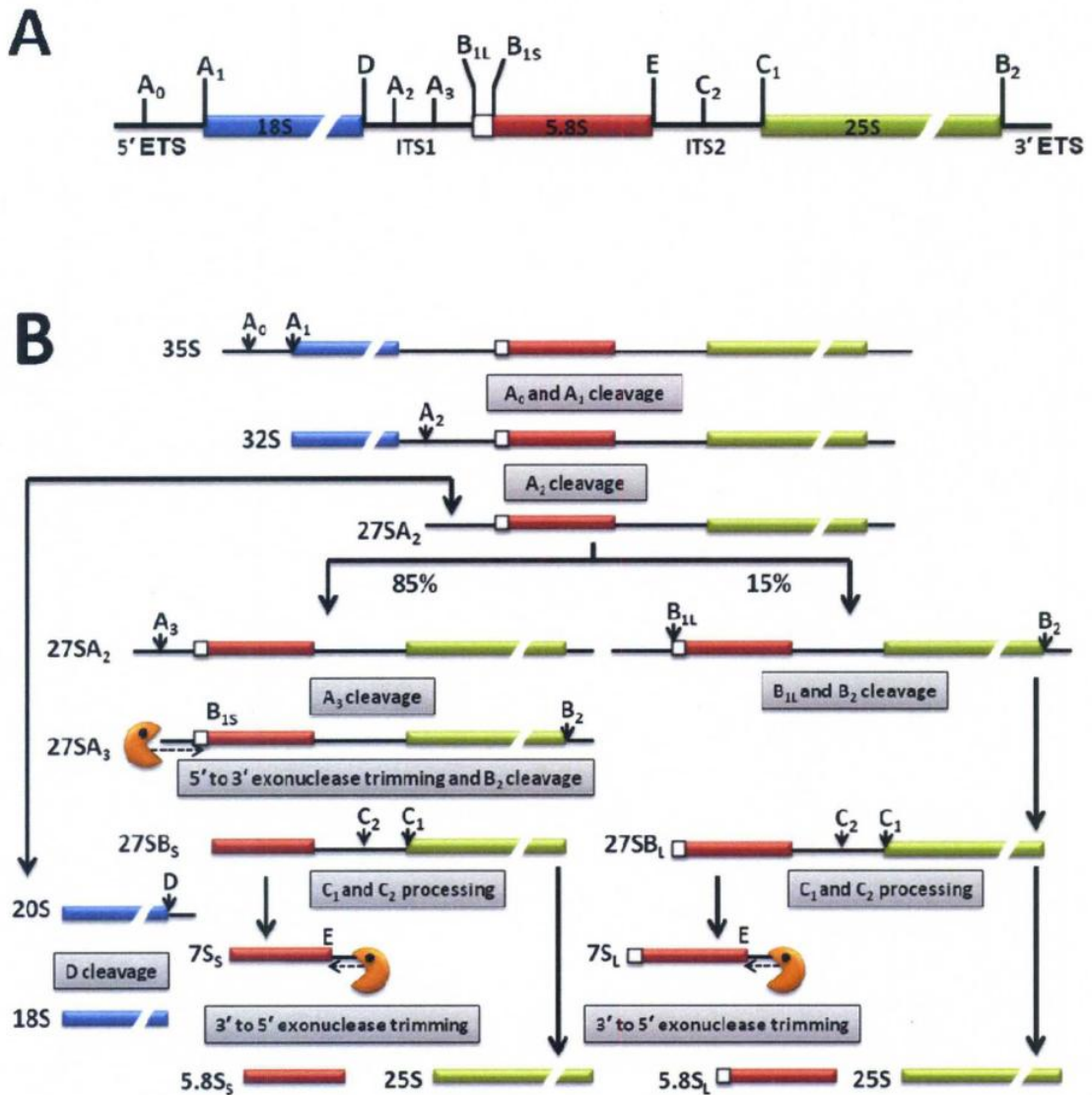
Figure 2. *Saccharomyces cerevisiae* **rRNA processing.** (A) Yeast 35S pre-rRNA transcript containing mature 18S, 5.8S, and 25S rRNAs. Vertical lines indicate cleavage sites, which are labeled. (B) Schematic diagram of the major and minor yeast rRNA processing pathways described in the text.

In addition to nucleotide modification and rRNA processing, the nascent ribosome undergoes a complex series of remodeling steps that are driven by the coordinated binding of different ribosomal proteins, and by the organized association and dissociation of trans-acting assembly factors (Venema and Tollervey 1999; Dinman 2009). Many of these trans-acting factors include GTPases, ATP dependent RNA helicases, AAA-ATPases, and chaperones. This pathway advances with the development of distinct ribosome assembly intermediates; with the earliest detectable intermediate being the 90S pre-ribosomal particle. The composition of the early 90S particle is distinct from later pre-40S and pre-60S ribosomes. For instance, the 90S particle is rich in 40S processing factors, but notably deficient in those required for 60S subunit assembly (Fromont-Racine, Senger et al. 2003). This suggests that 60S subunit assembly factors associate much later in the ribosome maturation process and explains why disruption of early pre-rRNA processing (i.e. A_0-A_2 cleavage events) does not significantly interfere with the production of 60S ribosomal subunits (Grandi, Rybin et al. 2002).

As previously noted, the early 90S ribosome is rapidly converted to 43S and 66S assembly intermediates within the nucleolus (Udem, Kaufman et al. 1971; Trapman, Retel et al. 1975). The 43S pre-ribosome is exported to the cytoplasm where it is completely matured and activated via a final rRNA cleavage event. Maturation of the 66S pre-ribosome is far more complicated than that of the early 43S particle. For instance, prior to its nuclear export to the cytoplasm, the 66S particle undergoes numerous remodeling and rRNA processing steps involving the development of approximately five 66S intermediates while en route from the nucleolus to the

nucleoplasm. Presumably, 60S subunit pre-rRNA processing is largely complete in the nucleoplasm and contains mature 25S, 5.8S, and 5S rRNAs prior to the pre-60S subunit's export to the cytoplasm.

Both large and small subunits are independently exported through nuclear pore complexes, a process which is facilitated via the export receptor Xpo1/Crm1 and RanGTP (Johnson, Ho et al. 2001; Moy and Silver 2002; Thomas and Kutay 2003). Although much is unknown concerning subunit nuclear export, genetic studies in yeast have identified a few trans-acting factors that are essential for this process. For instance, prior to attaining export competence, 60S subunits must bind ribosomal protein L10, which in turn binds the Nmd3 adaptor protein providing the nuclear export signal (NES), which is finally recognized by the Xpo1/Crm1 export receptor protein (Ho, Kallstrom et al. 2000; Gadal, Strauss et al. 2001; Senger, Lafontaine et al. 2001). During nuclear export, ribosomal subunits contain a limited number of non-ribosomal proteins. In addition to Nmd3, these factors include the anti-association factor Tif6, and an uncharacterized protein Arx1. These proteins are absent from ribosomes that are actively engaged in translation (Hung and Johnson 2006). Thus, during the late cytoplasmic stages of 60S ribosomal subunit maturation, translational competency is achieved after their dissociation. These factors are then recycled back to the nucleus, where they participate in additional rounds of nuclear export (Hung and Johnson 2006). It is likely that factors residing in the cytoplasm play an active role in this process of ribosome activation and nuclear export factor recycling. A significant number of studies have shown that two proteins, Efl1 and Sdo1 may also be involved in 60S subunit activation (Becam, Nasr et al. 2001; Senger, Lafontaine et al. 2001; Menne, Goyenechea et al.

2007). Efl1 is a cytoplasmic GTPase whereas Sdo1 is the yeast ortholog of SBDS, the protein responsible for SDS. Genetic studies in yeast have positioned these factors in the late cytoplasmic steps of 60S subunit maturation where Sdo1 appears to function in concert with Efl1 to promote Tif6 release, allowing for subsequent subunit joining (Menne, Goyenechea et al. 2007).

Ribosome Synthesis is Regulated at Multiple Levels

Ribosome biogenesis is a highly regulated process and is closely associated with both cell growth and proliferation (Ruggero and Pandolfi 2003). Rates of ribosome production are rapidly increased in response to various stimuli such as alterations in nutrient availability and mitogenic stimulation. Increases in ribosome numbers are ultimately dependent upon the rate of synthesis of ribosomal RNA and proteins, both of which are mediated by posttranslational modification of specific transcription factors that modulate Polymerase I and Polymerase III activity. A key regulator of the transcriptional activity of RNA Pol I is the transcription factor UBF (upstream binding factor) (Beckmann, Chen et al. 1995; Cavanaugh, Hempel et al. 1995; Brandenburger, Jenkins et al. 2001). UBF is directly targeted by several serine/threonine kinases, as well as tumor suppressor proteins (i.e. RB and p53), which can enhance or repress UBF activity thereby influencing cellular rates of rRNA synthesis (O'Mahony, Xie et al. 1992; Voit, Schnapp et al. 1992; Voit, Kuhn et al. 1995; Ruggero and Pandolfi 2003).

Enhanced ribosome production in response to growth factors and nutrient signaling also involves the enhanced translation of a series of mRNAs containing 5' terminal oligopyrimidine tracts (5'-TOP) via an unknown mechanism (Ruggero and

Pandolfi 2003). The 5'-TOP containing genes encode elongation factors, ribosomal proteins, and ribosome biogenesis factors. The pathway(s) mediating their regulation is unknown, however, the earliest events identified following mitogenic stimuli is the phosphorylation of Rps6 via S6 kinases S6K1 and S6K2 (Tang, Hornstein et al. 2001). Experiments correlating mitogen stimulation with the S6K1-mediated phosphorylation of Rps6 and concomitant enhanced translational efficiency of 5'-TOP containing messages, led to the proposal that phosphorylation of ribosomal protein S6 increases the affinity of ribosomes for 5'-TOP containing messages (Thomas 1986; Jefferies, Reinhard et al. 1994; Jefferies and Thomas 1994). Although a number of correlative studies have supported this model, the translational control of 5'-TOP mRNAs is purely speculative and has not been experimentally validated to be mediated by S6K1. A more recent study challenges this paradigm and suggests an alternate means of 5'-TOP gene expression that is dependent on the phosphotidyl inositol 3-kinase (PI3K) signaling pathway, and independent of both S6 kinase activity and the phosphorylation status of Rps6 (Stolovich, Tang et al. 2002). Despite this debate, it appears that ribosome biogenesis is under multiple modes of regulation, which involves both transcriptional and translational control mechanisms.

Indeed, proper ribosome assembly and regulation is crucial to the health of the cell. Perturbations in the ribosome biosynthetic pathway as well as circumstances of unregulated cell growth (i.e. oncogenesis) require growth arrest or apoptosis to assist in the elimination of affected cells. Not surprisingly, a growing body of evidence suggests that the tumor suppressor proteins RB (retinoblastoma) and p53 play an important role in mediating these processes. For instance, both RB (Cavanaugh, Hempel et al. 1995; Voit,

Schafer et al. 1997; Ciarmatori, Scott et al. 2001) and p53 (Budde and Grummt 1999; Zhai and Comai 2000) negatively regulate Pol I and Pol III activity by interfering with transcriptional complex formation at the promoter regions of genes encoding rRNA and non-coding RNAs (5S rRNA, snoRNAs, & tRNA), respectively, thereby repressing ribosome biogenesis and subsequent protein synthesis (Ruggero and Pandolfi 2003). The hindrance of transcriptional complex assembly, as mediated by RB and p53, is accomplished via their direct interactions with key transcription factors (i.e. UBF, TIF-1B/SL1, TFIIIB) (Ruggero and Pandolfi 2003). The p19ARF tumor suppressor also negatively regulates ribosome biogenesis by blocking rRNA synthesis and processing (Sugimoto, Kuo et al. 2003). The enhanced expression of these tumor suppressors in response to stress signals results in repression of ribosome biogenesis and cell cycle inhibition (Liu and Ellis 2006). The tumor suppressor p53 can also detect aberrations in rRNA processing/synthesis or perturbations in ribosome assembly and inhibit cell cycle progression or induce apoptosis (Ashcroft, Taya et al. 2000; Pestov, Strezoska et al. 2001). These stress response pathways, involving the activation of p53 in response to defects in ribosome biogenesis, have great implications for the mechanisms underlying the pathophysiology of disorders linked to defects in ribosome biogenesis, especially Diamond-Blackfan anemia and Shwachman-Diamond syndrome.

Diamond-Blackfan Anemia

Historical Introduction and Clinical Features

In 1938, Harvard Medical School physicians, Louis K. Diamond and Kenneth D. Blackfan, first described congenital erythroid hypoplastic anemia, a disorder which was later termed as Diamond-Blackfan anemia (DBA; OMIM 105650). Almost two decades later, Diamond and colleagues published work detailing their 25 year longitudinal studies of 30 patients with congenital hypoplastic anemia, and it was with these studies where the first association between DBA and skeletal abnormalities was noted (Diamond, Allen et al. 1961). As these early studies indicated, DBA, like many other bone marrow failure syndromes, is a complex disease presenting with a multitude of symptoms which include both hematologic and nonhematologic manifestations. DBA is clinically defined as a pure red cell hypoplasia leading to anemia, though the involvement of additional hematopoietic lineages have been reported (Giri, Kang et al. 2000; Vlachos, Federman et al. 2001; Lipton and Ellis 2009). DBA typically presents in early infancy manifesting symptoms of anemia with macrocytosis, reticulocytopenia, and normocellular bone marrow with a deficiency of red cell progenitors (Diamond, Wang et al. 1976; Dokal and Vulliamy 2008). Additional supportive features of a DBA diagnosis include elevated fetal hemoglobin levels and raised erythrocyte adenosine deaminase (eADA) activity; the physiological significance of these associated increases are unknown (Dokal, Rule et al. 1997; Lipton and Ellis 2009).

The incidence of cancer in DBA patients is relatively low compared to other IBMFS, but is substantially higher than that observed in healthy individuals. Both hematological (i.e. MDS and AML) and non-hematological (i.e. osteosarcoma, breast

cancer, hepatocellular carcinoma) malignancies have been identified in DBA patients (Lipton and Ellis 2009). Reports from the Diamond-Blackfan Anemia Registry (DBAR) show solid tumors are more prevalent among DBA patients compared to other malignancies (Lipton, Federman et al. 2001). In addition to an increased incidence of cancer, approximately one-third of patients exhibit somatic abnormalities such as craniofacial anomalies (cleft lip, palate), triphalangeal thumbs, genitourinary system defects, and cardiac irregularities (Lipton, Atsidaftos et al. 2006; Dokal and Vulliamy 2008; Ganapathi and Shimamura 2008; Lipton and Ellis 2009).

The Ribosome is a Target of Many Pathogenic Mutations in DBA

Diamond-Blackfan anemia has an autosomal-dominant mode of inheritance. In 1999, 42 out of 172 DBA patients were found to harbor disease-associated pathogenic mutations in a gene locus encoding a small ribosomal subunit protein, Rps19 (Draptchinskaia, Gustavsson et al. 1999). Interestingly, DBA represents the first and only known inherited disease resulting from mutations in a structural component of the ribosome. DBA is often referred to as a "ribosomapathy," a term which describes a disorder resulting from a failure to produce adequate quantities of ribosomes (Dianzani and Loreni 2008). This term gained even greater acceptance with the emergence of other mutated ribosomal proteins in DBA. Currently, of the 80 structural proteins comprising the human ribosome, nine have been identified as mutant in approximately 50% of DBA patients (Dianzani and Loreni 2008). These ribosomal proteins include both small and large ribosomal subunit proteins: Rps7 (Gazda, Sheen et al. 2008), Rps10 (Doherty, Sheen et al. 2010), Rps17 (Cmejla, Cmejlova et al. 2007), Rps19 (Draptchinskaia,

18

Gustavsson et al. 1999), Rps24 (Gazda, Grabowska et al. 2006), Rps26 (Doherty, Sheen et al. 2010), Rpl5 (Gazda, Sheen et al. 2008), Rpl11 (Gazda, Sheen et al. 2008), and Rpl35A (Farrar, Nater et al. 2008). Most of these ribosomal proteins, in both yeast and mammalian cells, are required for the biogenesis of their respective subunits (Choesmel, Bacqueville et al. 2007; Flygare, Aspesi et al. 2007; Idol, Robledo et al. 2007; Farrar, Nater et al. 2008; Gazda, Sheen et al. 2008). As mutations in these genes only account for approximately 50 percent of reported cases of DBA, there are undoubtedly a number of other genetic targets yet to be discovered. Efforts are currently underway to sequence all 80 ribosomal subunit protein genes in DBA patients from the North American DBA registry, a project which is being led by a consortium of DBA investigators in collaboration with the NHLBI Resequencing and Genotyping Service.

Most of the genetic mutations linked to DBA are heterozygous loss-of-function mutations which result in gene product haploinsufficiency. *RPS19* is the gene most commonly mutated in DBA and accounts for approximately 25% of all of the reported cases. For this reason, *RPS19* has been extensively studied and a total of 77 disease-related mutations have been described in the literature (Campagnoli, Ramenghi et al. 2008). These mutations include translocations, gene deletions, truncation mutations (i.e. nonsense or frameshift), and missense mutations (Campagnoli, Ramenghi et al. 2008; Dianzani and Loreni 2008). *In vitro* studies following the fate of mutated Rps19 demonstrate various mutations to decrease protein stability or lead to alterations in nucleolar localization (Angelini, Cannata et al. 2007; Cretien, Hurtaud et al. 2008). In each case, these mutant Rps19 proteins are incapable of being assembled into functional ribosomes (Angelini, Cannata et al. 2007).

DBA Etiology and Pathophysiology

Pioneering work in DBA provided evidence that its characteristic red cell hypoplasia was the result of an intrinsic disorder of erythropoiesis. Freedman and colleagues (1976) showed that a small number of DBA patients had reduced amounts of early committed myeloid progenitors in bone marrow aspirates (Freedman, Amato et al. 1976). These observations were re-enforced by another group of investigators based in Boston, who showed a reduction in committed erythroid precursors (both erythroid burst-forming units [BFU-E] and erythroid colony-forming units [CFU-E]) in eleven DBA patients. These authors concluded that these reductions were a consequence of a delay in differentiation prior to the earliest committed phase of erythroid development (BFU-E) (Nathan, Clarke et al. 1978). While a number of these earlier studies highlighted a paucity of red cell precursors in DBA, later investigation revealed a number of DBA patients to possess marrow with normal numbers of both BFU-E and CFU-E myeloid progenitors, however their differentiation to mature erythrocytes was interrupted (Lipton, Kudisch et al. 1986). These data, although contradictory, suggest that DBA is a heterogeneous disorder and further supports it as a disease which results from an intrinsic progenitor defect – a defect which later studies propose related to both impaired differentiation and reduced proliferative capacity of red cell precursors (Flygare, Kiefer et al. 2005; Miyake, Flygare et al. 2005).

Molecular studies investigating DBA pathophysiology lagged for some time as *in vivo* animal models, which recapitulate the human disease phenotype, were not available and initial attempts to construct them were unsuccessful. The first reported DBA mouse model was developed in 2004 and utilized gene targeted disruption of murine *RPS19*

(Matsson, Davey et al. 2004). Mice heterozygous for this *RPS19* null allele had no observable disease phenotype and mice which were homozygous for the null allele were early embryonic lethal (Matsson, Davey et al. 2004). More recently, two groups successfully created zebrafish models of DBA via the morpholino-mediated knockdown of *Rps19* (Danilova, Sakamoto et al. 2008; Uechi, Nakajima et al. 2008). Intriguingly, both of these zebrafish models recapitulate certain characteristics of the human disease, including defective erythropoiesis and developmental abnormalities. Uechi and colleagues (Uechi, Nakajima et al. 2008), in addition to *RPS19*, also investigated the depletion of a myriad of other ribosomal proteins and demonstrated three others, one of those being *RPL35A* (Farrar, Nater et al. 2008), to also affect erythropoiesis in zebrafish. A large-scale chemical mutagenesis screen for mice with a dark skin phenotype (de Angelis, Flaswinkel et al. 2000) led to the serendipitous identification of missense mutations in *RPS19* and *RPS20*, denoted as DSK3 and DSK4, respectively (McGowan, Li et al. 2008). McGowan and colleagues demonstrated *Rps19*^{DSK3} heterozygous mice manifest a mild DBA-like phenotype. These mice had normocellular marrow, but suffered from a hypoproliferative-proapoptotic anemia and growth retardation (McGowan, Li et al. 2008). In light of the available data, the current view is that DBA is the result of an intrinsic erythroid progenitor defect characterized by a proapoptotic phenotype and an impaired capacity to differentiate (Lipton, Kudisch et al. 1986; Tsai, Arkin et al. 1989; Perdahl, Naprstek et al. 1994; Ohene-Abuakwa, Orfali et al. 2005; Miyake, Utsugisawa et al. 2008). Notably, the disease phenotypes observed in zebrafish (Danilova, Sakamoto et al. 2008) and mouse (McGowan, Li et al. 2008) DBA models are ameliorated by inactivating p53. Thus, it has been hypothesized that the proapoptotic

phenotype of myeloid precursors observed in DBA is linked to p53 stabilization and activation, referred to as the "ribosomal stress hypothesis (Dianzani and Loreni 2008)." This hypothesis suggests that a reduction in ribosomal protein and/or rRNA synthesis promotes the stabilization and concomitant activation of p53, an event which ultimately results in premature cell senescence or apoptosis. These events are then thought to be responsible for the observed clinical features associated with DBA (i.e. anemia, developmental delays, and malformations) (Dianzani and Loreni 2008).

A potential mechanism by which abortive ribosome assembly or nucleolar stress could signal to activate the p53 tumor suppressor involves the interaction of certain ribosomal proteins with MDM2 (Murine Double Minute), the most central negative regulator of p53. MDM2 is essential for maintaining low cellular levels of active p53 by binding and blocking p53's transcriptional activity (Chen, Marechal et al. 1993; Ruggero and Pandolfi 2003), inducing p53's nuclear export (Boyd, Tsai et al. 2000; Geyer, Yu et al. 2000), and initiating p53's ubiquitination thereby promoting its proteasome-mediated degradation. MDM2 mediates p53 degradation through its function as a RING finger-containing E3 ubiquitin ligase (Haupt, Maya et al. 1997; Kubbutat, Jones et al. 1997). Three large ribosomal subunit proteins (Rpl5, Rpl11, and Rpl23) have been confirmed to directly interact with MDM2, an interaction which is associated with a reduction in the ubiquitin ligase activity of MDM2 and a concomitant stabilization of p53 (Marechal, Elenbaas et al. 1994; Lohrum, Ludwig et al. 2003; Zhang, Wolf et al. 2003; Dai, Zeng et al. 2004; Jin, Itahana et al. 2004). In addition, a small ribosomal subunit protein (Rps7) has also been shown to interact with MDM2 and elicit the stabilization and activation of p53, although with a weaker affinity than those of the large subunit (Chen, Zhang et al.

2007). These interactions have mostly been investigated under conditions that disrupt the assembly of both 40S and 60S ribosomal subunits, either by the inhibition of RNA polymerase I activity or by genetic inactivation of rRNA processing enzymes (Perry and Kelley 1970; Pestov, Strezoska et al. 2001; Yuan, Zhou et al. 2005). In the context of these studies, ribosome biogenesis is disrupted at early stages which results in the subsequent diversion of ribosomal proteins from their normal assembly pathway to other fates within cells. Some studies suggest that ribosomal proteins synthesized in excess of what is required for ribosome assembly are rapidly degraded by the proteasome (Lam, Lamond et al. 2007). Despite this, sufficient evidence exists to indicate that ribosomal proteins diverted from assembling into maturing ribosomal subunits can act as important modulators of MDM2 activity leading to the stabilization and activation of p53. The importance of p53 in ribosome stress pathways has been documented in zebrafish and mouse models of DBA (Danilova, Sakamoto et al. 2008; McGowan, Li et al. 2008). Thus, signaling through unassembled ribosomal proteins could potentially bridge the divide between abortive ribosome assembly and the proapoptotic phenotype of erythroid progenitors in DBA patients.

In addition to the inhibitory effects imposed by the binding of specific ribosomal proteins to MDM2, the ability of MDM2 to target p53 can also be affected by its interaction with the ARF tumor suppressor protein (Lindstrom, Deisenroth et al. 2007). Interestingly, interactions between ARF and nucleophosmin (B23), a multifunctional protein involved in ribosome synthesis and nuclear export, suggest an alternative pathway in which nucleolar stress may induce p53 activation in DBA (Maggi, Kuchenruether et al. 2008). It is believed that the relative amounts of ARF, MDM2, and B23 play an

important role in coupling cell cycle regulation to ribosome biogenesis (Brady, Yu et al. 2004). The relative contribution of this pathway to DBA pathogenesis or the degree to which it cooperates with other nucleolar stress signaling pathways, particularly those involving ribosomal proteins liberated from abortively assembled intermediates, is currently unknown.

Shwachman-Diamond Syndrome

Historical Introduction and Clinical Features

Shwachman-Diamond syndrome (SDS; OMIM 260400) was first identified in 1964 and so was named after two Harvard Medical School clinicians, Harry Shwachman and Louis K. Diamond (also of Diamond-Blackfan anemia), who described it in five patients suffering from leucopenia and pancreatic insufficiency (Shwachman, Diamond et al. 1964). The clinical phenotype of SDS, which often manifests in infancy, is frequently complex presenting with multisystemic anomalies that include abnormal myelopoiesis, exocrine pancreatic insufficiency, skeletal abnormalities (i.e. metaphyseal dysostosis), and cancer predisposition (Coccia, Ruggiero et al. 2007; Burroughs, Woolfrey et al. 2009). The most common hematological abnormality among SDS patients is neutropenia (88-100% of patients), however, other hematological manifestations have been observed. These include anemia, thrombocytopenia, and pancytopenia, with anemia being the second most common cytopenia observed in SDS patients (Smith, Hann et al. 1996). In addition to bone marrow failure, retrospective studies of SDS patients reveal a high propensity for malignant transformation to myelodysplastic syndrome (MDS) and acute myeloid leukemia (Alter 2007; Coccia, Ruggiero et al. 2007).

24

Exocrine pancreatic dysfunction is considered one of the hallmark clinical features of SDS and is an essential component of its diagnosis. Histological analyses of pancreases from SDS patients reveal a scarcity of pancreatic acinar cells replaced by fatty deposits within the gland causing a reduction/absence of trypsin, lipase, and amylase in pancreatic fluid (Shimamura 2006). As a result, SDS patients with exocrine pancreatic insufficiency generally suffer from malabsorption of nutrients and steatorrhea with symptoms typically becoming evident within the first 6 months of life. Pancreatic function in SDS patients has been reported to improve with age (Hall, Dale et al. 2006). In addition to these characteristic hematological abnormalities and pancreatic dysfunction, other clinical features in SDS include genitourinary tract irregularities, cardiac defects, and intellectual difficulties (Aggett, Cavanagh et al. 1980; Savilahti and Rapola 1984; Kent, Murphy et al. 1990).

SDS Genetics: Gene Conversions and Disruptions in Coding Potential

Shwachman-Diamond syndrome has an autosomal-recessive mode of inheritance. In 2002, pathogenic mutations in the *SBDS* (Shwachman—Bodian—Diamond Syndrome) gene were shown to be responsible for the disease (Boocock, Morrison et al. 2003). This highly conserved gene, which maps to chromosome 7q11, spans a region of 7.9 kb and is composed of five exons. Distally located to the *SBDS* locus is a paralogous pseudogene (*SBDSP*) whose transcript shares 97% identity with *SBDS* and contains numerous inactivating mutations. The high degree of sequence similarity among *SBDS* and *SBDSP* may explain why most of the mutated alleles associated with SDS (approximately 75%) are the result of gene conversion events between *SBDS* and its adjacent pseudogene (Boocock, Morrison et al. 2003). Coding region alterations

identified in affected individuals with SDS include missense and frameshift modifications. The most common mutations among SDS patients are the truncating *SBDS* mutations, 183-184 TA→CT and 258+2T→C (both gene conversion events), which result from the introduction of an in-frame stop codon or the mutation of a donor splice site which causes a concomitant frameshift, respectively (Boocock, Morrison et al. 2003). Both of these mutations result in severely truncated Sbds proteins. Most SDS patients are compound heterozygotes. Several harbor the 183-184 TA→CT and 258+2T→C biallelic mutations with a large majority (about 89%) of patients having at least one of these early truncating *SBDS* mutations (Boocock, Morrison et al. 2003). No patient is homozygous for the 183-184 TA→CT mutant allele, suggesting that patients are likely hypomorphs deriving small amounts of functional protein from the splice site allele. This observation is supported by a mouse model for SDS where it was shown that a complete loss of *SBDS* (*Sbds$^{-/-}$*) results in embryonic lethality (Zhang, Shi et al. 2006). In the same study, *Sbds$^{+/-}$* heterozygous mice lacked an observable phenotype that was distinct from wild-type littermates. These reports suggest the molecular pathogenesis and related clinical features of SDS are the consequence of residual expression from mutated *SBDS* alleles.

SBDS Protein: The Structure and Proposed Function

The *SBDS* locus encodes a polypeptide of 250 amino acids whose function is largely unknown. The *SBDS* mRNA and protein are broadly expressed throughout many human tissues at both the message and protein levels (Boocock, Morrison et al. 2003; Woloszynek, Rothbaum et al. 2004; Burroughs, Woolfrey et al. 2009). The Sbds protein

is present in both the cytoplasm and the nucleus of cells, but is particularly concentrated within the nucleolus (Woloszynek, Rothbaum et al. 2004; Austin, Leary et al. 2005). SBDS is a highly evolutionarily conserved protein with putative orthologues present in archaeal and eukaryotic kingdoms. No orthologue has been identified in eubacteria (Savchenko, Krogan et al. 2005). The only known structural information concerning SBDS is based on X-ray structures of the archaeal orthologues from *Archaeoglobus fulgidus* (afSBDS) and *Methanothermobacter thermautotrophicus* (mthSBDS) (Savchenko, Krogan et al. 2005; Shammas, Menne et al. 2005; Ng, Waterman et al. 2009). These X-ray studies reveal the SBDS protein possesses a tripartite structure with three characteristic domains consisting of a novel N-terminal FYSH domain (fungal, YHR087Wp, Shwachman), a common three-helical bundle domain, and a C-terminal domain possessing a ferredoxin-like fold (Figure 3).

Figure 3. **Ribbon diagram modeled after the crystal structure of the** *Methanothermobacter thermautotrophicus* **SBDS protein (mthSBDS).** Ribbon is constructed with colors that merge from the color blue (N-terminus) to red (C-terminus). Protein folding domains are labeled I (residues 1-88), II (residues 89-162), and III (residues 163-232) and correspond to the N-terminal FYSH domain, three-helical bundle domain, and C-terminal ferredoxin-like fold containing domain, respectively. Image adapted from Ng, Waterman et al. 2009.

The X-ray crystallographic structure of SBDS bares no obvious homology to common protein functional domains and thus function is difficult to infer based on structural characteristics alone. It is noteworthy that the novel N-terminal FYSH domain of the human SBDS protein is often the target of disease related mutations in Shwachman-Diamond syndrome and that it also possesses the highest sequence conservation among the archaeal and eukaryotic SBDS proteins (Boocock, Morrison et al. 2003; Nicolis, Bonizzato et al. 2005; Boocock, Marit et al. 2006). The N-terminal FYSH domain shares some sequence similarity to another yeast protein (YHR087Wp) that has genetic interactions with proteins involved in rRNA processing (Savchenko, Krogan et al. 2005). These observations suggested that the N-terminal FYSH domain of the SBDS protein was likely important for its function and that this function may involve pathways involved in RNA metabolism or ribosome biogenesis.

Initial reports, based largely on studies in archaebacteria and yeast, also hinted at a role for the SBDS family of proteins in RNA metabolism. For example, *SBDS* was shown to reside within a predicted superoperon encoding components of the exosome, a complex of RNases and RNA-binding proteins involved in numerous RNA processing reactions (Koonin, Wolf et al. 2001). Also, microarray expression studies in yeast demonstrated that the *SBDS* yeast ortholog, *SDO1* (*YLR022C*), is regulated in a coordinate fashion with genes encoding proteins involved in RNA processing and ribosome maturation (Wu, Hughes et al. 2002; Peng, Robinson et al. 2003). Congruent with these previous results, affinity purification of TAP tagged Sdo1 in yeast demonstrated a number of physical interactions with proteins involved in rRNA

processing, as well as with protein components of the 60S ribosomal subunit (Savchenko, Krogan et al. 2005).

The Molecular Pathogenesis of SDS Remains Elusive

Early studies pointed to an intrinsic defect in hematopoietic stem cells as the underlying cause of bone marrow failure in SDS patients. These studies demonstrated defective proliferative potential and diminished numbers of committed myeloid progenitors in the marrow of SDS patients, underscored by a paucity of granulocyte-monocyte colony-forming units (CFU-GM) and erythrocyte burst-forming units (BFU-E) (Saunders, Gall et al. 1979; Woods, Krivit et al. 1981; Suda, Mizoguchi et al. 1982). Almost two decades later, Dror and Freedman demonstrated that SDS patient derived bone marrow aspirates contained marked reductions in the quantity of CD34^{+} hematopoietic progenitors in comparison to normal individuals; they also showed SDS patient derived CD34^{+} cells to possess a reduced proliferative capacity discernible by diminished progenitor colony development and impaired long-term colony formation. Finally, they were able to show that stromal cells derived from SDS marrow exhibit an impaired ability to support normal CD34^{+} cells in long-term colony formation assays (Dror and Freedman 1999). These data suggest an inherent stem-cell defect together with an aberrant bone marrow stroma or defective hematopoietic microenvironment as contributing factors in SDS associated marrow dysfunction. Increased apoptosis is implicated as a central pathogenic mechanism in SDS. Both accelerated apoptosis and enhanced expression of the p53 tumor suppressor protein have been reported in bone marrow derived from SDS patients. These observations provide a potential explanation

for the decreased numbers of CD34$^+$ cells in SDS patients and their reduced ability to form hematopoietic colonies (Dror and Freedman 2001; Elghetany and Alter 2002; Rujkijyanont, Watanabe et al. 2008).

In vitro and *in vivo* animal studies have demonstrates that SBDS is essential for hematopoiesis and pancreatic development. Morpholino-mediated knockdown of Sbds in zebrafish results in aberrant exocrine pancreas morphogenesis and abnormal granulocyte development and distribution within embryos (Venkatasubramani and Mayer 2008). Further, lentiviral-mediated RNAi knockdown of Sbds in murine hematopoietic progenitor cells lead to defective granulocytic differentiation *in vitro* and impair both short-term hematopoietic engraftment and homing of hematopoietic progenitors to bone marrow following *in vivo* transplantation (Rawls, Gregory et al. 2007). In addition to these studies recapitulating some of the human pathologic characteristics associated with SDS, they also, in part, support additional roles for SBDS in chemotaxis and/or cell motility (Stepanovic, Wessels et al. 2004; Wessels, Srikantha et al. 2006; Orelio and Kuijpers 2009). This view is substantiated by numerous studies, which demonstrate SDS patient-derived neutrophils have chemotactic and mobility abnormalities (Aggett, Harries et al. 1979; Aggett, Cavanagh et al. 1980; Ruutu, Savilahti et al. 1984; Repo, Savilahti et al. 1987; Dror, Ginzberg et al. 2001).

Many studies suggest that members of the SBDS family of proteins function in ribosome synthesis. Consistent with this view, SBDS has been shown to reside predominantly within the nucleolus (Austin, Leary et al. 2005). Human cell studies have also shown that SBDS co-sediments with 60S ribosomal subunits in sucrose gradients, but not with mature subunits actively participating in translation. This association was

31

confirmed by SBDS co-precipitatation with 28S rRNA, an RNA component of 60S ribosomal subunits (Ganapathi, Austin et al. 2007). Ganapathi and colleagues (Ganapathi, Austin et al. 2007) also demonstrated that SDS patient derived cells have a hypersensitivity to low doses of the rRNA transcription inhibitor, actinomycin D, indicative of defective ribosome assembly. In these reports, the loss of SBDS was not associated with any discrete rRNA processing defects or with quantitative decreases in 60S ribosomal subunits (Ganapathi, Austin et al. 2007). Contrary to these earlier reports, later studies reveal cells derived from an SDS mouse model exhibit a diminution in large ribosomal subunits (Ball, Zhang et al. 2009). Proteomic analyses of SBDS binding partners show that it is complexed with nucleophosmin (NPM), a multifunctional nucleolar protein connected to both ribosome biogenesis and oncogenesis (Okuwaki, Tsujimoto et al. 2002; Grisendi, Mecucci et al. 2006; Ganapathi, Austin et al. 2007). In addition, both yeast two-hybrid and GST pull-down assays revealed SBDS associates with Nip7, a conserved large ribosomal subunit associated protein involved in the terminal steps of 60S subunit maturation (Zanchin, Roberts et al. 1997; Hesling, Oliveira et al. 2007). Further studies in HEK293 cells failed to demonstrate any effects of SBDS depletion on ribosome biogenesis, however, rRNA processing defects were evident (Hesling, Oliveira et al. 2007). These studies also showed that depletion of SBDS leads to alterations in both mRNA message abundance and translational efficiency of vital genes involved in blood cell differentiation and proliferation, bone morphogenesis, and nervous system development (Hesling, Oliveira et al. 2007).

As previously noted, studies on the yeast *SDO1* gene reveal a role for this protein in 60S subunit maturation. Menne and colleagues proposed that Sdo1 functions to

promote the dissociation and concomitant recycling of anti-association factor Tif6 from

nascent 60S subunits in the cytoplasm to the nucleolus (Menne, Goyenechea et al. 2007).

Yeast Tif6, the ortholog of mammalian eIF6, is an essential protein that is required for

60S subunit maturation and nuclear export (Basu, Si et al. 2001; Ceci, Gaviraghi et al.

2003). Further, *in vitro* studies show that Tif6 functions as a subunit anti-association

factor that prevents 60S subunits from prematurely associating with 40S subunits prior to

appropriate initiation complex formation (Si and Maitra 1999). Interestingly, mutations

in Tif6 rescue the slow growth phenotype associated with the complete loss of Sdo1

(Menne, Goyenechea et al. 2007). To date, mutations in *TIF6* that rescue the slow

growth phenotype of *SDO1* mutants, map to a single surface of Tif6, which presumably

mediates its interaction with 60S ribosomal subunits. These mutations are thought to

reduce the affinity of Tif6 for 60S subunits. Based on these observations, it is proposed

that Sdo1 functions to release Tif6 from subunits once they reach the cytoplasm. Sdo1

may not, however, function alone in facilitating the release of Tif6 from 60S subunits.

Mutations in *EFL1*, a yeast gene encoding a cytoplasmic GTPase, which shares

homology to elongation factor EF-G/EF-2, give rise to phenotypes similar to loss-of-

function mutations in *TIF6*. Mutations in both genes result in a severe slow growth

phenotype underscored by comparable pre-rRNA processing defects, 60S subunit

deficits, and impaired 60S subunit nuclear export (Basu, Si et al. 2001; Senger,

Lafontaine et al. 2001). *In vitro* studies show that Efl1 functions to dissociate Tif6 from

60S subunits, and intriguingly, mutations in *TIF6* suppress phenotypes associated with

EFL1 mutations (Senger, Lafontaine et al. 2001). Thus, genetic analysis clearly

demonstrates an epistatic relationship between *SDO1* and *EFL1*, and suggests that both

proteins function together to promote the dissociation of Tif6 from 60S ribosomal subunits. Once released, Tif6 can be recycled back to the nucleolus where it participates in additional rounds of 60S subunit maturation (Menne, Goyenechea et al. 2007). Recent data from Zhang and colleagues indicate reduced amounts of 60S subunits in embryonic fibroblasts derived from an SDS mouse model suggesting that the mammalian Sbds protein may have a similar role in 60S subunit biogenesis (Ball, Zhang et al. 2009).

Collectively, these studies home in on potential cellular processes and pathways that could potentially bridge the gap between aberrations in ribosome synthesis and SDS related marrow dysfunction. The specific molecular mechanisms relating SDS associated defects in ribosome biogenesis to the heterogeneous phenotype observed in SDS patients remain to be explained, as do those mechanisms that make SDS pathologically distinct from other bone marrow failure disorders whose molecular bases are also linked to defects in ribosome biogenesis, such as DBA.

Dissertation Overview

Overall Goal

The work presented in this dissertation is focused on *in vivo* models of Shwachman-Diamond syndrome and Diamond-Blackfan anemia. Here I made use of yeast models for both diseases, each targeting the 60S ribosomal subunit. The overall goal was to explore the molecular mechanisms by which the maturation of 60S subunits was affected in both disease models. Further, concerning the yeast SDS model, the objective was to analyze the function of Sdo1 in 60S subunit maturation from the perspective of its potential role as a regulator of protein acetylation. Investigation of

34

these disease models may reveal commonalities and/or differences among their underlying molecular defects, potentially leading to the elucidation of unique mechanisms and/or signaling pathways that could explain their inimitable clinical manifestations, as well as potentially lead to the identification of prospective therapeutic targets.

Hypothesis and Research Aims

I hypothesized that both DBA and SDS yeast models would result in a deficit in functional 60S ribosomal subunits, though by divergent mechanisms. In aim I, I demonstrated distinct ribosome maturations defects among yeast models of DBA and SDS. With the discovery that histone deacetylase inhibitors partially reverse the growth defect of the yeast SDS model, in aim II, I focused on the role of acetylation in ribosome maturation and its implications for SDS pathophysiology and treatment.

CHAPTER II

DISTINCT RIBOSOME MATURATION DEFECTS IN YEAST MODELS OF
DIAMOND-BLACKFAN ANEMIA AND SHWACHMAN-DIAMOND SYNDROME

Introduction

As previously noted, both DBA and SDS are congenital bone marrow failure
syndromes linked to defects in ribosome synthesis and/or function (Liu and Ellis 2006).
They are also characterized by a heterogeneous collection of congenital anomalies and a
predisposition to cancer. Although both diseases share these general features, there are
substantial differences in their clinical manifestations. DBA is characterized by a red
blood cell hypoplasia, whereas SDS is frequently characterized by neutropenia, although
other hematopoietic lineages may also be affected in both disorders. Patients with SDS
also display exocrine pancreatic deficiency, which is not observed in DBA (Hall, Dale et
al. 2006). The congenital anomalies in SDS include short stature, skeletal defects, and
neurological problems. Patients with DBA also have short stature, but in contrast to
SDS, craniofacial anomalies are the most commonly associated congenital malformations
along with other abnormalities, including triphalangeal thumbs and genitourinary tract,
and cardiac defects (Freedman 2000; Lipton, Atsidaftos et al. 2006). Both diseases carry
an increased risk of cancer, but differ in neoplastic potential and associated types of
malignancies. Approximately 30-40% of SDS patients progress to develop
myelodysplastic syndrome and/or acute myelogenous leukemia. The incidence of cancer

in DBA patients is lower, approximately 2%. Both solid tumors and blood-based cancers have been observed in patients with DBA (Lipton, Atsidaftos et al. 2006).

The molecular underpinnings of both DBA and SDS converge on a common target, the ribosome. To date, the genes involved in DBA all encode structural components of the ribosome. Three of these genes, *RPS17, RPS19*, and *RPS24* encode ribosomal proteins of the 40S subunit (Draptchinskaia, Gustavsson et al. 1999; Gazda, Grabowska et al. 2006; Cmejla, Cmejlova et al. 2007). More recently, *RPL5, RPL11*, and *RPL35A* genes encoding 60S subunit ribosomal proteins have also been shown to harbor pathogenic mutations in DBA (Farrar, Nater et al. 2008; Gazda, Sheen et al. 2008). Several studies show that ribosomal proteins affected in DBA are required for the maturation of ribosomal subunits indicating that the basis for the clinical features of DBA resides in abortive ribosome synthesis (Choesmel, Bacqueville et al. 2007; Flygare, Aspesi et al. 2007; Idol, Robledo et al. 2007; Farrar, Nater et al. 2008; Gazda, Sheen et al. 2008). In SDS, the gene affected is *SBDS*, which encodes a protein associated with 60S ribosomal subunits (Ganapathi, Austin et al. 2007). SBDS is not a structural component of the ribosome. The yeast ortholog of SBDS, Sdo1, has been reported to be required for the biogenesis and function of the 60S ribosomal subunit (Menne, Goyenechea et al. 2007). In contrast, there have been conflicting reports regarding the role of SBDS in the biogenesis of 60S ribosomal subunits in mammalian cells (Ganapathi, Austin et al. 2007). While these data indicate that both DBA and SDS may arise through defects in ribosome synthesis and/or function, little is known about how these changes in this common target result in the distinct clinical presentations of the two diseases.

Studies in animal models of DBA have recently shown that the tumor suppressor p53 plays an important role in developmental and hematologic phenotypes (Danilova, Sakamoto et al. 2008; McGowan, Li et al. 2008; Uechi, Nakajima et al. 2008). These findings are generally interpreted in the context of a model in which some form of nucleolar stress signaling promotes p53 stabilization and activation (Pestov, Strezoska et al. 2001). Two pathways appear ideally suited to link features of abortive ribosome assembly to growth control and apoptosis. Both involve MDM2, a zing-finger ubiquitin ligase, which targets p53 for proteasomal degradation. Several ribosomal proteins bind to MDM2 and inhibit its ubiquitin ligase activity resulting in p53 stabilization and activation (Lindstrom, Deisenroth et al. 2007). In this model, ribosomal proteins are liberated from productive assembly into ribosomal subunits and are free for signaling through MDM2. Alternatively, nucleolar stress can also signal through the ARF tumor suppressor (Gjerset 2006). This latter pathway appears to involve nucleophosmin, a nucleolar protein recently shown to be involved in ribosome trafficking from the nucleus to the cytoplasm (Maggi, Kuchenruether et al. 2008).

The recent discoveries of genes encoding 60S subunit ribosomal proteins mutated in DBA allowed me to focus on the large ribosomal subunit as a common target in yeast models for DBA and SDS (Farrar, Nater et al. 2008; Gazda, Sheen et al. 2008). These models employed yeast strains mutated in *RPL33A*, the yeast ortholog of *RPL35A* mutated in DBA (Freedman 2000), and *SDO1*, the ortholog of *SBDS* mutated in SDS (Boocock, Morrison et al. 2003). The overall goal was to determine whether there are molecular features that differentiate the two disease models. Here I show that both models affect the production of 60S subunits, but do so by distinct biochemical

38

mechanisms which affect different stages of the subunit maturation pathway. The subunit deficit in the DBA model is linked to an assembly defect that results in immature particles that are rapidly degraded. This assembly defect is associated with a substantial increase in the amount of extra-ribosomal 5S ribosomal RNA (rRNA). This observation is intriguing in light of the observation that, in mammalian cells, ribosomal proteins Rpl5 and Rpl11, in complex with 5S rRNA, interact with MDM2 and promote p53 stabilization and activation (Horn and Vousden 2008). In contrast to the data obtained for the DBA model, the subunit deficit in the SDS model is linked to defects later in the subunit maturation pathway. As a consequence of this rather late maturation defect, a significant fraction of the 60S subunit precursors found in the SDS model are retained within the nucleoplasm associated with 5S rRNA. Thus, the two disease models differ dramatically in terms of their effects on subunit assembly and the potential for subsequent diversion of ribosomal components from their normal assembly pathway to potential interactions with other growth regulatory factors within cells. These models, therefore, provide a mechanistic basis for how differing effects on 60S subunit maturation could potentially trigger alternative signaling pathways within cells that give rise to the distinct clinical phenotypes of DBA and SDS.

Design and Methods

Yeast Strains

The yeast strains used in these studies were generated by the Saccharomyces genome deletion project and were obtained from either Research Genetics or Euroscarf. Heterozygous diploids for SDO1 (20519D: MAT a/α *ura3-1/ura3-1, his3-11/his3-11,*

leu2-3_112/leu2-3_112,   trp1Δ2/trp1Δ2,   ade2-1/ade2-1,   can1-100/can1-100, sdo1::kanMX4/SDO1) and *RPL33A* (22109: MAT a/α *his3Δ1/ his3Δ1, leu2Δ0/leu2Δ0, lys2Δ0/+, met15Δ0/+, ura3Δ0/ura3Δ0, rpl33A::kanMX4/RPL33A*) were sporulated and resulting haploid strains were employed. Because the genetic background of the *SDO1* mutant was W303 and the *RPL33A* strain was BY4743, the *RPL33A* disruption was backcrossed into the W303 background for the experiments reported here. The genotype of the *RPL33A* strain used was MAT a/α *ura3-1/ura3-1, his3-11/his3-11, leu2-3_112/leu2-3_112,   trpΔ2/trp1Δ2,   ade2-1/ade2-1,   can1-100/can1-100, rpl33A::kanMX4/RPL33A*. Because of a high spontaneous suppression rate of both *SDO1* and *RPL33A* mutants, haploid strains were freshly derived for each experiment.

Polysome profiling, northern hybridization, and pulse-chase analyses

Cell extracts were prepared for polysome analysis as previously described (Leger-Silvestre, Caffrey et al. 2005). Yeast strains were inoculated into 100 ml of glucose rich media (YPD) and were allowed to grow to mid-log phase at 30°C. At this time, 5 mg of cycloheximide was added to flasks containing cells and media, swirled, and poured into chilled nalgene® centrifuge bottles. Cells were harvested at 5,000 RPM (~3,000 x g) for 10 minutes. Following centrifugation, the supernatant was decanted, and cell pellets were resuspended in 5 ml of polysome buffer (10 mM Tris-HCl [pH 7.5], 100 mM NaCl, 30 mM MgCl₂, 50 μg/ml cycloheximide, 100 μg/ml heparin, 0.2 μl/ml DEPC). Cell suspensions were then transferred to 12 ml pop-top tubes, centrifuged again, and the washing step repeated with polysome buffer. Cell pellets were resuspended in 1 ml of polysome buffer and 0.30 grams of 425-600 micron glass beads were added. Cell/glass

bead suspensions were then mechanically lysed by vortexing at high speed, 8 times, 15 seconds each, with 30 second cool down periods between bursts. Following cell lysis, 1.5 ml of polysome buffer was added and extracts centrifuged at 5,000 x g at 4°C for 5 minutes to remove unbroken cells and debris. Supernatants were decanted into new 12 ml pop-top tubes, centrifuged again at 10,000 x g for 5 minutes, and supernatants saved. Polysome extracts (1 ml of 1:100 $A_{260} \sim 0.15$) were loaded onto 7-47% stepwise sucrose gradients and centrifuged at 28,000 rpm for 6 hours in an SW28.1 rotor (Beckman Instruments, Inc., Fullerton, CA, USA). Sucrose gradients were fractionated and the absorbance at 254 nm monitored using an ISCO model 185 gradient fractionator interfaced to a UA-6 absorbance detector (Teledyne Isco, Inc., Lincoln, NE, USA).

RNA was recovered from sucrose gradient fractions after precipitation with 2 volumes of absolute ethanol. Precipitates were collected by centrifugation for 10 min at 10,000xg and then suspended in 0.3 mL of 20 mM Tris-HCl pH 7.4, 2.5 mM EDTA, 100 mM NaCl, and 1% sodium dodecyl sulfate. Suspensions were extracted twice with phenol/chloroform and RNA in the aqueous phase was precipitated overnight at -20°C with 2.5 volumes of ethanol. RNA was collected by centrifugation, washed once with 70% ethanol, dried *in vacuo*, and suspended in DEPC-treated water. RNA was resolved on 1.5% formaldehyde-agarose gels, transferred to Zeta-Probe (Bio-Rad Laboratories, Hercules, CA, USA), and hybridized with oligonucleotides labeled at their 5' ends with ^{32}[P]. Oligonucleotides were radio-labeled using polynucleotide kinase and γ-^{32}[P]-ATP. The oligonucleotides employed were: 5S rRNA probe 5'-CAGTTGATCGGACGGGAACA-3', 5.8S rRNA probe 5'-CGTATCGCATTTCGCTGCGTTC-3', and C_2-ITS2 probe 5'-

GGCCAGCAATTTCAAGTTA-3'. The procedures for pulse-chase analysis are described elsewhere (Leger-Silvestre, Caffrey et al. 2005). Data were scanned and digitized using Adobe Photoshop.

Live cell fluorescence imaging

Yeast strains were transformed with PRS316-RPL25eGFP (URA3) and pUN100-DsRed-NOP1 (LEU2) vectors using an Alkali-Cation™ Yeast Kit (Qbiogene, Inc., Carlsbad, CA, USA) as directed by the manufacturer. Isolated transformants were grown to mid-log phase in synthetic complete liquid media lacking leucine and uracil. One milliliter aliquots were centrifuged at 10,000 RPM (~9,000 x g) for 15 s to pellet the cells. The supernatant was discarded and the resulting pellet was washed with 0.5 mL of KPO_4/sorbitol wash solution (1.2M sorbitol, 0.1M potassium phosphate, pH 7.5). Cell pellets were re-suspended in 300 μL of KPO_4/sorbitol wash solution and 1 μl of 10 μg/ml 4',6-diamidino-2-phenylindole (DAPI) nuclear stain added. Cell/DAPI suspensions were incubated at room temperature for 10 min, washed twice with KPO_4/sorbitol solution, re-suspended in 200 μL of KPO_4/sorbitol, and 2.5 μL of this cell suspension placed on glass microscope slides. Cells were subjected to fluorescent imaging using a Zeiss Axiovert 200 multi-channel fluorescence microscope (Carl Zeiss MicroImaging, Inc., Thornwood, NY, USA).

Results

Yeast strains heterozygous for RPL33A and SDO1 deletions were obtained from Euroscarf or Research Genetics. The diploid strains were sporulated, tetrads dissected, and resulting haploid progeny grown on rich media. Compared with wild-type cells, cells harboring either deletion had a pronounced growth deficit (Figure 4). To assess the effect of the *RPL33A* and *SDO1* deletions on the steady-state level of 60S subunits, extracts were prepared in a magnesium free buffer in which polysomes and 80S monosomes dissociate completely into 40S and 60S ribosomal subunits. The ratio of 60S to 40S subunits was used to examine the selective effect of these mutations on 60S subunit levels beyond any overall reduction in ribosome synthesis linked to reduced growth rate. Figure 5 illustrates that both yeast strains exhibit a reduction in the quantity of 60S subunits relative to 40S subunits when compared to wild-type cells. The relative reduction of 60S subunits in the two mutant strains differed by approximately 10% with the Δ*RPL33A* showing the greater overall reduction.
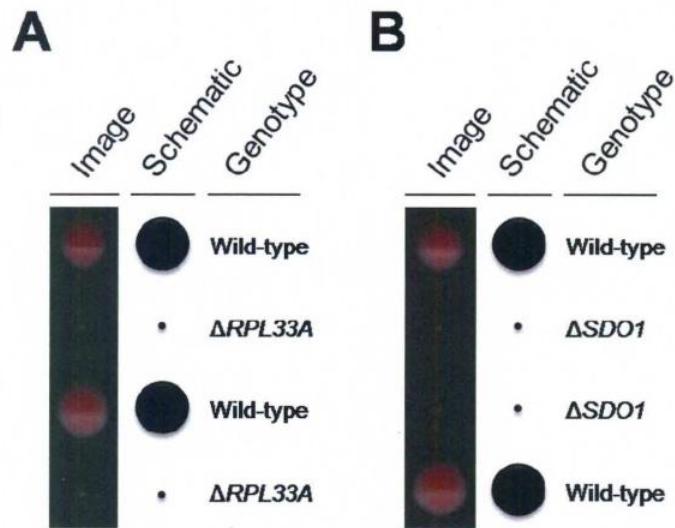
Figure 4. **Haploid yeast strains possessing deletions in *RPL33A* or *SDO1* have a pronounced growth defect.** (A) Δ*RPL33A* and (B) Δ*SDO1* heterozygous diploid strains were sporulated, their tetrads dissected and resultant haploid progeny grown on glucose rich media. Photographic images containing four haploid daughter cells from one dissected tetrad are shown and are accompanied by a schematic diagram representing colony size with corresponding genotypes labeled.
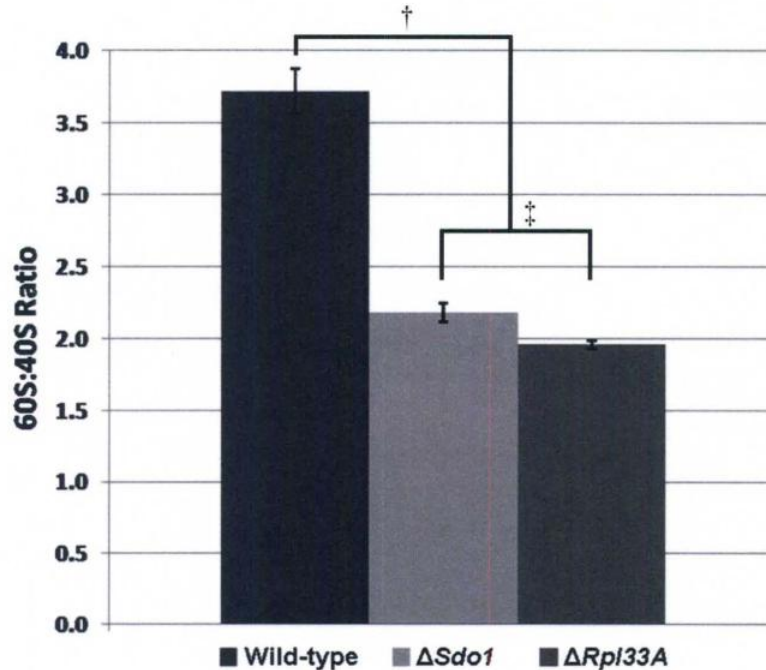
Figure 5. **Yeast models of DBA and SDS both exhibit deficits in the relative amount of 60S to 40S ribosomal subunits.** Extracts for subunit analysis were prepared as described for polysome isolation except magnesium was omitted from the buffers. Ribosomal subunits were resolved on 7-47% stepwise sucrose gradients via centrifugation. Gradients were fractionated and the absorbance at 254 nm monitored using a gradient fractionator interfaced to a UA-6 absorbance detector. Ribosomal subunits were quantified by determining the area under the curve (peak integration) in resultant absorbance tracings. The bar graph reports the ratio of 60S to 40S in wild-type, $\Delta SDO1$, and $\Delta RPL33A$ strains. Error bars corresponding to the standard error of the mean (SEM) are shown. Statistical significance was assessed by Student's t test. [†]Wild-type strain versus mutant strains ($p<0.0001$). [‡]$\Delta SDO1$ strain versus $\Delta RPL33A$ strain ($p<0.02$).

I used pulse-chase analysis of pre-rRNA processing for a more detailed characterization of subunit maturation in the DBA and SDS disease models. The yeast pre-rRNA processing pathway is shown in Figure 6A. Relative to the wild-type strain, the *RPL33A* mutant shows a pronounced delay in the production of mature 25S rRNA such that by 10 min of chase the amount of radio-label in 25S rRNA relative to 18S rRNA is significantly less than the approximate 2:1 ratio observed in wild-type cells (Figure 6B top panel). This selective effect on 25S rRNA synthesis is accompanied by delayed maturation of several pre-rRNA precursors including 35S, 23S, and 27S pre-rRNA. The delayed maturation of 35S and 23S pre-rRNA is the result of an ill-defined feedback system in which early steps in pre-rRNA processing are slowed in mutants that affect the maturation of 60S subunits (Venema and Tollervey 1999). The delayed maturation of 27S pre-rRNA species, on the other hand, accounts for the selective effect of the $\Delta RPL33A$ mutant on the maturation of 60S subunits. The top panel of Figure 6B shows a 27S pre-rRNA doublet that persists through the 10-min chase period. This doublet consists of 27S A_2/A_3 species (upper band) and 17S B (lower band). The primary effect of the *RPL33A* deletion is a delay in maturation of 27S A_2/A_3 pre-rRNA as evidenced by the increased ratio of 27S A_2/A_3 to 27S B pre-rRNA observed by northern analysis (Figure 6C). The data from the $\Delta SDO1$ strain, on the other hand, revealed a more complex effect on 60S subunit maturation. As for the $\Delta RPL33A$ strain, there was a delay in 35S and 23S pre-rRNA processing, consistent with the feedback effect of a reduction in 60S subunits on early steps in pre-rRNA processing. The persistence of 35S and 23S pre-rRNA in the $\Delta SDO1$ strain indicates that cleavage steps A_0 and A_1 involved in the maturation of the 5' end of 18S rRNA may be more adversely affected when

compared with the ΔRPL33A strain. Moreover, there was clearly a delay in 27S B pre-rRNA processing apparent by pulse-chase analysis in the ΔSDO1 mutant relative to wild-type cells (Figure 6B, bottom panel); this delay could also be observed by northern analysis (Figure 6C). Surprisingly, however, the effect of this delay on the production of 25S rRNA did not appear to be as great as that observed in the ΔRPL33A strain since the ratio of 25S to 18S rRNA in this strain was still greater than one.
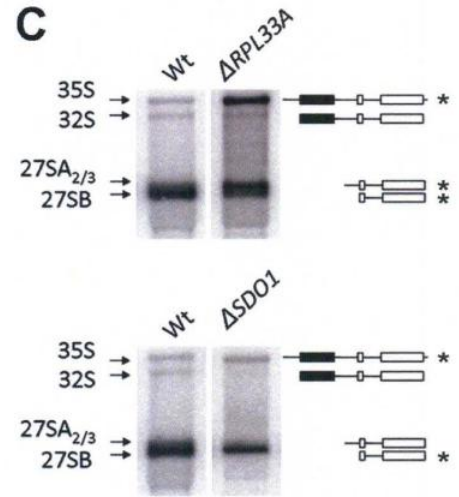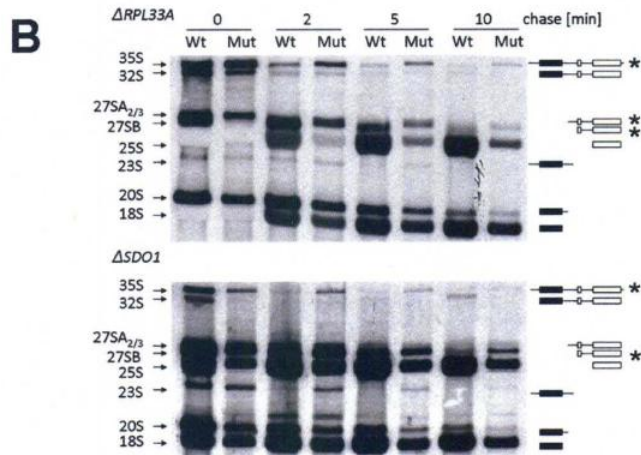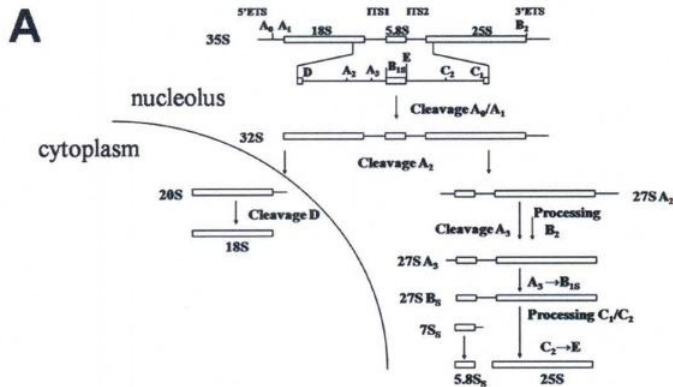
Figure 6. **Yeast models of DBA and SDS display discrete pre-rRNA processing defects.** (A) The major pre-rRNA processing pathways in S. *cerevisiae.* Mature rRNA species are respresented by boxes. External and internal transcribed sequences are shown as thin lines. Numbered letters indicate processing sites. Horizontal arrows represent exonucleolytic cleavages; other cleavage steps are endonucleolytic. An alternative pathway (not shown) has cleavage at site A_2 preceding cleavages at sites A_0 and A_1 giving rise to 23S pre-rRNA. (B) Pulse-chase analysis of pre-rRNA processing in yeast models of DBA and SDS. Top panel, $\Delta RPL33A$ strain (Mut) and isogenic wild-type (Wt); bottom panel, $\Delta SDO1$ strain (Mut) and isogenic wild-type (Wt). Cells were pulse-labeled for 2 min with [methyl-^{3}H]-methionine and chased in the presence of 1 mg/mL methionine for the indicated times. Total RNA was prepared and fractionated as outlined in the Design and Methods section. Mature and pre-rRNA species are labeled to the left of each panel. Schematic diagrams to the right correlate to each of the rRNA processing intermediates noted to the left. RNAs showing delayed processing relative to wild-type are marked with an asterisk. (C) Northern blot analysis of pre-rRNA processing in yeast models of DBA and SDS. Total RNA was prepared and resolved as outlined in the Design and Methods section. A radiolabeled oligonucleotide probe that hybridizes to the C_2 processing site located within internal transcribed spacer 2 (ITS2) was used for northern analyses. Membranes were exposed to BioMax MS film at -80° C using a BioMax LE intensifying screen and then subjected to phosphorimage analysis.

A more comprehensive analysis of the protein synthetic apparatus in the two disease models was based on polysome profiles. Polysome profiles from the ∆*RPL33A* strain showed a marked reduction in free 60S subunits relative to wild-type and the appearance of half-mer polysomes (Figure 7, middle panel). Half-mer polysomes are polysomes with stalled 48S initiation complexes and are a common characteristic of yeast strains with a deficit of 60S subunits (Rotenberg, Moritz et al. 1988). The polysome profiles from the ∆*SDO1* strain also exhibited half-mer polysomes, but in contrast to the ∆*RPL33A* strain, there was a significant pool of free 60S subunits and a noteworthy decrease in mean polysome size (Figure 7, bottome panel). These data differ from previously reported polysome data from *SDO1* mutants when neither half-mer polysomes nor a free pool of 60S subunits was observed (Menne, Goyenechea et al. 2007). Both mutant strains show a peak to the left of the 40S peak which is absent in the wild-type strain. This peak contains 20S RNA, an endogenous virus-like particle (termed the 20S replicon) induced by various forms of translational stress (Wickner 1996).
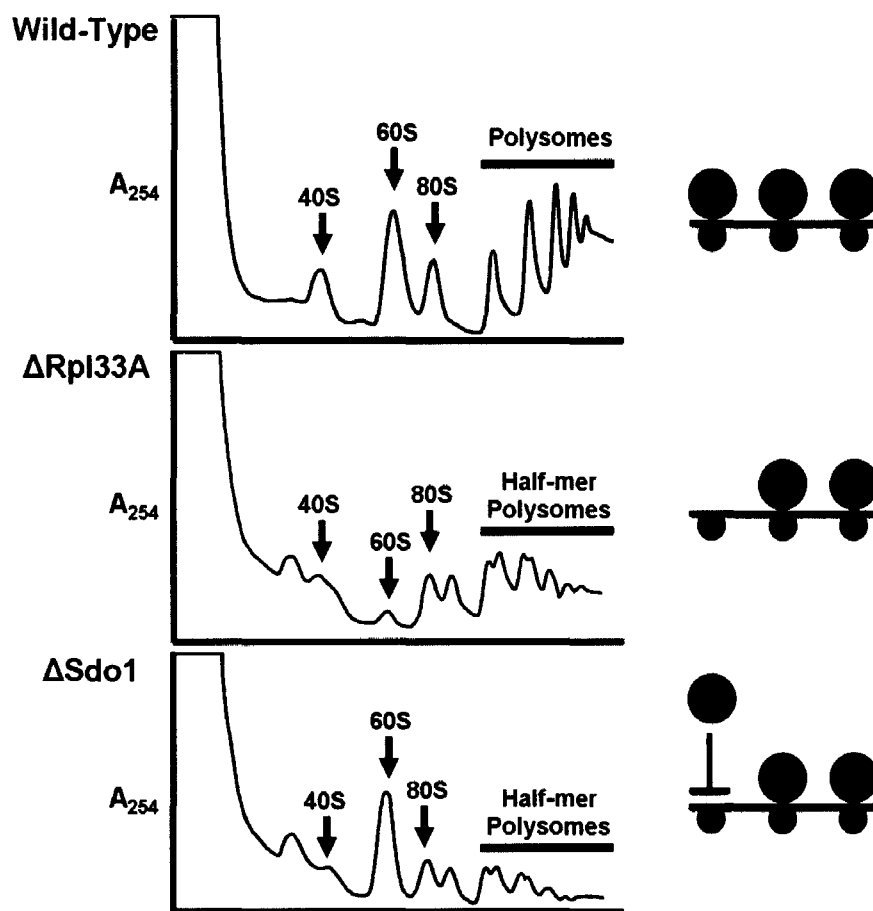
Figure 7. **Polysome profiles from yeast models of DBA and SDS differ in the amount of free 60S subunits.** Top panel, wild-type; middle panel, $\Delta RPL33A$; bottom panel, $\Delta SDO1$. Cell extracts were prepared and fractionated as outlined in the Design and Methods section. Subunit peaks were identified by analyzing the rRNA species co-sedimenting with each peak. The left hand side of each panel represents the top of the sucrose gradient. The schematic diagrams to the right of the mutant profiles indicate that half-mer polysomes arise as a consequence of a 60S subunit deficit in the $\Delta RPL33A$ strain whereas in the $\Delta SDO1$ strain 60S subunits are present but unable to engage in translation. Polysome analysis was performed in triplicate for each strain. The profile shown is representative.

51

To evaluate the intracellular distribution of 60S subunits in the two disease models, 60S subunits were tracked using a GFP-Rpl25 fusion protein. Several studies have shown that this protein is assembled into 60S subunits and can be used to monitor the distribution of such subunits within cells. In wild-type cells GFP fluorescence was distributed throughout nuclear and cytoplasmic regions but was reduced in intensity in the region corresponding to resident vacuoles (Figure 8, top panel). In ΔRPL33A cells, cytoplasmic GFP fluorescence intensity was diminished, with discrete regions of enhanced GFP fluorescence that coincided with Nop1 and DAPI staining (Figure 8, middle panel). Rpl33, like many yeast ribosomal proteins, is encoded by duplicated genes that are nearly identical. Therefore, the cytoplasmic staining within these cells presumably results from the incorporation of Rpl33B into 60S subunits. The nucleolar localized GFP fluorescence observed in the ΔRPL33A strain likely represents the modest accumulation of immature 60S subunits as a consequence of delayed pre-rRNA processing at sites A_2 and A_3. The overall reduction in GFP-Rpl25 staining in the ΔRPL33A strain relative to wild-type indicates that these immature precursors are subject to enhanced decay. In contrast, ΔSDO1 strains showed a pronounced accumulation of fluorescence in regions that broadly encompass Nop1 and DAPI staining and likely represent the retention of more fully matured 60S subunits in the nucleoplasm (Figure 8, bottom panel). Given the relative reduction of 60S subunits in the ΔSDO1 strain observed from the subunit profiles in Figure 5, I believe a fraction of these more fully matured subunits accumulating in the absence of Sdo1 undergo degradation, albeit at a much slower rate than that observed for immature subunits in the ΔRPL33A strain.
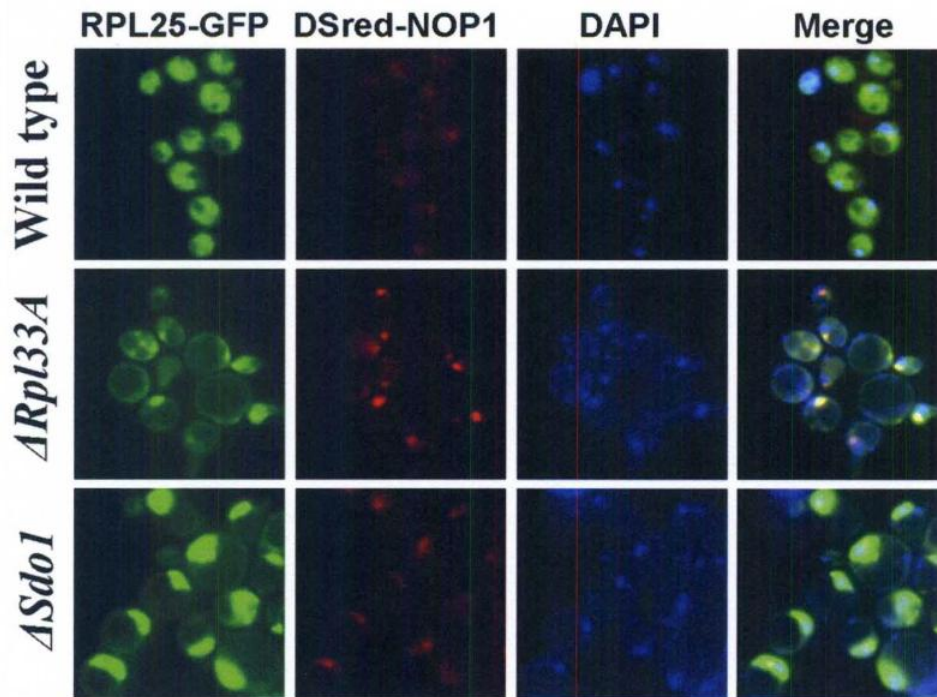
Figure 8. **Nuclear retention of pre-60S subunits in the yeast SDS model.** Live cell fluorescence images corresponding to wild-type (top row), Δ*RPL33A* (middle row), and Δ*SDO1* (bottom row) strains. Wild-type and mutant strains were transformed with Rpl25-GFP (a component of 60S ribosomal subunits) and Nop1-DSred (nucleolar protein). Left column, Rpl25-GFP fluorescence; middle left column, Nop1-RFP; middle right column, DAPI stain; right column, merge of all three images. Images depicted were chosen to be accurate representations of a collection of fluorescence studies performed in triplicate.

Collectively, these data indicate that the defect in 60S subunit maturation between the two disease models occurs at a later step in the $\Delta SDO1$ strain than in the $\Delta RPL33A$ strain, resulting in the accumulation of more fully matured precursors in the former relative to the latter.

Based on the emerging role for the 5S rRNA subcomplex in signaling abortive ribosome assembly to p53 activation in mammalian cells, I examined the fate of 5S rRNA in the yeast models of DBA and SDS. In wild-type cells, 5S rRNA is found in fractions corresponding to 60S subunits, 80S monosomes, and polysomes, with only a small fraction of extra-ribosomal 5S rRNA found near the top of the gradient (Figure 9). In $\Delta RPL33A$ extracts there is a dramatic increase in the amount of extra-ribosomal 5S rRNA found near the top of the gradient (~41% of the total 5S RNA relative to ~11% for wild-type extracts), while in other regions of the gradient the amount of 5S rRNA is reduced. This latter observation is consistent with the absorbance tracings of the gradient profiles which show an almost complete loss of free 60S subunits and a lower level of polysomes including half-mer polysomes, relative to wild-type (Figure 7). As for the $\Delta RPL33A$ strain, extracts from the $\Delta SDO1$ strain show a significant reduction in the amount of 5S rRNA in the polysome region of the gradient compared to wild-type. In contrast to extracts of the $\Delta RPL33A$ strain, $\Delta SDO1$ extracts show a substantial peak of 5S rRNA in the 60S region with this peak being comparable to that of the wild-type strain. The ratio of 5S to 5.8S rRNA in this peak is similar to that found in 80S and polysome regions indicating that this free pool of 60S subunits contains stoichiometric amounts of these two mature rRNA species.
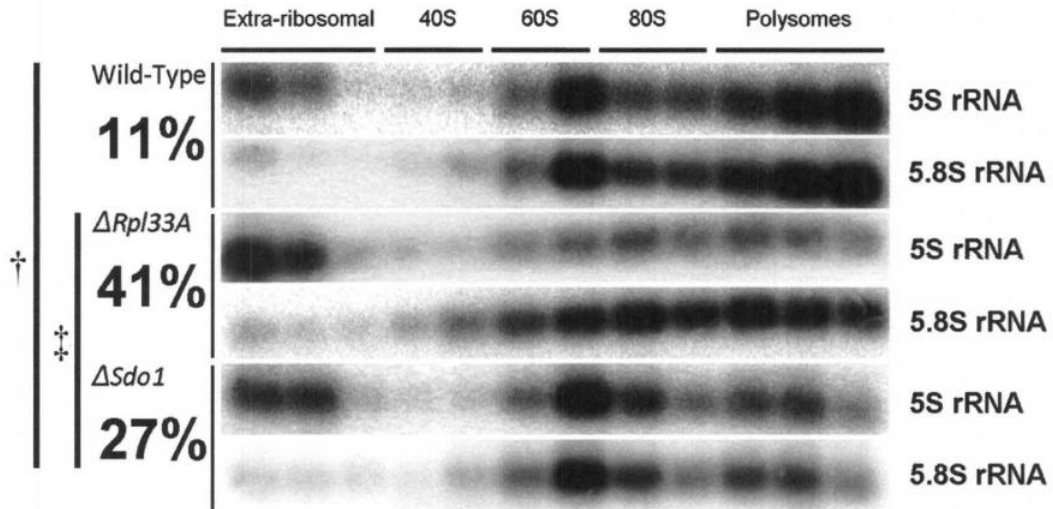
Figure 9. **The yeast DBA model has an increased amount of extra-ribosomal 5S rRNA.** Each row depicts a total of 12 precipitated RNA fractions spanning the 7-47% stepwise sucrose density gradients of resolved polysome extracts corresponding to wild-type (top rows), $\Delta RPL33A$ (middle two rows), and $\Delta SDO1$ (bottom two rows) yeast strains. RNA samples were immobilized to nylon membranes via UV crosslinking and incubated with radiolabeled oligonucleotide probes to either 5S or 5.8S rRNA (labels are shown to the right). The percentage of extra-ribosomal 5S rRNA for each yeast strain is depicted to the left of each northern blot and is expressed as a mean. Student's t test was used to test for statistical significance. The percentage of extra-ribosomal 5S rRNA is representative of the ratio of 5S rRNA at the top of the gradient divided by the total 5S rRNA within a gradient. [†]Wild-type versus mutant strains (p<0.004); [‡] $\Delta RPL33A$ versus $\Delta SDO1$ (p<0.01).

The increase in 5S rRNA in the 60S region in Δ*SDO1* extracts is associated with a small amount of extra-ribosomal 5S rRNA (~27% of total 5S RNA) found near the top of the gradient when compared with the Δ*RPL33A* strain. Thus, the two disease models differ dramatically in their effect on subunit assembly and stability including differences in the fate of 5S rRNA as a consequence of these distinct effects on 60S subunit maturation.

Discussion

The recent finding that DBA can be caused by mutations in genes encoding large subunit ribosomal proteins has a number of implications (Farrar, Nater et al. 2008; Gazda, Sheen et al. 2008). This observation now suggests that any of the approximately 60 genes encoding large subunit ribosomal proteins could be mutated in DBA patients with unknown genetic lesions. Furthermore, this observation continues to support the notion that DBA is caused by mutations in genes encoding structural components of the ribosome and that either subunit can be affected. For the purposes of this study, the finding that 60S subunit ribosomal proteins are affected in DBA allowed for a more direct comparison of the underlying molecular bases for DBA and SDS, as the target in SDS also appears to be the 60S ribosomal subunit (Ganapathi, Austin et al. 2007; Menne, Goyenechea et al. 2007).

The yeast models of DBA and SDS examined here are both associated with a selective reduction in the amount of 60S ribosomal subunits. This reduction is more severe in the Δ*RPL33A* extracts relative to Δ*SDO1* extracts when total subunit analysis is performed. In both cases, the reduced amount of 60S subunits is associated with the appearance of half-mer polysomes upon polysome analysis. Half-mer polysomes are

polysomes with stalled 48S initiation complexes generally linked to defects in 60S subunit synthesis (Rotenberg, Moritz et al. 1988). In this case, subunit joining is delayed in forming 80S initiation complexes leaving 48S initiation complexes stalled at the initiation codon. The reduction in 60S subunits in the $\Delta RPL33A$ strain occurs at the level of 27S A_2/A_3 pre-rRNA processing, which results in delayed production of 27S B pre-rRNA and reduced amounts of mature 5.8S and 25S rRNA. A related defect in the production of 60S ribosomal subunits has recently been demonstrated for a yeast strain harboring a missense mutation in $RPL33A$ (Martin-Marcos, Hinnebusch et al. 2007).

In the yeast model of SDS, half-mer polysomes are observed in cells that still have a substantial pool of free 60S ribosomal subunits. These results differ dramatically from those in a previous study of a $\Delta SDO1$ deletion strain in which half-mer polysomes were not observed despite an apparent reduction in the amount of 60S subunits (Menne, Goyenechea et al. 2007). These previous findings are difficult to explain since studies have shown that a reduction in 60S subunits gives rise to half-mer polysomes (Venema and Tollervey 1999). My data reveal that there is also a delay in pre-rRNA processing in the $\Delta SDO1$ strain, but that this delay occurs at the level of 27S B pre-rRNA, downstream of the effect observed in cells depleted of Rpl33A. This delay is also associated with the retention of a significant fraction of 60S subunits within the nuclei of $\Delta SDO1$ cells. Thus, the effect of the SDO1 mutation on the amount of 60S subunits available for translation in the cytoplasm represents a combined effect of both delayed pre-rRNA processing and nuclear retention. This interpretation is in general agreement with conclusions reached previously on the role of Sdo1 in recycling Tif6 from the cytoplasm

57

to the nucleus where it is involved in 60S subunit maturation, but differs significantly from the previous report in the supporting data (Menne, Goyenechea et al. 2007).

Comparing the two disease models, I have shown that they differ in their effect on the maturation of 60S subunits (Figure 10). Both 35S pre-rRNA and 5S rRNA are found in 90S pre-ribosomal particles assembled early in the ribosome maturation pathway (Zhang, Harnpicharnchai et al. 2007). The maturation defect in the DBA model occurs earlier in the pathway and is accompanied by the rapid degradation of incompletely assembled precursors. In contrast, the maturation defect in the SDS model is associated with delayed export, and accumulation of 60S-like particles in the nucleoplasm. Thus, the differences in the mechanism by which ribosome maturation is disrupted in these yeast models of DBA and SDS could form the basis for different types of nucleolar/nuclear stress signaling and be responsible for the distinct clinical presentations of the two diseases in humans.
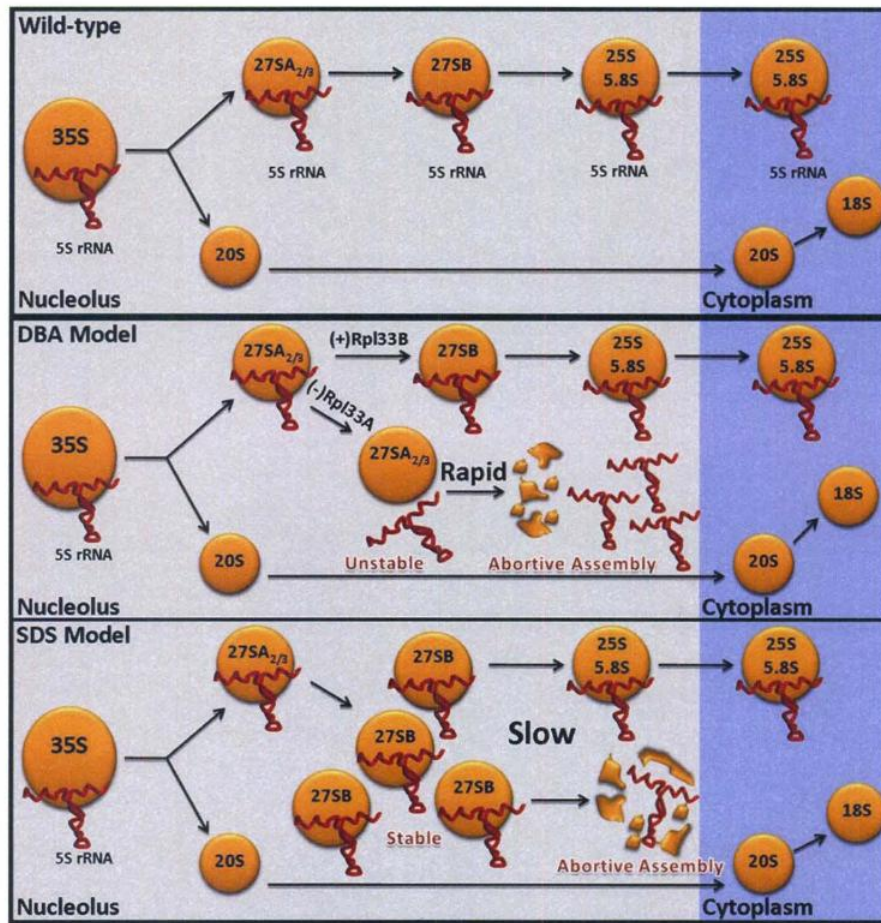
Figure 10. **Ribosomal subunit maturation in ∆*RPL33A* and ∆*SDO1* strains.**
Diagrammatic representations of ribosomal subunit maturation in wild-type (top panel),
∆*RPL33A* (middle panel), and ∆*SDO1* (bottom panel) yeast strains are shown and are
described in detail in the text. Orange circles represent either the 90S pre-ribosomal
particle or 40S or 60S ribosomal subunit precursors. Fractured circles represent
precursor degradation. Relevant steps in pre-rRNA processing are labeled. 5S rRNA is
labeled and is shown in red.

Accumulating data suggest that nucleolar stress signaling linked to abortive ribosome assembly plays an important role in the pathophysiology of DBA. Studies in zebra fish (Danilova, Sakamoto et al. 2008) and mouse (McGowan, Li et al. 2008) models of DBA suggest that p53 stabilization and activation promoted by nucleolar stress signaling is critical for phenotypes associated with ribosomal protein haploinsufficiency. While many potential mechanisms can explain p53 activation and stabilization under conditions of stress, recent studies have identified mechanisms more specific to nucleolar stress induced by abortive ribosome assembly (Lindstrom, Deisenroth et al. 2007; Sun, Dai et al. 2007). Three large subunit ribosomal proteins bind to MDM2 and promote p53 stabilization and activation. Two of these proteins, Rpl5 and Rpl11, bind synergistically with MDM2, most likely mediated through their interaction with 5S rRNA (Horn and Vousden 2008). Therefore, I was interested in following the fate of 5S rRNA in the yeast models of DBA and SDS to determine whether the maturation defects outlined above influenced 5S rRNA assembly.

Intriguingly, both disease models show an increase in extra-ribosomal 5S rRNA relative to wild-type. 5S rRNA is distinct from the other three mature rRNA species in that 5S rRNA is transcribed by RNA polymerase III, distinct from the 35S polycistronic precursor transcribed by RNA polymerase I, which gives rise to 25S, 18S, and 5.8S rRNA (Venema and Tollervey 1999). Moreover, 5S rRNA forms a subcomplex with Rpl5, Rpl11 and specific assembly factors within 60S subunit precursors (Zhang, Harnpicharnchai et al. 2007). Whether this subcomplex forms prior to joining 60S subunit precursors or after individual components of the subcomplex are incorporated into maturing subunits has not yet been determined (Zhang, Harnpicharnchai et al. 2007).

According to the data reported here, the extra-ribosomal pool of 5S rRNA in wild-type

cells accounts for only about 10% of the total 5S rRNA on sucrose gradients. This extra-

ribosomal pool increases to approximately 40% of total 5S rRNA in $\Delta RPL33A$ extracts

(Figure 9). This increase could be a reflection of the inability of assembly intermediates

lacking Rpl33A to stably incorporate components of the 5S rRNA subcomplex into 60S

subunit precursors. The extent to which components of the 5S subcomplex depend on

Rpl33A for incorporation into assembling 60S subunits is currently unknown (Nissan,

Bassler et al. 2002). The observation that depletion of Rpl33A blocks pre-rRNA

processing upstream of 27S B pre-rRNA, which accumulates in cells depleted of

components of the 5S subcomplex (Dechampesme, Koroleva et al. 1999; Zhang,

Harnpicharnchai et al. 2007), is consistent with Rpl33A acting earlier in the pathway than

components of the 5S subcomplex. It cannot, however, rule out the possibility that the

increased extra-ribosomal 5S rRNA observed in cells depleted of Rpl33A results from the

release of bound 5S subcomplex from abortive assembly intermediates targeted for

degradation.

In contrast to the data obtained with the $\Delta RPL33A$ strain, my data show that 5S

rRNA co-sediments with the large pool of free 60S subunits observed in $\Delta SDO1$ cells.

The localization data indicate that a considerable fraction of this pool of free 60S subunits

in $\Delta SDO1$ cells is retained within the nucleus. This pool of free 60S subunits likely

represents pre-60S subunit precursors containing either 27S B pre-rRNA or pre-60S

subunit precursors even further along the maturation pathway containing mature 25S and

5.8S rRNA (Harnpicharnchai, Jakovljevic et al. 2001). The ratio of 5S to 5.8S rRNA in

the free 60S subunit peak is similar to the ratio of 5S to 5.8S rRNA in functional 60S

subunits found in the polysome fractions, indicating that 5S rRNA has been incorporated into the nuclear-retained subunits in $\Delta SDO1$ cells. The decreased amount of total 60S subunits in these cells suggests that this pool of pre-60S subunits may be turned over at a higher rate than mature 60S subunits that reach the cytoplasm. It is an interesting possibility that the increased amounts of extra-ribosomal 5S rRNA in $\Delta SDO1$ strains may be a consequence of the release of the 5S subcomplex from pre-60S particles targeted for degradation.

Some caveats should be considered in regarding an integral role for components of the 5S rRNA subcomplex in signaling mechanisms that link abortive ribosome assembly to p53 stabilization and activation as a molecular basis for DBA. First, it is the general view that the assembly of 60S ribosomal subunits is largely independent of the assembly of 40S subunits, suggesting that haploinsufficiency for a small subunit ribosomal protein should not interfere with steps in 60S subunit assembly. However, recent results from mammalian systems reveal that disruption of 40S subunit maturation results in an up-regulation of translation of Rpl11 (Fumagalli, Di Cara et al. 2009). This up-regulation presumably results in Rpl11 being synthesized in excess of that needed for 60S subunit assembly which in turn, interacts with MDM2 leading to p53 activation. These studies did not however, address whether Rpl11 functions in concert with other components of the 5S rRNA subcomplex in this signaling pathway. A second caveat with regard to a critical role for Rpl5 and Rpl11 signaling in the pathophysiology of DBA is the finding that *RPL5* and *RPL11* are both mutated in DBA (Gazda, Sheen et al. 2008). Here it is difficult to envision how proteins that presumably limit ribosome assembly in an affected patient could also have an important role in signaling via an interaction with

MDM2. The observation that patients with mutations in *RPL5* have distinct clinical phenotypes suggests that alternative signaling pathways may operate in patients with mutations in *RPL5* and *RPL11* (Gazda, Sheen et al. 2008).

Despite the caveats, these yeast data support a potential role for the 5S ribonucleoprotein subcomplex in the pathogenesis of DBA. Moreover, the differences in the mechanisms by which 60S subunit maturation is affected in the DBA and SDS models and their influence on the 5S subcomplex suggest that this subcomplex may also be important in explaining how defects in the maturation of 60S ribosomal subunits can give rise to distinct clinical phenotypes.

CHAPTER III

THE SBDS FAMILY OF PROTEINS REGULATE 60S SUBUNIT MATURATION BY
MODULATING PROTEIN ACETYLATION

Introduction

Shwachman-Diamond syndrome (SDS) is a member of a group of rare congenital

bone marrow failure syndromes whose molecular basis has been connected to faulty

ribosome biosynthesis or function. Patients with this disorder manifest a wide collection

of clinical features, which notably include hematological abnormalities, pancreatic

dysfunction, growth retardation, and enhanced cancer susceptibility.   The typical

hematological profile of an SDS patient involves intermittent or persistent neutropenia,

though other cell lineages may be affected.   A paucity of neutrophils in the peripheral

blood together with exocrine pancreatic insufficiency and metaphyseal chondrodysplasia

are considered hallmark diagnostic features of SDS.   Patients may also present with

developmental delays and other congenital abnormalities.

In 2003, mutations of the *SBDS* locus were found to be present in most patients

with SDS (~89%) (Boocock, Morrison et al. 2003). Studies on *SDO1*, the yeast ortholog

of *SBDS*, support a role for the SBDS family of proteins in 60S subunit maturation. Sdo1

appears to perform this function by controlling the dissociation of the anti-association

factor Tif6 from nascent 60S subunits in the cytoplasm. Without Sdo1, Tif6 remains

associated with 60S subunits in the cytoplasm thereby preventing its recycling to the

nucleolus where it participates in late steps in subunit maturation (Menne, Goyenechea et al. 2007). Human studies have demonstrated physical interactions between SBDS and 60S subunits (Ganapathi, Austin et al. 2007) and further studies investigating an SDS murine model revealed that Sbds is necessary for 60S subunit biogenesis (Ball, Zhang et al. 2009). Together, these observations suggest a potential role for the SBDS family of proteins in large subunit maturation and/or function. My studies in yeast demonstrate that Sdo1 is required for the late stages of 60S subunit maturation (Moore IV, Farrar et al. 2009). I also show yeast strains depleted of Sdo1 possess half-mer polysomes as a consequence of a reduction in the number of functional 60S ribosomal subunits in the cytoplasm. In addition to its suggested role in subunit maturation, SBDS plays a role in chemotaxis (Stepanovic, Wessels et al. 2004; Wessels, Srikantha et al. 2006; Orelio and Kuijpers 2009), and also functions in mitotic spindle stabilization and the maintenance of genomic stability (Austin, Gupta et al. 2008). Thus, the SBDS family of proteins appears to possess multiple cellular functions. The molecular mechanisms by which they coordinate and/or function in these cellular processes are currently unknown.

In collaborative efforts with the laboratory of Paul de Figueiredo at Texas A&M University, we demonstrate a novel role for the SBDS family of proteins in the maintenance of protein acetylation by acting as endogenous inhibitors of cellular histone deacetylase (HDAC) activities. The de Figueiredo laboratory demonstrated that Sdo1 physically and genetically interacts with yeast class I (Rpd3) and class II (Hda1) histone deacetylases to antagonize their activity (submitted to *Cell*). In a collaboration with the de Figueiredo laboratory, we demonstrated that pharmacological and genetic inactivation of class I and class II HDAC enzymes ameliorates the ribosome biogenesis defect

associated with the depletion of Sdo1 in a yeast model of SDS. This amelioration is manifested by a restoration of growth, an increase in mean polysome size, and a partial resolution of half-mer polysomes. These observations suggest that Sdo1 might regulate 60S subunit maturation by modulating one or more protein acetylation events. Fluorescence localization studies revealed the relocalization of nucleolar retained GFP tagged 60S ribosomal subunits to the cytoplasm upon inhibition of HDAC activity in yeast strains depleted of Sdo1 (Paul de Figueiredo; unpublished results). In light of these observations, I hypothesized that the inhibition of HDAC activity by Sdo1 was necessary for the efficient export of 60S subunits to the cytoplasm through its ability to modulate the association of Tif6 with 60S ribosomal subunits. In support of this model, I show ribosome-enriched extracts contain a higher content of Tif6 in *SDO1* mutants relative to wild-type strains. Moreover, the enhanced association of Tif6 with 60S subunits can become partially reversed by the pharmacological or genetic inactivation of histone deacetylase activities. Overall, these studies establish a novel relationship between the function of the SBDS family of proteins, protein acetylation, and ribosome maturation. This work also has implications for SDS pathophysiology and predicts a new potential class of therapeutic agents for treating patients with SDS.

Design and Methods

Yeast strains

Most of the haploid strains employed in these studies are derivatives of BY4743

(MAT a/α his3Δ/his3Δ, leu2Δ/leu2Δ, lys2D/+, met15Δ/+, ura3Δ/ura3Δ) or W303 (MAT

a/α his3/his3, leu2/leu2, ura3/ura2, trp1/trp1, ade2/ade2, can1/can1) yeast genetic

backgrounds supplied by Dr.'s Jinbai Guo and James Huang. The strains and relevant

genotypes utilized in these studies are shown in table 1.

Trichostatin A drug treatments

A 3mM stock solution of TSA was prepared by reconstitution of lyophilized TSA

powder (InvivoGen, Inc., San Diego, CA, USA) in dimethylsulfoxide. The stock solution

was diluted (in growth media) to concentrations employed in individual experiments.

Polysome analysis and protein precipitation

Yeast strains were grown to mid-log phase in YPG, YPD, or YPD containing 0.5,

1.0, 2.0, or 5.0μM TSA. Cell extracts were prepared for polysome analysis as outlined

previously (Leger-Silvestre, Caffrey et al. 2005). Extracts were centrifuged at 28,000

RPM for 6 hours in an SW28.1 rotor (Beckman Instruments, Inc., Fullerton, CA, USA).

Following centrifugation, stepwise sucrose gradients (7-47%) were fractionated and the

absorbance at 254nm monitored using an ISCO model 185 gradient fractionator

interfaced to a UA-6 absorbance detector (Teledyne Isco, Inc., Lincoln, NE, USA).

Resultant polysome profiles were subjected to peak integration (corresponding to 60S,

80S, and polysome regions) to determine relative percent areas under the curve.

Table 1

<u>Yeast Strains Utilized</u>

Strain	Relevant Genotype
4D	MAT ? *HIS3MX6::GAL1-SDO1-GFP::kanMX6, erg6Δ::LEU2, pdr5::TRP1, snq2Δ, ura3Δ*
BY4741	MAT a *his3Δ, leu2Δ, met15Δ, ura3Δ*
JHY980	MAT ? *HIS3MX6::GAL1-SDO1, his3Δ, leu2Δ, ura3Δ*
SRYR35	MAT a *hda1::TRP1, rpd3::LEU2, ade2, his3*
JGY040	MAT a *kanMX6::GAL-SDO1, hda1::TRP1, rpd3::LEU2, his3, ura3, ade2*
ΔRPD3, ΔHDA1, ΔSDO1	MAT a *sdo1::kan, rpd3::LEU2, hda1::TRP1, his3, ura3, ade2*
W303 ΔSDO1	MAT ? *sdo1::kanMX4/SDO1, his3, ura3, ade2, leu2, trp1Δ2, can1*
BY ΔSDO1	MAT ? *sdo1::kanMX4/SDO1, his3Δ, leu2Δ, ura3Δ*

Protein was recovered from sucrose gradient fractions after precipitation with 1:100 volumes of 2% sodium deoxycholate (DOC) and 1:5 volumes of trichloroacetic acid (TCA). Eppendorf tubes containing precipitated protein fractions were placed on ice for 1 hour and centrifuged at 13,000 RPM (~16,000 x g) in a tabletop centrifuge at 4°C for 15 minutes. The resultant supernatant was carefully discarded (aspirated off) and 600 μL of -20°C acetone added to wash pelleted proteins. This washing step was repeated prior to allowing pelleted proteins to air-dry in an inverted position on paper towels. Protein precipitates were resuspended in NuPAGE® LDS sample dilution buffer (under reducing conditions) and resolved on NuPAGE® 4-12% Bis-Tris Gels (Invitrogen™, Carlsbad, CA, USA).

Preparation of yeast whole cell extracts

Yeast strains were grown in 100 mL of glucose rich media (YPD) to mid-log phase. Cells were centrifuged for 10 minutes at 5,000 RPM (~3,000 x g) and washed two times with cell lysis buffer (20 mM Tris-HCl [pH 7.6], 10 mM NaF, 10 mM sodium pyrophosphate, 0.5 mM EDTA, 0.1% deoxycholate). Cell pellets were resuspended in 100 μLs of cell lysis buffer and 0.30 grams of 425-600 micron glass beads were added. Cell suspensions were then vortexed at high speed, 8 times, 30 seconds each, with 30 second cool down periods between bursts. Following this cell lysis procedure, extracts were centrifuged at 5,000 x g at 4°C for 1 minute to remove unbroken cells. Lastly, using a gel-loading pipette tip, extracts are withdrawn from the top of glass bead slurries, placed in eppendorf tubes, and stored in -80°C for later use.

Differential centrifugation and ribosome enrichment

Ribosome enriched fractions were derived from polysome extracts isolated via a variation of a method outlined previously for polysome analysis (Leger-Silvestre, Caffrey et al. 2005). Yeast strains were inoculated into 100 ml of glucose rich media (YPD) and were allowed to grow to mid-log phase at 30°C. Cycloheximide (5 mg) was added to flasks containing cells and media, swirled, and poured into chilled nalgene® centrifuge bottles. Cells were collected by centrifugation at 5,000 RPM (~3,000 x g) for 10 minutes, supernatants decanted, and resultant pellets resuspended in 5 ml of polysome buffer (10 mM Tris-HCl [pH 7.5], 100 mM NaCl, 30 mM $MgCl_2$, 50 μg/ml cycloheximide, 100 μg/ml heparin, 0.2 μl/ml DEPC). Cell suspensions were transferred to 12 ml pop-top tubes, centrifuged again, and the washing step repeated with polysome buffer. Cell pellets were resuspended in 400 μl of polysome buffer and 0.30 grams of 425-600 micron glass beads were added. Cell suspensions were then mechanically lysed by vortexing at high speed, 8 times, 30 seconds each, with 30 second cool down periods between bursts. Following cell lysis, extracts were centrifuged at 5,000 x g at 4°C for 1 minute to remove unbroken cells and debris. Next, approximately 400 μl of cell extracts were withdrawn from glass bead slurries using gel-loading pipette tips, and placed in 11 x 34 mm Beckman thickwall polycarbonate tubes (Beckman Coulter, Inc., Brea, CA, USA). Differential centrifugation was carried out using a TLA-100.2 fixed-angle rotor (Beckman Coulter, Inc., Brea, CA, USA). First, samples were centrifuged at 17,000 RPM (10,000 x g) for 10 minutes to pellet cell walls, nuclei, and organelles. Resultant supernatants were then transferred to new Beckman polycarbonate tubes and centrifuged at 75,000 RPM (200,000 x g) for 30 minutes to isolate ribosome pellets. Following the

final high speed (75,000 RPM) centrifugation step, ribosome pellets were suspended (using polysome buffer) in volumes required to attain final concentrations of 5 mg/ml.

Western blot analysis

Protein extracts were resolved on NuPAGE® 4-12% Bis-Tris Gels (Invitrogen™, Carlsbad, CA, USA), using standard 1X MES SDS running buffer, and electrophoretically transferred to nitrocellulose membranes. Membranes were then blocked for 1 hour in blocking buffer (1X TBS, 0.1% Tween-20 with 5% w/v nonfat dry milk), rinsed with TBS-T (1X TBS, 0.1% Tween-20), and incubated overnight at 4°C with primary antibodies in primary antibody dilution buffer (1X TBS, 0.1% Tween-20 with 5% BSA). Primary antibodies employed include: rabbit polyclonal against acetylated-lysine (Cell Signaling Technology, Inc., Danvers, MA, USA), mouse monoclonal against beta Actin [mAbcam 8224] (Abcam, Inc., Cambridge, MA, USA), rabbit polyclonal against human EIF6 (Proteintech Group, Inc., Chicago, IL, USA), and mouse polyclonal against RPLP0 (Abnova Corporation, Taipei, Taiwan). The RPLP0 antibody cross-reacts with yeast Rpl4, which was used as a control. Following incubation with primary antibodies, membranes were washed three times, for 10 minutes each, with TBS-T and then incubated with the appropriate HRP-conjugated secondary antibodies in blocking buffer for 1 hour at room temperature. Secondary antibodies employed include: HRP-linked goat to rabbit IgG [#7074] (Cell Signaling Technology, Inc., Danvers, MA, USA) and HRP-linked rabbit to mouse IgG [mAbcam 6728] (Abcam, Inc., Cambridge, MA, USA). Again, following this incubation period, membranes were washed three times for 5 minutes each with TBS-T wash buffer. Proteins were detected

using the ECL Plus Western Blotting Detection System from GE Healthcare (GE Healthcare Biosciences, Piscataway, NJ, USA), as suggested by the manufacturers instructions.

Results

We have recently entered into collaboration with the laboratory of Dr. Paul de Figueiredo (Texas A&M University) who had performed a high throughput screen of more than 160,000 unique small molecules in an effort to identify potential compounds that ameliorate or suppress the growth defect associated with the depletion of Sdo1. The overall goal of this screen was to gain a better understanding of the molecular function of Sdo1 and to identify potential lead compounds for therapeutic development. A diversity of structural classes of compounds was identified in this screen including a number of histone deacetylase inhibitors. I chose one of these inhibitors, trichostatin A (TSA), for further study. The structure of TSA is shown in Figure 11, panel A. TSA is a commercially available antifungal antibiotic, which acts as a specific and potent inhibitor of class I and class II histone deacetylases (HDACs). HDACs function as parts of large multi-subunit complexes that have essential roles in various cellular processes (Yang and Seto 2003; Yang and Seto 2008). HDACs are categorized into four groups according to sequence homology, as well as function, and include the "classical" family, which is grouped into classes I, II, and, IV (Yang and Seto 2008), and the the sirtuin family of NAD^+-dependent deacetylases which constitute class III. Most class I HDACs are subunits of multimeric nuclear complexes that modulate chromatin structure and transcriptional activity, whereas class II HDACs regulate processes in the cytoplasm or

function to transmit signals between the cytoplasm and nucleus by shuttling between the two compartments (Yang and Seto 2008). Little is known about the class IV group, and based on its sequence similarities to other HDACs, is considered a unique class of its own (Yang and Seto 2008).

To test the efficacy of TSA in suppressing the slow growth phenotype associated with the loss of Sdo1, an inducible *SDO1* deletion strain (4D) was treated with increasing concentrations of this pharmacological HDAC inhibitor (Figure 11, Panel B). *SDO1* expression in this strain was under the control of a galactose-inducible/glucose-repressible *GAL1-10* promoter (*pGAL-SDO1*). In addition, this strain also contained deletions in three multi-drug resistance genes (*PDR5*, *SNQ2*, and *ERG6*) to aid in drug delivery and cellular retention. In panel B of Figure 11, cellular growth was severely impaired under conditions where *SDO1* expression was repressed (in the presence of glucose). TSA treatment resulted in a dose-dependent increase in growth rate of the Sdo1-depleted yeast strain with increasing concentrations of TSA up to 5 μM. TSA treated Sdo1-depleted yeast strains also exhibited a dose-dependent increase in polysome size and partial resolution of half-mer polysomes, as evidenced by polysome analysis in panel C of Figure 11.
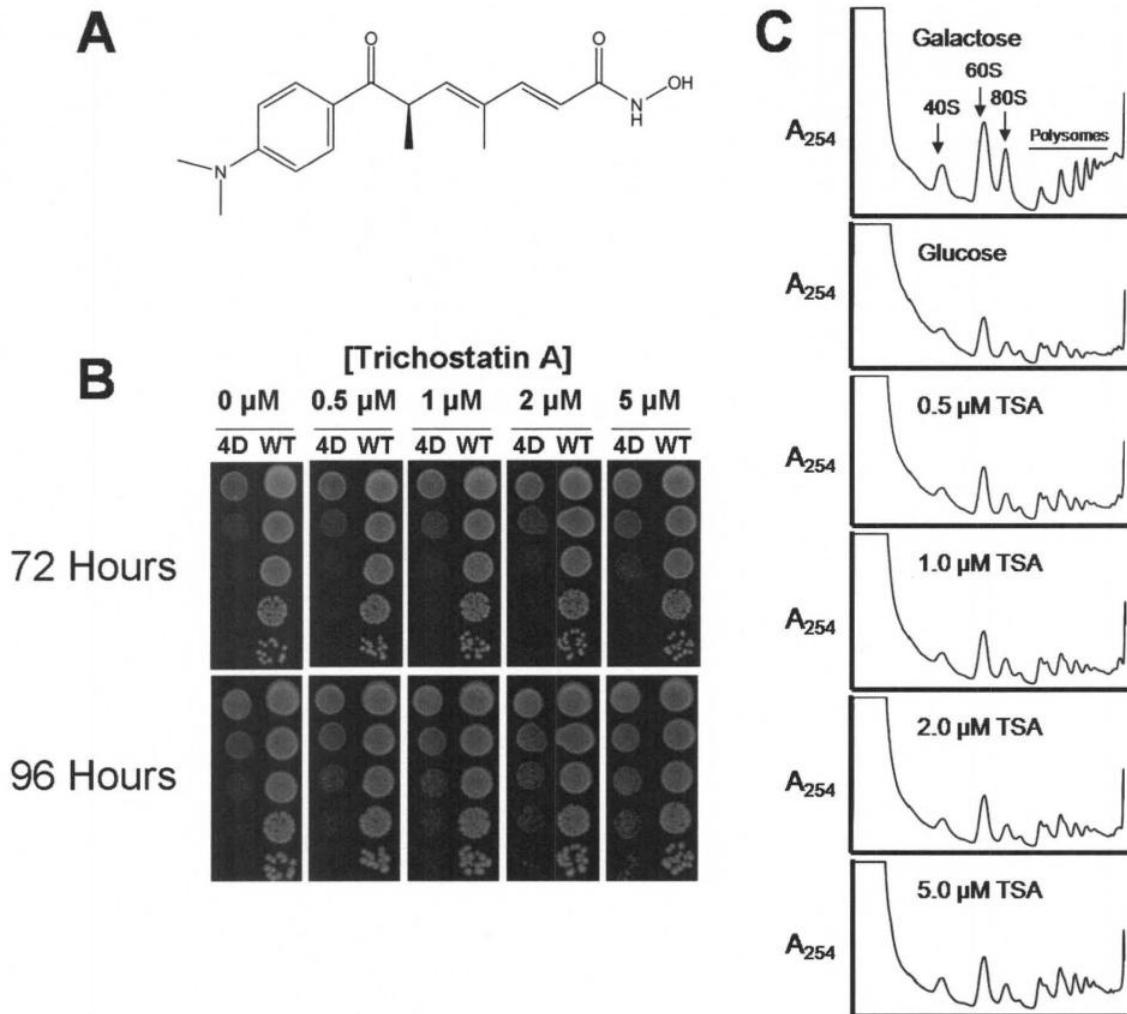
Figure 11. **TSA partially rescues the slow growth phenotype associated with the depletion of Sdo1.** (**A**) The structure of the pharmacological class I and class II HDAC inhibitor, trichostatin A. (**B**) 4D and wild-type (WT) yeast strains were pre-grown for 24 hours in glucose rich liquid media. Following this incubation period, five serial dilutions were prepared and spotted on solid YPD media, from top to bottom, with increasing dilution. From left to right the media contained increasing concentrations of TSA (0, 0.5, 1, 2, or 5 μM). Cells were grown at 30^0 C and imaged at 72 hrs (top) and 96 hrs (bottom). (**C**) Polysome analysis of strain 4D grown in galactose (Sdo1 expressed), glucose (Sdo1 depleted), or glucose rich media containing 0.5, 1.0, 2.0, or 5.0 μM TSA.

74

A semi-quantitative analysis of 5 μM TSA treated and untreated Sdo1-deficient polysome profiles was performed by determining the relative percent area of 60S, 80S, and polysome regions in absorbance tracings (Figure 12). The relative percent of areas for these specific regions (i.e. 60S, 80S, and polysome regions) are represented as the peak area divided by the total area (includes all three regions). Relative to untreated strains, the Sdo1-depleted yeast strains treated with 5 μM TSA revealed a net decrease in the percentage of free 60S subunits and 80S monomers, with a corresponding overall increase in polysomes (Figure 12, Panel B). My previous work has demonstrated that the loss of Sdo1 interferes with the nucleo-cytoplasmic transport of 60S ribosomal subunits, which results in nuclear retention of pre-60S particles, a severe reduction in the quantity of functional polysomes, and the appearance of half-mer polysomes (polysome peaks possessing shoulders) containing stalled 48S initiation complexes (Moore IV, Farrar et al. 2009). Because of this block in nuclear export, the polysomes profiles of Sdo1 mutant strains possess a large free 60S peak, composed primarily of 60S pre-ribosomes retained in the nucleus. In Figure 12, the size of this peak is reduced in TSA treated cells with a corresponding increase in total polysomes. These data suggest that TSA partially rescues the ribosome maturation defect associated with the loss of Sdo1 and enhances the availability of 60S subunits to participate in translation. Based on this evidence, I hypothesize that TSA treatment enhances 60S subunit transport from the nucleus to the cytoplasm and consequently makes more large ribosomal subunits accessible for translation in the Sdo1 depleted strain. Questions remained as to the mechanisms by which this HDAC inhibitor resolves the ribosome defect associated with the depletion of Sdo1.
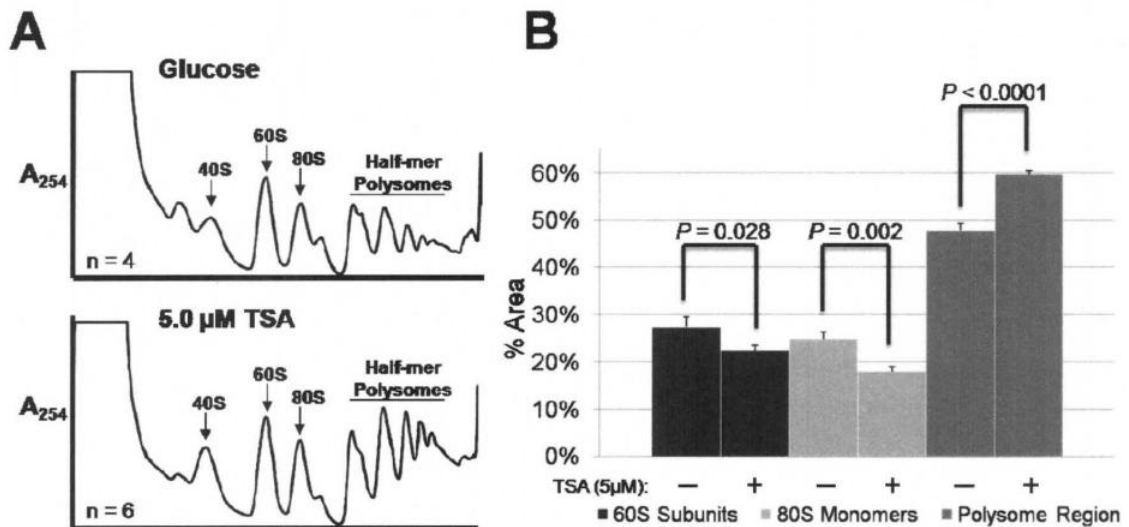
Figure 12. **Trichostatin A treatment partially corrects the ribosome maturation defect associated with the loss of Sdo1.** (A) Representative polysome profiles from strain 4D harvested from glucose containing media (SDO1 expression repressed) or glucose containing media with 5.0 μM TSA. The number of trials used for quantitative analysis is denoted with the letter n. (B) Quantification of 4D polysome absorbance tracings. Relative percent area (% area) of 60S, 80S monomers, or polysome regions were determined and averages shown. Columns representative of TSA treated samples are labeled with plus signs (+), and those untreated are labeled with minus signs (-). Error bars corresponding to the standard error of the mean (SEM) are shown. Statistical significance was assessed by Student's t test and *P*-values are displayed.

Since TSA is a known histone deacetylase inhibitor, it seemed reasonable to determine if genetically eliminating the enzyme target of TSA could also partially compensate for the absence of Sdo1. Yeast possess 13 annotated HDAC genes which include: *RPD3, HDA1, HDA2, HDA3, HOS1, HOS2, HOS3, HOS4, HST1, HST2, HST3, HST4*, and *SIR2*. Of these genes, *RPD3* and *HDA1* (*HDA1* activity requires *HDA2* and *HDA3*), the major yeast class I and class II HDACs, respectively, are inhibited by TSA (Bernstein, Tong et al. 2000). The class III NAD$^+$-dependent (*HST1, HST2, HST3, HST4*, and *SIR2*) deacetylases and *HOS3* (*HOS3* shows similarity to *RPD3* and *HDA1*) deacetylases are insensitive to TSA; little is known regarding *HOS1, HOS2*, and *HOS4* (Bernstein, Tong et al. 2000; Yang and Seto 2008). Using a serial dilution-plating assay, the Paul de Figueiredo laboratory at Texas A&M monitored the growth of Sdo1-deficient yeast strains that also harbored deletions in each of the 13 annotated yeast HDAC genes (unpublished results). Most strains did not show measurable improvement in growth, however, strains harboring deletions in either *RPD3* or *HDA1* showed a marked increase in growth. These data suggested that *SDO1* cooperates in a genetic pathway involving the class I and/or class II family of HDAC genes. A strain was therefore created that contained the *pGal-SDO1* construct as the only source of Sdo1 together with null alleles of *RPD3* and *HDA1*. The ability of the loss of these histone deacetylases to compensate for the reduced amounts of Sdo1 was assessed by growth on glucose (Figure 13, Panel C).
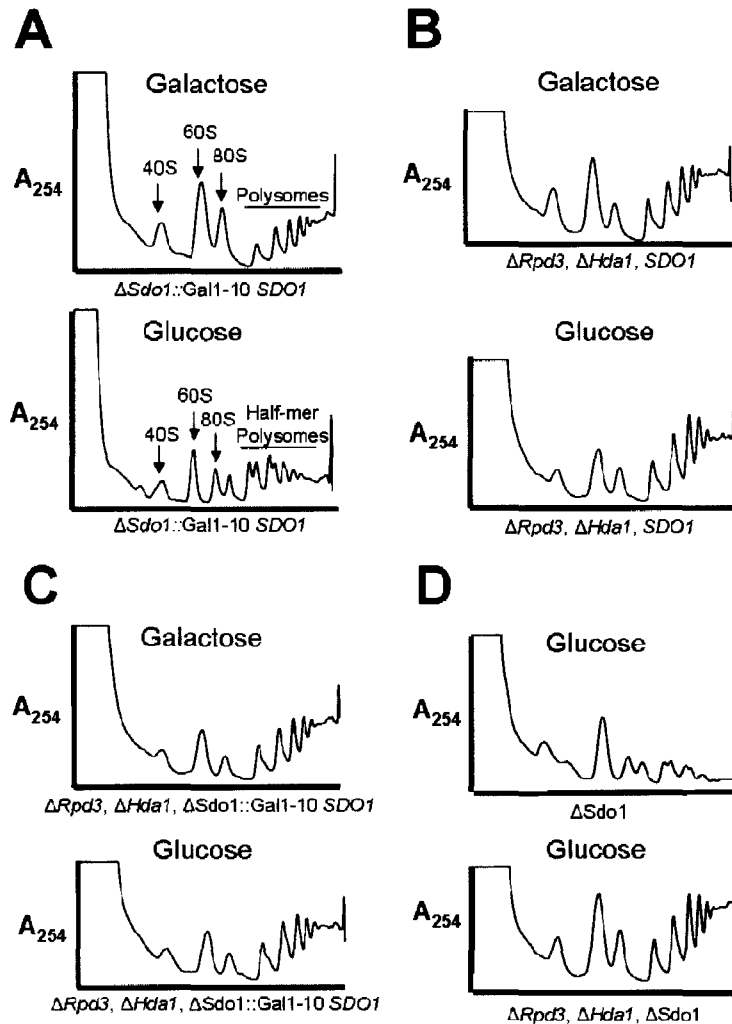
Figure 13. **Loss of major class I and class II HDAC enzymes rescues the ribosome maturation defect associated with the loss of Sdo1.** Polysome analysis of yeast strains: **(A)** Strain JHY980, conditional *pGal-SDO1* strain grown in galactose (top) or glucose (bottom). **(B)** Strain SRYR35, control strain containing wild-type *SDO1* and two null alleles for *RPD3* and *HDA1*, grown in galactose (top) or glucose (bottom). **(C)** Strain JGY040, conditional *pGal-SDO1* strain containing *RPD3* and *HDA1* null alleles, grown in galactose (top) or glucose (bottom). **(D)** Sdo1-deletion strain (W303 *ΔSDO1*) grown in glucose (top) and *RPD3*, *HDA1*, *SDO1* triple-deletion strain grown in glucose (bottom).

As previously demonstrated, under conditions where *SDO1* expression is repressed (Figure 13, Panel A, glucose), absorbance tracings show evidence of translational stress underscored by a dramatic decrease in polysomes and the appearance of half-mer polysomes relative to strains grown in galactose (Figure 13, Panel A, galactose). As predicted, the effects of Sdo1 depletion were largely rescued by the absence of *RPD3* and *HDA1*. Panel C of figure 13 (glucose) shows that polysome profiles from the strain lacking Rpd3 and Hda1 have a marked increase in translation with only a modest presence of half-mer polysomes that were virtually indistinguishable from the strain grown in galactose (Figure 13, Panel C, galactose). In a control strain, containing wild-type *SDO1*, deletion of *RPD3* and *HDA1* (both of which are not essential) in the presence of galactose or glucose did not produce any observable affects on the translational machinery of cells (Figure 13, Panel B).

The transcriptional activity of a gene is largely influenced by chromatin structure (Wolffe 1998). Further, covalent modification of histones via the acetylation of lysine residues can alter chromatin structure to activate gene transcription. Thus, suppression of the Sdo1-depleted phenotype in the conditional *pGal-SDO1* strain (grown in glucose) mediated by the deletion of two major cellular HDACs, *RPD3* and *HDA1*, may actually be the result of de-repression of the galactose-inducible promoter used to deplete cells of Sdo1. To address this concern, polysome analysis was performed on a triple-deletion strain where an *SDO1* null allele was combined with deletions in *RPD3* and *HDA1* (Figure 13, Panel D). Thus, we were asking whether the loss of Rpd3 and Hda1 could compensate for the complete loss of Sdo1. The polysome profile of the triple deletion strain, like that obtained with the conditional *pGal-SDO1* strain (Figure 13, Panel C,

glucose), revealed a mean increase in polysome size and a resolution of half-mer polysomes when compared with an Sdo1 deletion strain alone.

Taken as a whole, these experiments demonstrate the loss of major class I and class II HDAC enzymes, either by pharmacological inhibition (TSA-mediated) or by genetic inactivation, rescues the ribosome biogenesis defect associated with the loss of Sdo1. These observations suggest that Sdo1 may participate in 60S subunit maturation by modulating protein acetylation through its function as an endogenous histone deacetylase inhibitor. I hypothesize that in the absence of Sdo1, unregulated deacetylase activity disrupts normal nucleo-cytoplasmic 60S ribosomal subunit transport. Moreover, these data indicate that inhibition of histone deacetylase activity with a small molecule pharmacological agent can partially compensate for the loss of Sdo1 and overcome this defect.

I suspect that one or more proteins positioned in this export pathway require acetylation for efficient 60S subunit export from the nucleus to the cytoplasm. Whole cell immunoblots using antisera raised to acetylated-lysine revealed differences in acetylation between wild-type and *SDO1*-null cells (Figure 14, Panel A). Consistent with Sdo1's proposed role as an HDAC inhibitor, both the conditional Sdo1-depleted strains (4D) and the *SDO1*-deletion strains (BYΔSdo1) show a relative reduction in lysine acetylation of numerous low molecular weight proteins (~15-50 kDa range) compared to wild-type strains. Notably, this hypo-acetylated phenotype is more pronounced in the *SDO1*-deletion strains than that of the Sdo1-depleted strains (Figure 14, Panel A).
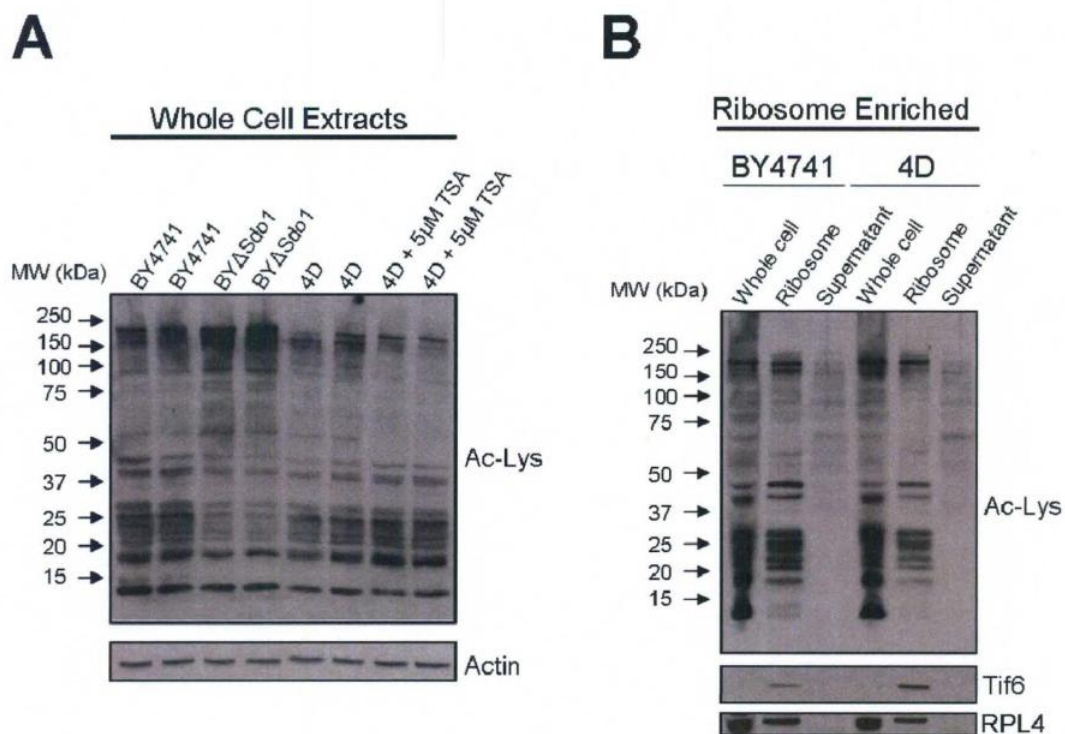
Figure 14. **The loss of Sdo1 is associated with alterations in protein acetylation.** Western blot analysis of **(A)** whole cell extracts derived from BY4741, BYΔSDO1, 4D, or 4D yeast strains treated with 5 μM TSA and **(B)** cellular fractions (whole cell, ribosome, and supernatant) obtained by differential centrifugation of BY4741 or 4D yeast strains. Whole cell extracts were centrifuged at 17,000 RPM (low-speed) and then at 75,000 RPM (high-speed) to pellet soluble/cytosolic ribosomes. Whole cell extracts, ribosome enriched fractions, and resultant high-speed supernatants were diluted in equal volumes of buffer and equivalent volumes resolved on 4-12% SDS-PAGE gels. Antibodies used include acetylated-lysine antibody (Ac-Lys; 1:1000 dilution), beta-actin antibody (Actin; 1:1000 dilution), Tif6 antibody (1:1500 dilution), and RPLP0 antibody (1:500 dilution). The RPLP0 antibody is a mouse polyclonal IgG raised against the human ribosomal protein RPLP0 and has confirmed cross-reactivity with the yeast large ribosomal subunit protein L4 (RPL4).

In addition, the conditional Sdo1-depleted strains (4D) prepared in glucose containing 5 μM TSA showed evidence that this HDAC inhibitor was capable of rescuing protein acetylation whereas several low molecular weight proteins (~15-50 kDa range) in treated strains possessed modest increases in lysine acetylation relative to untreated strains. Despite the apparent differences among wild-type and *SDO1*-null cells, the large number of proteins acetylated in whole cell extracts interfered with the ability to identify specific protein targets of Sdo1p-regulated acetylation/deacetylation.

To minimize the number of acetylated proteins detected and, more importantly, home in on translational machinery components whose acetylation is modulated by the presence or absence of Sdo1, I decided to enrich for ribosomal proteins and associated factors by isolating crude ribosome fractions via differential centrifugation of whole cell extracts (Figure 14, Panel B). These fractions were then immunoblotted with anti-acetylated lysine antibodies. In Figure 14, the ribosome-enriched fractions revealed evidence of differential acetylation among wild-type and Sdo1-depleted yeast strains. Unexpectedly, the ribosome-enriched fractions also revealed that a large number of ribosomal proteins are apparently subject to ε-amino-lysine side chain acetylation. This particular posttranslational modification (PTM) had not been reported for ribosomal proteins. Interestingly, while I was were bewildered by the relatively large number of ribosomal proteins that possess acetylation of their lysine residues, Choudhary and colleagues recently reported that a substantial number of mammalian ribosomal proteins are subject to lysine acetylation (Choudhary, Kumar et al. 2009). The biological significance of these modifications remains largely unknown. As with whole cell acetylated-lysine immunoblots, insufficient resolution of acetylated proteins limited the

ability to identify individual proteins differentially acetylated between wild-type and *SDO1*-null derived ribosome extracts (Figure 14, Panel B).

Further fractionation of acetylated proteins was performed by immunoblotting precipitated proteins isolated from polysome extracts, which were resolved on 7-47% sucrose gradients. In Figure 15, the acetylated-lysine immunoblots of fractionated polysomes revealed that proteins of both 40S and 60S ribosomal subunits were acetylated. Moreover, acetylation was observed in both free subunits and subunits actively engaged in translation. The relative amount of acetylation in fractions across the gradients of fractionated polysome profiles from wild-type, conditional Sdo1-depleted, and TSA treated Sdo1-depleted yeast strains showed a rough correspondence with the total protein in each fraction. This can be observed by comparing acetylated-lysine immunoblots with Coomassie stained gels below each blot in Figure 15 (bottom two panels). Because of the number of ribosomal proteins acetylated and the limited resolution of 1-dimensional gels, I was not able to identify specific ribosomal proteins or ribosome associated factors whose acetylation was specifically modulated by the presence or absence of Sdo1.
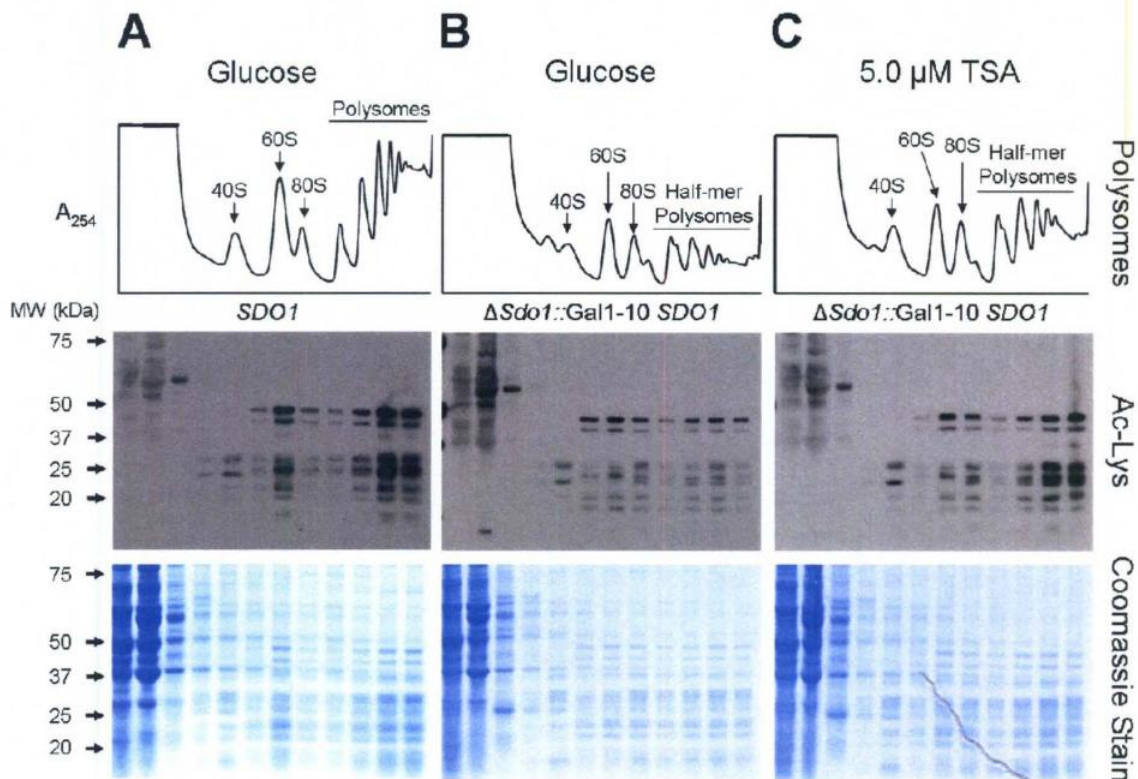
Figure 15. **Sucrose density fractionation reveals proteins of both the 40S and 60S ribosomal subunits are subject to lysine acetylation.** Yeast cell extracts from strains grown in glucose-containing media were subjected to polysome analysis (top panel). **(A)** BY4741 (Wild-type *SDO1*) strain, **(B)** 4D (*ΔSdo1::Gal1-10 SDO1*) strain, or **(C)** 4D (*ΔSdo1::Gal1-10 SDO1*) strain grown in the presence of 5 μM TSA. Proteins were precipitated and recovered from each of the corresponding fractions (12 in total) and resolved on 4-12% SDS-PAGE gels. Resultant gels were immunoblotted with anti-aceylated lysine antibody (Ac-Lys; 1:1000 dilution) (middle panel) or stained with Colloidal Coomassie Blue stain (bottom panel).

84

As I have previously demonstrated, cells lacking Sdo1 accumulate half-mer polysomes as a consequence of the failure to efficiently transport pre-60S subunits from the nucleus to the cytoplasm (Moore IV, Farrar et al. 2009). This transport defect is rescued by pharmacological or genetic inhibition of major class I and class II histone deacetylases. My efforts towards the identification of key proteins whose degree of acetylation is reduced in Sdo1 mutants and restored by TSA, have been hampered by the limited resolution of 1-dimensional gels. I therefore asked a more specific question pertaining to the role of acetylation in 60S subunit transport from the nucleus to the cytoplasm. Previous studies implicated the protein Tif6 in the mechanism of action of Sdo1 (Menne, Goyenechea et al. 2007). These studies suggested that Sdo1 is necessary for the release of Tif6 from 60S ribosomal subunits in the cytoplasm so it can be recycled to the nucleolus to participate in further rounds of 60S subunit export. In the absence of Sdo1, nuclear Tif6 becomes depleted and subsequently accumulates in the cytoplasm, presumably due to it's inability to be recycled from nascent 60S subunits (Menne, Goyenechea et al. 2007) (reviewed in Figure 16).
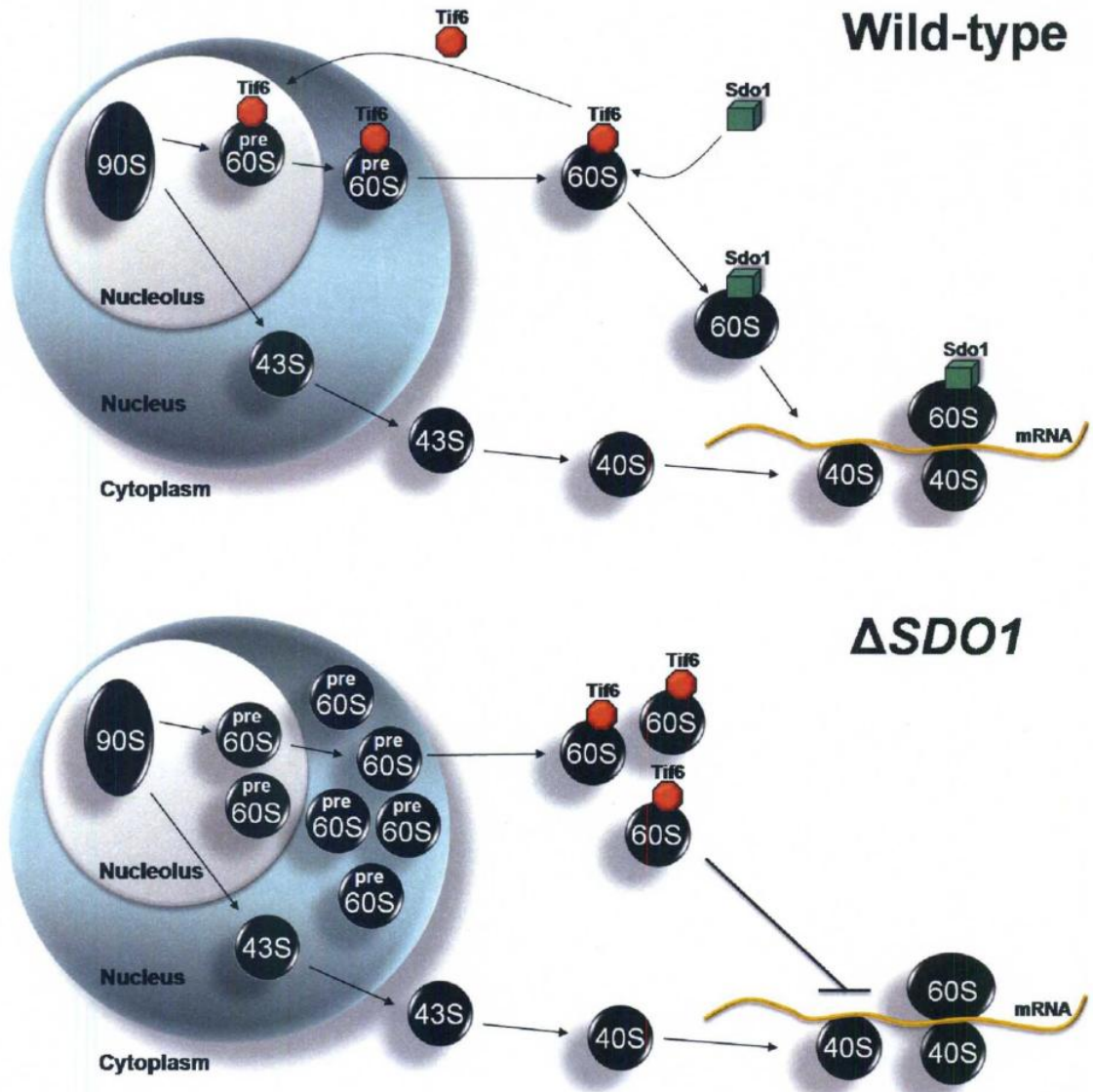
Figure 16. **Sdo1 and Tif6 cooperate in a pathway required for the maturation, nuclear export, and translational activation of 60S ribosomal subunits.** Wild-type (top panel) and Δ*SDO1* (bottom panel) are shown. Black circles represent various ribosomal particles. Tif6 (translation initiation factor 6) and Sdo1 (Shwachman-Diamond ortholog protein) are labeled and are represented by red octagons or green cubes, respectively. Messenger RNA (mRNA) is depicted by the yellow lines.

In Figure 14, I show an inverse relationship between ribosomal protein acetylation and the presence of Tif6 in ribosome fractions. Thus, there is a greater amount of Tif6 co-sedimenting with ribosomal subunits in the Sdo1-depleted yeast strain relative to wild-type cells. These observations also held true in yeast strains derived from both BY and W303 genetic backgrounds (Figure 17, panel B) and are consistent with a role for Sdo1 in modulating the release of Tif6 from 60S ribosomal subunits by acting as an inhibitor of histone deacetylase activity. I further investigated the role of lysine acetylation in mediating the interaction of Tif6 with 60S ribosomal subunits by addressing whether the increase in the amount of Tif6 associated with ribosome fractions from Sdo1-deficient strains could be reversed by the chemical or genetic inhibition of HDAC activity (Figure 17). To determine if the association of Tif6 with ribosome extracts is influenced by histone deacetylase activity, the amount of Tif6 co-sedimenting with ribosomal subunits in Sdo1-depleted yeast strains was assessed in both the presence and absence of 5.0 μM TSA. Sdo1-depleted strains grown in the presence of TSA showed a reduction in the amount of Tif6 co-sedimenting with the ribosome fractions relative to untreated yeast strains depleted of Sdo1 (Figure 17, panel C). To confirm that this result was a consequence of the inhibition of class I and class II HDAC enzyme activities, the amount of Tif6 present in ribosome fractions was assessed in strains harboring null alleles of *RPD3* and *HDA1*.
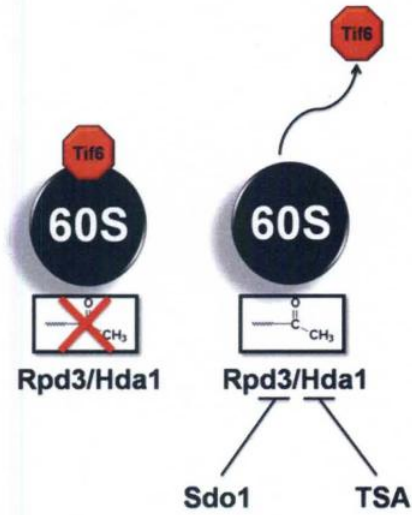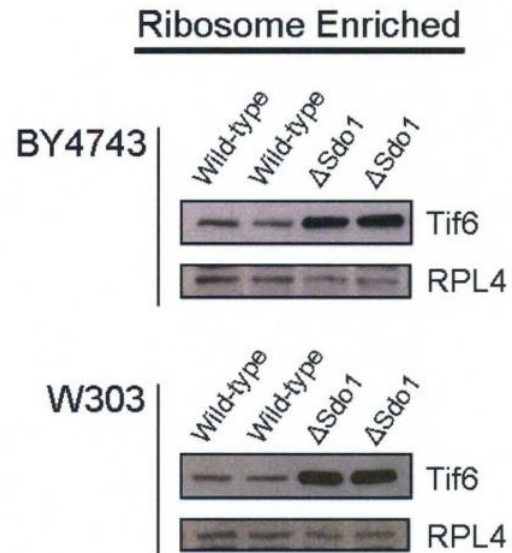
Figure 17. **The inhibition of yeast class I and class II HDACs reverse the enhanced association of Tif6 with ribosomal fractions in SDO1-depleted yeast strains.** (A) Schematic hypotheses for the role of lysine acetylation in modulating the interactions of Tif6 with 60S subunits. Left, in the absence of Sdo1, unregulated HDAC activities of Rpd3 and Hda1 result in the loss of protein acetylation and the enhanced association of Tif6 with 60S ribosomal subunits. Right, the inhibition of Rpd3/Hda1 HDACs via genetic inactivation or TSA exposure, results in protein hyperacetylation, which in turn favors the dissociation of Tif6 from 60S ribosomal subunits. (B) Immunoblot analyses of crude ribosome fractions derived from ΔSdo1 or isogenic wild-type yeast strains in either BY4743 (top) or W303 (bottom) genetic backgrounds and (C) 4D conditional Sdo1-depleted (ΔSdo1), 4D conditional Sdo1-depleted grown in 5 μM TSA (ΔSdo1 + 5μM TSA), or triple-deletion (ΔSdo1 ΔRpd3 ΔHda1) yeast strains. Cells were mechanically lysed with glass beads and ribosome fractions isolated using previously described differential centrifugation techniques. For each sample, 10μg of protein was loaded and resolved on 4-12% SDS-PAGE gels. Immunoblot analyses was performed using anti-Tif6 antibodies (1:1500 dilution) or antibodies raised to RPLP0 (1:500 dilution). As was previously noted, the RPLP0 antibody cross-reacts with the yeast large ribosomal subunit protein L4 (RPL4).

Panel C of Figure 17, shows a dramatic decrease in the amount of Tif6 in ribosome

fractions of cells lacking Rpd3 and Hda1. The release of Tif6 from ribosome fractions

was greater in strains missing Rpd3 and Hda1 relative to strains treated with TSA. The

amount of Tif6 present in the ribosome fractions correlated with the degree of

suppression of the Sdo1-mutant phenotypes by similar treatments (Figures 13 and 14).

These data suggest the HDAC-inhibitory activity of Sdo1 is important for mediating

interactions between Tif6 and 60S ribosomal subunits and that in the absence of Sdo1,

pharmacological inhibition of HDAC activities can ameliorate the subunit export defect

associated with its loss by aiding in the dissociation of Tif6 from 60S ribosomal subunits.

Discussion

Numerous studies show that the SBDS family of proteins function in the

maturation of 60S ribosomal subunits (Ganapathi, Austin et al. 2007; Menne,

Goyenechea et al. 2007; Ball, Zhang et al. 2009; Luz, Georg et al. 2009; Moore IV,

Farrar et al. 2009). In addition, *SBDS* has extra-ribosomal functions in cell motility and

in stabilizing the mitotic spindle (Stepanovic, Wessels et al. 2004; Wessels, Srikantha et

al. 2006; Austin, Gupta et al. 2008; Orelio and Kuijpers 2009). The multifunctional

character of the SBDS protein may explain the complex clinical phenotypes observed in

SDS patients. The molecular mechanisms by which *SBDS* functions in these diverse

processes is unknown. In the studies described above, I investigated a novel role for

Sdo1, the yeast ortholog of the human Shwachman-Diamond syndrome protein, in

modulating protein acetylation via its function as a histone deacetylase inhibitor. The

pleiotropic nature of this proposed function for Sdo1 and other members of the SBDS protein family provide an explanation for their involvement in diverse cellular processes.

A role for Sdo1 in regulating lysine acetylation was suggested by the observation that the severe growth defect associated with the loss of Sdo1 function in yeast was partially ameliorated by treatment with histone deacetylase inhibitors. I have since demonstrated that the HDAC inhibitor, TSA, rescues the slow growth phenotype in a yeast model of SDS. The impaired growth observed in cells depleted of Sdo1 is linked to a defect in the transport of pre-60S subunits from the nucleus to the cytoplasm. This results in a deficit of functional 60S ribosomal subunits in the cytoplasm and a global decrease in translation (Menne, Goyenechea et al. 2007; Moore IV, Farrar et al. 2009). The translational defect is evident by the accumulation of half-mer polysomes (polysome peaks appearing as doublets) and a marked decrease in polysome size (Moore IV, Farrar et al. 2009). The polysome profiles of Sdo1-depleted strains treated with increasing concentrations of TSA demonstrate a dose-dependent decrease in the quantity of half-mers and an increased amount of total polysomes (Figure 11). Closer inspection of polysome profiles revealed that, relative to controls, strains treated with TSA possess a statistically significant decrease in the pool of free 60S subunits and 80S monomers with a concomitant increase in polysome size. These data indicate that the amount of 60S subunits capable of functioning in translation is increased in *SDO1* mutants treated with TSA relative to untreated cells.

The effects of TSA on *SDO1*-null yeast strains had not been seen previously. In light of the fact that TSA is a known inhibitor of both class I and class II HDAC enzymes, these studies suggest that Sdo1 functions in a pathway that modulates the

activity of two major histone deacetylases within yeast cells. Given the evidence that

Sdo1 may function as a natural inhibitor of class I and II HDACs it seemed reasonable to

determine if genetically inactivating one or more of the genes encoding HDACs could

also rescue the Sdo1 phenotype. In this regard, of the 13 known yeast HDAC genes

investigated, the deletion of *RPD3* and *HDA1* was capable of rescuing the slow growth

phenotype associated with the loss of Sdo1 (unpublished data; de Figueiredo laboratory

of Texas A&M). This observation suggests that these two HDACs are the major targets

of Sdo1-mediated inhibition. Further, I demonstrated the double deletion of *RPD3* and

HDA1 also resolved the ribosome maturation defect associated with the depletion of

Sdo1. Interestingly, the rescue was greater with the genetic inactivation (Figure 13) than

with pharmacological inhibition (Figure 12), a result likely due to poor cellular uptake of

TSA. While these studies were ongoing, our collaborators in the de Figueiredo

laboratory demonstrated that Sdo1 physically interacts with both Rpd3 and Hda1 *in vivo*,

and inhibits their HDAC activity *in vitro*. Together, these data show that Sdo1 is an

inhibitor of HDAC activity and regulates 60S ribosomal subunit maturation via its action

on class I and class II HDAC enzymes.

I have shown both the pharmacological and genetic inhibition of HDAC activity

partially resolves the half-mer polysomes caused by a 60S subunit transport defect in

cells depleted of Sdo1. These observations suggested a role for lysine acetylation in the

maturation of 60S ribosomal subunits, specifically relating to the transport of 60S

subunits from the nucleus to the cytoplasm. Consistent with its role as a histone

deacetylase inhibitor, the loss of Sdo1 is associated with an overall loss of protein

acetylation, as expected in cells with unregulated histone deacetylase activity. The search

for potential acetylation targets revealed alterations in whole cell extracts between wild-type and Sdo1-depleted cells, but the large number of proteins subject to lysine acetylation precluded their identification using single dimension SDS-PAGE (Figure 14). In an attempt to enrich for acetylation targets involved in ribosome maturation, I analyzed crude ribosome fractions (Figure 14) and fractionated polysomes (Figure 15) for targets influenced by Sdo1. Here again the data revealed a surprisingly large number of yeast ribosomal proteins, of both the 40S and 60S ribosomal subunits, are subject to lysine acetylation. This finding was confirmed by a recent publication which demonstrated numerous ribosomal proteins and other components of the translational machinery components were subject to lysine acetylation in human cells (Choudhary, Kumar et al. 2009). The studies by Choudhary and colleagues also identified additional functional networks subject to lysine acetylation including networks involved in nuclear transport (Choudhary, Kumar et al. 2009).

Tif6, the yeast ortholog of mammalian eIF6, is a shuttling factor that plays a crucial role in ribosome maturation and nuclear export (Menne, Goyenechea et al. 2007). Tif6 and Sdo1 are thought to cooperate in 60S ribosomal subunit maturation, with Sdo1 functioning in the dissociation and concomitant recycling of Tif6 from nascent 60S ribosomal subunits in the cytoplasm back to the nucleus (Figure 16). In the nucleus, Tif6 plays a role in late steps in pre-rRNA maturation and 60S subunit export. In strains depleted of Sdo1, Tif6 relocates from the nucleus to the cytoplasm where it remains associated with 60S subunits (Menne, Goyenechea et al. 2007). In addition, the inability of Tif6 to cycle back to the nucleus also results in the nuclear accumulation of pre-60S subunits (Moore IV, Farrar et al. 2009). Mutations in *TIF6* have been shown to suppress

the slow growth phenotype and ribosome maturation defects in Sdo1-mutant strains by apparently lowering the affinity of Tif6 for 60S ribosomal subunits (Menne, Goyenechea et al. 2007). In Figure 17 (panel B), I observed an increased amount of Tif6 in enriched ribosome fractions obtained from *SDO1*-null strains relative to isogenic wild-type. Moreover, I have showed that the amount of Tif6 in the ribosome fraction was inversely proportional to the degree of lysine acetylation of ribosomal proteins (Figure 14). These observations suggest that Sdo1 may regulate the intracellular trafficking of Tif6 through an effect on the level of acetylation of ribosomal proteins and that it is through this mechanism that Sdo1 is involved in the export of 60S subunits from the nucleus.

A prediction of the foregoing discussion is that TSA will reverse the increased amount of Tif6 observed in the ribosome fraction of cells depleted of Sdo1. This prediction was confirmed as the amount of Tif6 cosedimenting with ribosome fractions was reduced in *SDO1*-null yeast strains by either treatment with TSA or double deletion of histone deacetylases (*RPD3* and *HDA1*), an observation suggesting that Tif6 may be actively recycling from nascent 60S subunits under these conditions. In this regard, our collaborators at Texas A&M University showed that treatment with TSA shifts the localization of RPL25-GFP from the nucleus to the cytoplasm in cells depleted of Sdo1 (unpublished data). Together, these data suggest that the HDAC inhibitory activity of Sdo1 modulates the interaction of Tif6 with pre-60S subunits. The proper modulation of these interactions is important, as the association of Tif6 with pre-60S subunits is necessary for late stages in their maturation and the release from 60S subunits is required for their translational activation in the cytoplasm (Basu, Si et al. 2001; Menne, Goyenechea et al. 2007). These studies raise a number of questions such as whether Tif6

is itself a target of Sdo1-regulated acetylation or if one or more other protein targets of Sdo1-regulated acetylation control the interaction of Tif6 with pre-60S subunits.

The finding that the Sdo1 protein functions as an inhibitor of HDAC activity, which is involved in ribosome maturation, represents a novel function for lysine acetylation of proteins. As their name implies, the primary targets of HDACs have long been thought to be histones. Acetylation of lysine residues is associated with a loss of positive charge and so is thought to weaken the binding of basic histone proteins with negatively charged DNA. In this regard, acetylation of lysine residues in histones results in reduced nucleosome structure and increased transcriptional activity. Thus, as a regulator of lysine acetylation, Sdo1 could have other potential functions within cells. Previous studies utilizing large-scale proteomic approaches to characterize multi-protein complexes in yeast have revealed potential interactions between Sdo1, chromatin structural components, and chromatin regulatory proteins. For instance, Sdo1 interacts with Hta2p, a histone H2A subtype, and has been shown to reside in a complex of proteins containing the histone deacetylase Rpd3 (Krogan, Cagney et al. 2006). Interestingly, Meskauskas and colleagues demonstrated the loss of Rpd3-associated histone deacetylase function in yeast to disrupt pre-rRNA processing (Meskauskas, Baxter et al. 2003). These data suggest that Sdo1 may influence ribosome biogenesis at multiple points in this complex pathway.

A multitude of biological mechanisms exists by which Sdo1 may influence ribosome biogenesis via its ability to modulate HDAC activities. HDACs have a tremendous influence on chromatin structure and thus could modify the transcriptional activity of genes encoding ribosomal RNAs and proteins. Both Rpd3 and Hda1 are

members of distinct HDAC complexes that function to regulate both chromatin silencing and transcriptional activation of a number of target genes (Thiagalingam, Cheng et al. 2003; Yang and Seto 2008). Interactions between Rpd3 and RP promoter elements have been reported (Kurdistani, Robyr et al. 2002; Robert, Pokholok et al. 2004) and, UBF, a major regulator of Pol I-mediated rRNA transcription, is regulated by acetylation (Pelletier, Stefanovsky et al. 2000).

A recent publication, which analyzed the human acetylome using high-resolution mass spectroscopy, revealed that over 1,500 proteins are subject to lysine acetylation (Choudhary, Kumar et al. 2009). Further, many of the proteins identified in this screen are constituents of functional networks including the ribosome, nuclear transport, actin cytoskeleton remodeling, cell cycle, and DNA damage repair. These observations offer a potential explanation for the complex clinical phenotypes of many SDS patients and highlight a potential molecular process whose disruption could explain the basis for many of the diverse cellular processes affected in SDS (i.e. ribosome maturation, chemotaxis, mitotic spindle stabilization, and p53 expression) (Dror 2002; Elghetany and Alter 2002; Austin, Gupta et al. 2008; Moore IV, Farrar et al. 2009; Orelio and Kuijpers 2009).

Our data suggests that Sdo1 modulates the activity of both Rpd3 (class I) and Hda1 (class II) HDACs. Of the yeast HDACs, Rpd3 and Hda1 have the highest degrees of sequence similarity with the mammalian class I histone deacetylase, HDAC1 and the mammalian class II histone deacetylase, HDAC6, respectively. HDAC6 is a major mammalian cytoplasmic HDAC whose activity targets the acetylation of numerous cytoskeletal elements, including both tubulin and cortactin (a protein involved in actin remodeling) (Zhang, Li et al. 2003; Gao, Hubbert et al. 2007; Tran, Marmo et al. 2007;

Zhang, Yuan et al. 2007). Alterations in the acetylation status of cortactin and tubulin as mediated by HDAC6 influences the dynamics of cell motility (Zhang, Yuan et al. 2007) and cellular adhesion (Tran, Marmo et al. 2007), respectively. The influence of tubulin acetylation on spindle stabilization and genomic stability has not been investigated. Another interesting target of lysine acetylation is the tumor suppressor p53, which is overexpressed in the bone marrow of SDS patients (Dror 2002). Mammalian HDACs 1, 2, and 3 decrease the transcriptional activity of p53 via deacetylation (Juan, Shia et al. 2000). These findings suggest that SBDS-mediated inhibition of histone deacetylase activity may also influence the regulation of p53 activity, which may be a contributing factor to the pathology observed in SDS.

The demonstration that the pharmacological inhibition of HDAC activity can partially compensate for the loss of Sdo1 in cell growth and ribosome biogenesis establishes a molecular foundation for the potential use of histone deacetylase inhibitors as a treatment for Shwachman-Diamond syndrome. Many HDAC inhibitors are currently in phase I-III clinical trials for use in the treatment of solid tumors and hematological malignancies (Munster, Marchion et al. 2009), and some have recently been licensed by the US FDA for the treatment of cutaneous T-cell lymphoma (i.e. Vorinostat and Romidepsin). Although their therapeutic modes of action are not well understood, many HDAC inhibitors inhibit proliferation of cancer cells by inducing cell cycle arrest, differentiation, and apoptosis (Marson 2009). Our work identified lysine acetylation as a process affected by the loss of members of the Sdo1/SBDS family of proteins. The pleiotropic effects of the disruption of this vital post-translational modification could

potentially explain how ribosome biogenesis, genome stability, and neutrophil chemotaxis could all be affected in SDS.

CHAPTER IV

CONCLUDING REMARKS

The current scientific consensus that ribosome synthesis is the principle molecular target in both Diamond-Blackfan anemia and Shwachman-Diamond syndrome provides a potential explanation for their common clinical features and raises questions concerning the foundation for their unique characteristics (Liu and Ellis 2006; Gregory, Aguissa-Toure et al. 2007; Menne, Goyenechea et al. 2007). In my work, I uncovered distinct molecular mechanisms by which yeast models of DBA and SDS influence 60S ribosomal subunit maturation. These observations point to potentially divergent signaling pathways that may form the basis for the distinct clinical features of these disorders. Further studies on the involvement of Sdo1 in 60S subunit maturation, from its perspective role as a regulator of protein acetylation in the SDS model, have established a molecular foundation for the potential use of histone deacetylase inhibitors as a therapeutic treatment for Shwachman-Diamond syndrome.

DBA is caused by mutations in genes encoding ribosomal proteins of both the 40S and 60S ribosomal subunits. To facilitate comparison with the yeast model of SDS, which is known to affect 60S subunit maturation, I created a yeast model of DBA that also affected maturation of 60S subunits. In both models, deficits of functional 60S subunits were observed. These deficits, however, were created by distinct mechanisms. Delays in pre-rRNA processing occurred at earlier stages in 60S ribosomal subunit

maturation in the DBA model compared to that of the SDS model. This delay, a consequence of abortive ribosome assembly, was associated with rapid degradation of assembly intermediates and the concomitant liberation and accumulation of substantial quantities of extra-ribosomal 5S rRNA. As previously noted, a potential mechanism by which abortive ribosome assembly (nucleolar stress) could signal to activate the p53 tumor suppressor involves the binding of certain ribosomal proteins with its negative regulator, MDM2. As 5S rRNA (in complex with Rpl5 and Rpl11) has been demonstrated to inhibit MDM2 and activate p53 in mammalian cells (Horn and Vousden 2008), these findings have implications for 5S rRNA-mediated stress signaling and p53 activation in DBA. *RPL33A*, used to create the yeast DBA model, is an ortholog of *RPL35A*, which was the first large subunit RP known to be affected in DBA (Farrar, Nater et al. 2008). My data indicate that haploinsufficiency for Rpl35A could disrupt large subunit assembly, liberating the 5S rRNA ternary complex making it available for interactions with MDM2 (Figure 18). Inhibition of MDM2, in turn, could lead to apoptosis and cell cycle arrest in a p53-dependent fashion. The ternary complex involved in signaling through MDM2 may arise from newly synthesized particles that fail to be properly assembled into newly maturing 60S ribosomal subunits in the absence of Rpl35A or from complexes released from partially assembled assembly intermediates destined for degradation.

A related signaling mechanism has also been proposed for DBA cases caused by defects in the assembly of small subunit proteins. Fumagalli and colleagues demonstrated the disruption of 40S subunit maturation leads to the translational up-

100
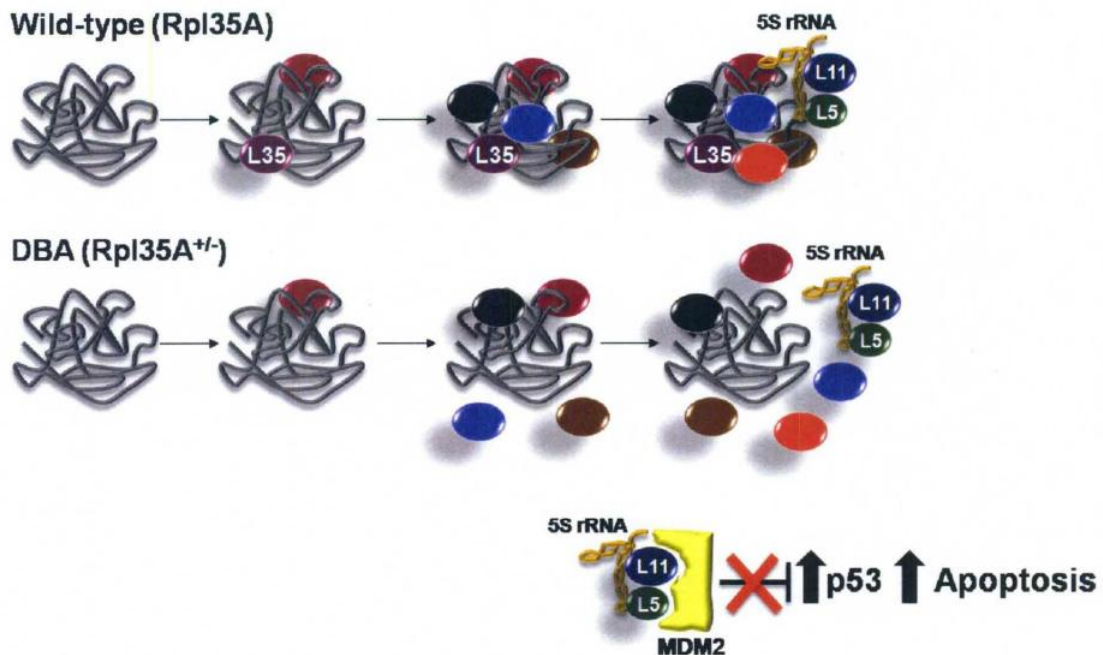
Figure 18. **A proposed mechanism for nucleolar stress signaling in cells haploinsufficient for Rpl35A.** *RPL35A* haploinsufficiency in DBA results in 60S ribosomal subunit abortive assembly, accumulation of extra-ribosomal 5S rRNA-Rpl5-Rpl11 ternary subcomplex, and successive signaling through the MDM2-p53 axis. Top, wild-type 60S subunit assembly with ribosomal subunit proteins shown as colored ovals and rRNA as grey-curvy lines. Ribosome assembly occurs in a hierarchical fashion with some RPs binding directly to rRNA, facilitating the assembly of additional proteins as rRNA folds into the functional active sites required for protein synthesis on the ribosome. Bottom, Rpl35A (L35) haploinsufficiency disrupts the assembly process, preventing productive interactions with later assembling ribosomal proteins. This results in the diversion of the 5S-L5-L11 ternary subcomplex from its normal assembly into 60S subunits to a potential interaction with MDM2 and subsequent p53 activation.

regulation of Rpl11, which is necessary for p53 activation (Fumagalli, Di Cara et al. 2009). Whether Rpl5 and 5S rRNA also participate in this signaling mechanism is unknown. In light of previous studies in mice and zebrafish models of DBA, which exhibited a p53-dependent disease phenotype (Danilova, Sakamoto et al. 2008; McGowan, Li et al. 2008), I believe the nucleolar stress pathway described here that links abortive ribosome assembly to p53 activation could be a major contributor to the pro-apoptotic phenotype of erythroid progenitors in DBA patients.

In contrast to the DBA model, the yeast SDS model affected a later step in 60S ribosomal subunit maturation resulting in the accumulation of relatively stable pre-60S particles containing associated 5S ribosomal RNA. These particles were largely retained in the nucleus. Consequently, the SDS model exhibited a reduced accrual of extra-ribosomal 5S rRNA compared to that of the DBA model, an observation which when extended to mammalian cells would suggest that nucleolar stress signaling via the interactions of the 5S rRNA subcomplex with MDM2 may have less significance in SDS disease pathophysiology.

The recent observation that histone deacetylase inhibitors partially rescue the severe growth defect of strains depleted of Sdo1 suggested a role for lysine acetylation in the pathophysiology of SDS (Guo, Knight et al. 2009). Here I demonstrated both the pharmacological and genetic inhibition of major class I (*RPD3*) and class II (*HDA1*) families of yeast HDAC enzymes partially resolve the ribosome maturation defect in cells depleted of Sdo1. These observations are not only the first to show a role for lysine acetylation in the maturation of 60S ribosomal subunits, but are also the first to reveal a novel role for Sdo1 as a modulator of cellular HDAC activities. In my analyses, the

inhibition of HDAC activity in the absence of Sdo1 increased the number of functional 60S ribosomal subunits reaching the cytoplasm. These findings were corroborated with fluorescence studies in *SDO1*-null yeast strains, which demonstrated a relocalization of RPL25-GFP from the nucleolus to the cytoplasm in the presence of TSA (unpublished data; Texas A&M University). Together, our work suggests that SBDS-mediated inhibition of cellular HDAC activities in human cells may also be necessary for efficient nuclear export of 60S ribosomal subunits (Figure 19).

The inverse relationship between ribosomal protein acetylation and Tif6 association with 60S subunits suggests that in the absence of Sdo1, the inability to release Tif6 from cytoplasmic 60S subunits interferes with Tif6 recycling and subsequent functions in subunit export from the nucleus. I showed that the enhanced association of Tif6 with 60S ribosomal subunits in Sdo1-deficient yeast strains is reduced by either pharmacological inhibition or genetic inactivation of Rpd3 and Hda1. The mammalian ortholog of Tif6, eIF6, is also required for 60S subunit biogenesis, and like its yeast counterpart also functions as an anti-association factor, preventing 40S and 60S subunits from non-productive interactions (Donadini, Giacopelli et al. 2006). This data suggests that eIF6 may also need Sbds-mediated inhibition of HDAC activity for efficient release of eIF6 from nascent 60S ribosomal subunits in the cytoplasm.

The demonstration that lysine acetylation targets numerous protein complexes and that this modification likely regulates many major cellular processes (Choudhary, Kumar et al. 2009) underscores the potential polyfunctional character of the SBDS family of proteins and places emphasis on a molecular process whose loss of function in SDS could be responsible for the complex clinical features of the disease. These functions include
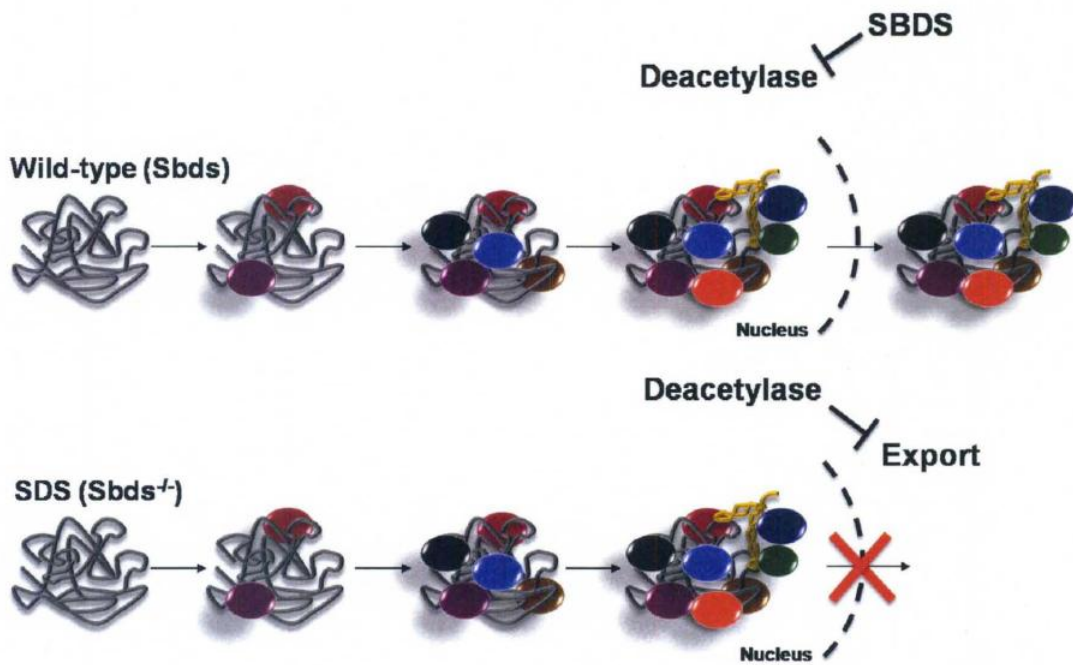
Figure 19. **A model showing a role for Sbds-mediated regulation of cellular histone deacetylase activity in the efficient export of pre-60S ribosomal subunits from the nucleus to the cytoplasm.** Top, wild-type 60S subunit maturation in the presence of wild-type SBDS. The late steps of 60S ribosomal subunit maturation require Sbds-mediated inhibition of deacetylase activity to facilitate transport from the nucleus to the cytoplasm. Bottom, the loss of Sbds is associated with unregulated deacetylase activity, which results in inefficient export of 60S ribosomal subunits to the cyctoplasm.

impaired neutrophil motility and chemotaxis, mitotic spindle destabilization and genomic instability, and as my data suggests, aberrations in ribosome maturation (Dror 2002; Elghetany and Alter 2002; Austin, Gupta et al. 2008; Moore IV, Farrar et al. 2009; Orelio and Kuijpers 2009).

The work presented here clearly illustrates different molecular mechanisms in 60S ribosomal subunit maturation between yeast models of DBA and SDS. The molecular differences presented in these models may actually form the basis for various types of nucleolar stress signaling and are likely a contributing factor to the unique clinical features of these two human disorders. Beyond its ability to influence the intracellular trafficking of Tif6 and ribosome maturation, the ability of Sdo1 to modulate protein acetylation through the inhibition of histone deacetylase activity implicates the involvement of the SBDS family of proteins in other diverse cellular processes. Finally, these studies strongly suggest that HDAC inhibitors may be of therapeutic benefit to patients suffering from Shwachman-Diamond syndrome.

REFERENCES

Aggett, P. J., N. P. Cavanagh, et al. (1980). "Shwachman's syndrome. A review of 21 cases." Arch Dis Child **55**(5): 331-347.

Aggett, P. J., J. T. Harries, et al. (1979). "An inherited defect of neutrophil mobility in Shwachman syndrome." J Pediatr **94**(3): 391-394.

Alter, B. P. (2007). "Diagnosis, genetics, and management of inherited bone marrow failure syndromes." Hematology Am Soc Hematol Educ Program: 29-39.

Angelini, M., S. Cannata, et al. (2007). "Missense mutations associated with Diamond-Blackfan anemia affect the assembly of ribosomal protein S19 into the ribosome." Hum Mol Genet **16**(14): 1720-1727.

Ashcroft, M., Y. Taya, et al. (2000). "Stress signals utilize multiple pathways to stabilize p53." Mol Cell Biol **20**(9): 3224-3233.

Austin, K. M., M. L. Gupta, et al. (2008). "Mitotic spindle destabilization and genomic instability in Shwachman-Diamond syndrome." J Clin Invest **118**(4): 1511-1518.

Austin, K. M., R. J. Leary, et al. (2005). "The Shwachman-Diamond SBDS protein localizes to the nucleolus." Blood **106**(4): 1253-1258.

Ball, H. L., B. Zhang, et al. (2009). "Shwachman-Bodian Diamond syndrome is a multi-functional protein implicated in cellular stress responses." Hum Mol Genet **18**(19): 3684-3695.

Ban, N., P. Nissen, et al. (2000). "The complete atomic structure of the large ribosomal subunit at 2.4 A resolution." Science **289**(5481): 905-920.

Basu, U., K. Si, et al. (2001). "The Saccharomyces cerevisiae TIF6 gene encoding translation initiation factor 6 is required for 60S ribosomal subunit biogenesis." Mol Cell Biol **21**(5): 1453-1462.

Becam, A. M., F. Nasr, et al. (2001). "Ria1p (Ynl163c), a protein similar to elongation factors 2, is involved in the biogenesis of the 60S subunit of the ribosome in Saccharomyces cerevisiae." Mol Genet Genomics **266**(3): 454-462.

Beckmann, H., J. L. Chen, et al. (1995). "Coactivator and promoter-selective properties of RNA polymerase I TAFs." Science **270**(5241): 1506-1509.

Bernstein, B. E., J. K. Tong, et al. (2000). "Genomewide studies of histone deacetylase function in yeast." Proc Natl Acad Sci U S A **97**(25): 13708-13713.

Boocock, G. R., M. R. Marit, et al. (2006). "Phylogeny, sequence conservation, and functional complementation of the SBDS protein family." Genomics **87**(6): 758-771.

Boocock, G. R., J. A. Morrison, et al. (2003). "Mutations in SBDS are associated with Shwachman-Diamond syndrome." Nat Genet **33**(1): 97-101.

Boyd, S. D., K. Y. Tsai, et al. (2000). "An intact HDM2 RING-finger domain is required for nuclear exclusion of p53." Nat Cell Biol **2**(9): 563-568.

Brady, S. N., Y. Yu, et al. (2004). "ARF impedes NPM/B23 shuttling in an Mdm2-sensitive tumor suppressor pathway." Mol Cell Biol **24**(21): 9327-9338.

Brandenburger, Y., A. Jenkins, et al. (2001). "Increased expression of UBF is a critical determinant for rRNA synthesis and hypertrophic growth of cardiac myocytes." FASEB J **15**(11): 2051-2053.

Budde, A. and I. Grummt (1999). "p53 represses ribosomal gene transcription." Oncogene **18**(4): 1119-1124.

Burroughs, L., A. Woolfrey, et al. (2009). "Shwachman-Diamond syndrome: a review of the clinical presentation, molecular pathogenesis, diagnosis, and treatment." Hematol Oncol Clin North Am **23**(2): 233-248.

Campagnoli, M. F., U. Ramenghi, et al. (2008). "RPS19 mutations in patients with Diamond-Blackfan anemia." Hum Mutat **29**(7): 911-920.

Cavanaugh, A. H., W. M. Hempel, et al. (1995). "Activity of RNA polymerase I transcription factor UBF blocked by Rb gene product." Nature **374**(6518): 177-180.

Ceci, M., C. Gaviraghi, et al. (2003). "Release of eIF6 (p27BBP) from the 60S subunit allows 80S ribosome assembly." Nature **426**(6966): 579-584.

Chen, D., Z. Zhang, et al. (2007). "Ribosomal protein S7 as a novel modulator of p53-MDM2 interaction: binding to MDM2, stabilization of p53 protein, and activation of p53 function." Oncogene **26**(35): 5029-5037.

Chen, J., V. Marechal, et al. (1993). "Mapping of the p53 and mdm-2 interaction domains." Mol Cell Biol **13**(7): 4107-4114.

Choesmel, V., D. Bacqueville, et al. (2007). "Impaired ribosome biogenesis in Diamond-Blackfan anemia." Blood 109(3): 1275-1283.

Choudhary, C., C. Kumar, et al. (2009). "Lysine acetylation targets protein complexes and co-regulates major cellular functions." Science 325(5942): 834-840.

Ciarmatori, S., P. H. Scott, et al. (2001). "Overlapping functions of the pRb family in the regulation of rRNA synthesis." Mol Cell Biol 21(17): 5806-5814.

Cmejla, R., J. Cmejlova, et al. (2007). "Ribosomal protein S17 gene (RPS17) is mutated in Diamond-Blackfan anemia." Hum Mutat 28(12): 1178-1182.

Coccia, P., A. Ruggiero, et al. (2007). "Shwachman Diamond Syndrome: an emergency challenge." Signa Vitae 2(2): 10-13.

Cretien, A., C. Hurtaud, et al. (2008). "Study of the effects of proteasome inhibitors on ribosomal protein S19 (RPS19) mutants, identified in patients with Diamond-Blackfan anemia." Haematologica 93(11): 1627-1634.

Culver, G. M. (2003). "Assembly of the 30S ribosomal subunit." Biopolymers 68(2): 234-249.

Dai, M. S. and H. Lu (2004). "Inhibition of MDM2-mediated p53 ubiquitination and degradation by ribosomal protein L5." J Biol Chem 279(43): 44475-44482.

Dai, M. S., S. X. Zeng, et al. (2004). "Ribosomal protein L23 activates p53 by inhibiting MDM2 function in response to ribosomal perturbation but not to translation inhibition." Mol Cell Biol 24(17): 7654-7668.

Danilova, N., K. M. Sakamoto, et al. (2008). "Ribosomal protein S19 deficiency in zebrafish leads to developmental abnormalities and defective erythropoiesis through activation of p53 protein family." Blood 112(13): 5228-5237.

de Angelis, M. H., H. Flaswinkel, et al. (2000). "Genome-wide, large-scale production of mutant mice by ENU mutagenesis." Nature Genetics 25(4): 444-447.

Decatur, W. A. and M. J. Fournier (2002). "rRNA modifications and ribosome function." Trends Biochem Sci 27(7): 344-351.

Dechampesme, A. M., O. Koroleva, et al. (1999). "Assembly of 5S ribosomal RNA is required at a specific step of the pre-rRNA processing pathway." J Cell Biol 145(7): 1369-1380.

Diamond, L. K., D. M. Allen, et al. (1961). "Congenital (erythroid) hypoplastic anemia. A 25-year study." Am J Dis Child 102: 403-415.

Diamond, L. K., W. C. Wang, et al. (1976). "Congenital hypoplastic anemia." <u>Adv Pediatr</u> **22**: 349-378.

Dianzani, I. and F. Loreni (2008). "Diamond-Blackfan anemia: a ribosomal puzzle." <u>Haematologica</u> **93**(11): 1601-1604.

Dinman, J. D. (2009). "The eukaryotic ribosome: current status and challenges." <u>J Biol Chem</u> **284**(18): 11761-11765.

Doherty, L., M. R. Sheen, et al. (2010). "Ribosomal Protein Genes RPS10 and RPS26 Are Commonly Mutated in Diamond-Blackfan Anemia." <u>Am J Hum Genet</u> **86**(2): 222-228.

Dokal, I., S. Rule, et al. (1997). "Adult onset of acute myeloid leukaemia (M6) in patients with Shwachman-Diamond syndrome." <u>Br J Haematol</u> **99**(1): 171-173.

Dokal, I. and T. Vulliamy (2008). "Inherited aplastic anaemias/bone marrow failure syndromes." <u>Blood Rev</u> **22**(3): 141-153.

Donadini, A., F. Giacopelli, et al. (2006). "GABP complex regulates transcription of eIF6 (p27BBP), an essential trans-acting factor in ribosome biogenesis." <u>FEBS Lett</u> **580**(8): 1983-1987.

Draptchinskaia, N., P. Gustavsson, et al. (1999). "The gene encoding ribosomal protein S19 is mutated in Diamond-Blackfan anaemia." <u>Nat Genet</u> **21**(2): 169-175.

Dror, Y. (2002). "P53 protein overexpression in Shwachman-Diamond syndrome." <u>Arch Pathol Lab Med</u> **126**(10): 1157-1158; author reply 1158.

Dror, Y. and M. H. Freedman (1999). "Shwachman-Diamond syndrome: An inherited preleukemic bone marrow failure disorder with aberrant hematopoietic progenitors and faulty marrow microenvironment." <u>Blood</u> **94**(9): 3048-3054.

Dror, Y. and M. H. Freedman (2001). "Shwachman-Diamond syndrome marrow cells show abnormally increased apoptosis mediated through the Fas pathway." <u>Blood</u> **97**(10): 3011-3016.

Dror, Y., H. Ginzberg, et al. (2001). "Immune function in patients with Shwachman-Diamond syndrome." <u>Br J Haematol</u> **114**(3): 712-717.

Elghetany, M. T. and B. P. Alter (2002). "p53 protein overexpression in bone marrow biopsies of patients with Shwachman-Diamond syndrome has a prevalence similar to that of patients with refractory anemia." <u>Arch Pathol Lab Med</u> **126**(4): 452-455.

Farrar, J. E., M. Nater, et al. (2008). "Abnormalities of the large ribosomal subunit protein, Rpl35a, in Diamond-Blackfan anemia." Blood **112**(5): 1582-1592.

Fatica, A. and D. Tollervey (2002). "Making ribosomes." Curr Opin Cell Biol **14**(3): 313-318.

Flygare, J., A. Aspesi, et al. (2007). "Human RPS19, the gene mutated in Diamond-Blackfan anemia, encodes a ribosomal protein required for the maturation of 40S ribosomal subunits." Blood **109**(3): 980-986.

Flygare, J., T. Kiefer, et al. (2005). "Deficiency of ribosomal protein S19 in CD34+ cells generated by siRNA blocks erythroid development and mimics defects seen in Diamond-Blackfan anemia." Blood **105**(12): 4627-4634.

Freedman, M. H. (2000). "Diamond-Blackfan anaemia." Baillieres Best Pract Res Clin Haematol **13**(3): 391-406.

Freedman, M. H., D. Amato, et al. (1976). "Erythroid colony growth in congenital hypoplastic anemia." J Clin Invest **57**(3): 673-677.

Fromont-Racine, M., B. Senger, et al. (2003). "Ribosome assembly in eukaryotes." Gene **313**: 17-42.

Fumagalli, S., A. Di Cara, et al. (2009). "Absence of nucleolar disruption after impairment of 40S ribosome biogenesis reveals an rpL11-translation-dependent mechanism of p53 induction." Nat Cell Biol **11**(4): 501-508.

Gadal, O., D. Strauss, et al. (2001). "Nuclear export of 60s ribosomal subunits depends on Xpo1p and requires a nuclear export sequence-containing factor, Nmd3p, that associates with the large subunit protein Rpl10p." Mol Cell Biol **21**(10): 3405-3415.

Ganapathi, K. A., K. M. Austin, et al. (2007). "The human Shwachman-Diamond syndrome protein, SBDS, associates with ribosomal RNA." Blood **110**(5): 1458-1465.

Ganapathi, K. A. and A. Shimamura (2008). "Ribosomal dysfunction and inherited marrow failure." Br J Haematol **141**(3): 376-387.

Gao, Y. S., C. C. Hubbert, et al. (2007). "Histone deacetylase 6 regulates growth factor-induced actin remodeling and endocytosis." Mol Cell Biol **27**(24): 8637-8647.

Garcia-Cuellar, M. P., R. Esteban, et al. (1997). "RNA-dependent RNA polymerase activity associated with the yeast viral p91/20S RNA ribonucleoprotein complex." RNA **3**(1): 27-36.

110

Gazda, H. T., A. Grabowska, et al. (2006). "Ribosomal protein S24 gene is mutated in Diamond-Blackfan anemia." <u>Am J Hum Genet</u> **79**(6): 1110-1118.

Gazda, H. T., M. R. Sheen, et al. (2008). "Ribosomal protein L5 and L11 mutations are associated with cleft palate and abnormal thumbs in Diamond-Blackfan anemia patients." <u>Am J Hum Genet</u> **83**(6): 769-780.

Geyer, R. K., Z. K. Yu, et al. (2000). "The MDM2 RING-finger domain is required to promote p53 nuclear export." <u>Nat Cell Biol</u> **2**(9): 569-573.

Giri, N., E. Kang, et al. (2000). "Clinical and laboratory evidence for a trilineage haematopoietic defect in patients with refractory Diamond-Blackfan anaemia." <u>Br J Haematol</u> **108**(1): 167-175.

Gjerset, R. A. (2006). "DNA damage, p14ARF, nucleophosmin (NPM/B23), and cancer." <u>J Mol Histol</u> **37**(5-7): 239-251.

Grandi, P., V. Rybin, et al. (2002). "90S pre-ribosomes include the 35S pre-rRNA, the U3 snoRNP, and 40S subunit processing factors but predominantly lack 60S synthesis factors." <u>Mol Cell</u> **10**(1): 105-115.

Green, R. and H. F. Noller (1996). "In vitro complementation analysis localizes 23S rRNA posttranscriptional modifications that are required for Escherichia coli 50S ribosomal subunit assembly and function." <u>RNA</u> **2**(10): 1011-1021.

Gregory, L. A., A. H. Aguissa-Toure, et al. (2007). "Molecular basis of Diamond-Blackfan anemia: structure and function analysis of RPS19." <u>Nucleic Acids Res</u> **35**(17): 5913-5921.

Grisendi, S., C. Mecucci, et al. (2006). "Nucleophosmin and cancer." <u>Nat Rev Cancer</u> **6**(7): 493-505.

Guo, J., C. Knight, et al. (2009). "Sdo1p Regulation of Histone Deacetylase Activity in Yeast." <u>Pediatric Blood & Cancer</u> **52**(6): 698-698.

Hage, A. E. and D. Tollervey (2004). "A surfeit of factors: why is ribosome assembly so much more complicated in eukaryotes than bacteria?" <u>RNA Biol</u> **1**(1): 10-15.

Hall, G. W., P. Dale, et al. (2006). "Shwachman-Diamond syndrome: UK perspective." <u>Arch Dis Child</u> **91**(6): 521-524.

Harnpicharnchai, P., J. Jakovljevic, et al. (2001). "Composition and functional characterization of yeast 66S ribosome assembly intermediates." <u>Mol Cell</u> **8**(3): 505-515.

Haupt, Y., R. Maya, et al. (1997). "Mdm2 promotes the rapid degradation of p53." Nature **387**(6630): 296-299.

Hesling, C., C. C. Oliveira, et al. (2007). "The Shwachman-Bodian-Diamond syndrome associated protein interacts with HsNip7 and its down-regulation affects gene expression at the transcriptional and translational levels." Exp Cell Res **313**(20): 4180-4195.

Ho, J. H., G. Kallstrom, et al. (2000). "Nmd3p is a Crm1p-dependent adapter protein for nuclear export of the large ribosomal subunit." J Cell Biol **151**(5): 1057-1066.

Horn, H. F. and K. H. Vousden (2008). "Cooperation between the ribosomal proteins L5 and L11 in the p53 pathway." Oncogene **27**(44): 5774-5784.

Hung, N. J. and A. W. Johnson (2006). "Nuclear recycling of the pre-60S ribosomal subunit-associated factor Arx1 depends on Rei1 in Saccharomyces cerevisiae." Mol Cell Biol **26**(10): 3718-3727.

Idol, R. A., S. Robledo, et al. (2007). "Cells depleted for RPS19, a protein associated with Diamond Blackfan Anemia, show defects in 18S ribosomal RNA synthesis and small ribosomal subunit production." Blood Cells Mol Dis **39**(1): 35-43.

Jefferies, H. B., C. Reinhard, et al. (1994). "Rapamycin selectively represses translation of the "polypyrimidine tract" mRNA family." Proc Natl Acad Sci U S A **91**(10): 4441-4445.

Jefferies, H. B. and G. Thomas (1994). "Elongation factor-1 alpha mRNA is selectively translated following mitogenic stimulation." J Biol Chem **269**(6): 4367-4372.

Jin, A., K. Itahana, et al. (2004). "Inhibition of HDM2 and activation of p53 by ribosomal protein L23." Mol Cell Biol **24**(17): 7669-7680.

Johnson, A. W., J. H. Ho, et al. (2001). "Nuclear export of the large ribosomal subunit." Cold Spring Harb Symp Quant Biol **66**: 599-605.

Juan, L. J., W. J. Shia, et al. (2000). "Histone deacetylases specifically down-regulate p53-dependent gene activation." J Biol Chem **275**(27): 20436-20443.

Kent, A., G. H. Murphy, et al. (1990). "Psychological characteristics of children with Shwachman syndrome." Arch Dis Child **65**(12): 1349-1352.

Khaitovich, P., T. Tenson, et al. (1999). "Peptidyl transferase activity catalyzed by protein-free 23S ribosomal RNA remains elusive." RNA **5**(5): 605-608.

Koonin, E. V., Y. I. Wolf, et al. (2001). "Prediction of the archaeal exosome and its connections with the proteasome and the translation and transcription machineries by a comparative-genomic approach." Genome Res 11(2): 240-252.

Kowalak, J. A., E. Bruenger, et al. (1995). "Posttranscriptional modification of the central loop of domain V in Escherichia coli 23 S ribosomal RNA." J Biol Chem 270(30): 17758-17764.

Krogan, N. J., G. Cagney, et al. (2006). "Global landscape of protein complexes in the yeast Saccharomyces cerevisiae." Nature 440(7084): 637-643.

Kubbutat, M. H., S. N. Jones, et al. (1997). "Regulation of p53 stability by Mdm2." Nature 387(6630): 299-303.

Kurdistani, S. K., D. Robyr, et al. (2002). "Genome-wide binding map of the histone deacetylase Rpd3 in yeast." Nat Genet 31(3): 248-254.

Lam, Y. W., A. I. Lamond, et al. (2007). "Analysis of nucleolar protein dynamics reveals the nuclear degradation of ribosomal proteins." Curr Biol 17(9): 749-760.

Leger-Silvestre, I., J. M. Caffrey, et al. (2005). "Specific Role for Yeast Homologs of the Diamond Blackfan Anemia-associated Rps19 Protein in Ribosome Synthesis." J Biol Chem 280(46): 38177-38185.

Lewicki, B. T., T. Margus, et al. (1993). "Coupling of rRNA transcription and ribosomal assembly in vivo. Formation of active ribosomal subunits in Escherichia coli requires transcription of rRNA genes by host RNA polymerase which cannot be replaced by bacteriophage T7 RNA polymerase." J Mol Biol 231(3): 581-593.

Lindstrom, M. S., C. Deisenroth, et al. (2007). "Putting a finger on growth surveillance: insight into MDM2 zinc finger-ribosomal protein interactions." Cell Cycle 6(4): 434-437.

Lipton, J. M., E. Atsidaftos, et al. (2006). "Improving clinical care and elucidating the pathophysiology of Diamond Blackfan anemia: an update from the Diamond Blackfan Anemia Registry." Pediatr Blood Cancer 46(5): 558-564.

Lipton, J. M. and S. R. Ellis (2009). "Diamond-Blackfan anemia: diagnosis, treatment, and molecular pathogenesis." Hematol Oncol Clin North Am 23(2): 261-282.

Lipton, J. M., N. Federman, et al. (2001). "Osteogenic sarcoma associated with Diamond-Blackfan anemia: a report from the Diamond-Blackfan Anemia Registry." J Pediatr Hematol Oncol 23(1): 39-44.

Lipton, J. M., M. Kudisch, et al. (1986). "Defective erythroid progenitor differentiation system in congenital hypoplastic (Diamond-Blackfan) anemia." Blood **67**(4): 962-968.

Liu, J. M. and S. R. Ellis (2006). "Ribosomes and marrow failure: coincidental association or molecular paradigm?" Blood **107**(12): 4583-4588.

Liu, S., H. Ishikawa, et al. (2006). "Increased susceptibility to apoptosis in CD45(+) myeloma cells accompanied by the increased expression of VDAC1." Oncogene **25**(3): 419-429.

Lodish, H. F. (1974). "Model for the regulation of mRNA translation applied to haemoglobin synthesis." Nature **251**(5474): 385-388.

Lohrum, M. A., R. L. Ludwig, et al. (2003). "Regulation of HDM2 activity by the ribosomal protein L11." Cancer Cell **3**(6): 577-587.

Luz, J. S., R. C. Georg, et al. (2009). "Sdo1p, the yeast orthologue of Shwachman-Bodian-Diamond syndrome protein, binds RNA and interacts with nuclear rRNA-processing factors." Yeast **26**(5): 287-298.

Maggi, L. B., Jr., M. Kuchenruether, et al. (2008). "Nucleophosmin serves as a rate-limiting nuclear export chaperone for the Mammalian ribosome." Mol Cell Biol **28**(23): 7050-7065.

Marechal, V., B. Elenbaas, et al. (1994). "The ribosomal L5 protein is associated with mdm-2 and mdm-2-p53 complexes." Mol Cell Biol **14**(11): 7414-7420.

Marson, C. M. (2009). "Histone deacetylase inhibitors: design, structure-activity relationships and therapeutic implications for cancer." Anticancer Agents Med Chem **9**(6): 661-692.

Martin-Marcos, P., A. G. Hinnebusch, et al. (2007). "Ribosomal protein L33 is required for ribosome biogenesis, subunit joining, and repression of GCN4 translation." Mol Cell Biol **27**(17): 5968-5985.

Matsson, H., E. J. Davey, et al. (2004). "Targeted disruption of the ribosomal protein S19 gene is lethal prior to implantation." Mol Cell Biol **24**(9): 4032-4037.

McGowan, K. A., J. Z. Li, et al. (2008). "Ribosomal mutations cause p53-mediated dark skin and pleiotropic effects." Nat Genet **40**(8): 963-970.

Menne, T. F., B. Goyenechea, et al. (2007). "The Shwachman-Bodian-Diamond syndrome protein mediates translational activation of ribosomes in yeast." Nat Genet **39**(4): 486-495.

Meskauskas, A., J. L. Baxter, et al. (2003). "Delayed rRNA processing results in significant ribosome biogenesis and functional defects." Mol Cell Biol 23(5): 1602-1613.

Miyake, K., J. Flygare, et al. (2005). "Development of cellular models for ribosomal protein S19 (RPS19)-deficient diamond-blackfan anemia using inducible expression of siRNA against RPS19." Mol Ther 11(4): 627-637.

Miyake, K., T. Utsugisawa, et al. (2008). "Ribosomal protein S19 deficiency leads to reduced proliferation and increased apoptosis but does not affect terminal erythroid differentiation in a cell line model of Diamond-Blackfan anemia." Stem Cells 26(2): 323-329.

Moore IV, J. B., J. E. Farrar, et al. (2009). "Distinct ribosome maturation defects in yeast models of Diamond Blackfan anemia and Shwachman Diamond syndrome." Haematologica.

Moore, P. B. (1997). "Ribosomes: protein synthesis in slow motion." Curr Biol 7(3): R179-181.

Moy, T. I. and P. A. Silver (2002). "Requirements for the nuclear export of the small ribosomal subunit." J Cell Sci 115(Pt 14): 2985-2995.

Munster, P., D. Marchion, et al. (2009). "Clinical and biological effects of valproic acid as a histone deacetylase inhibitor on tumor and surrogate tissues: phase I/II trial of valproic acid and epirubicin/FEC." Clin Cancer Res 15(7): 2488-2496.

Nathan, D. G., B. J. Clarke, et al. (1978). "Erythroid precursors in congenital hypoplastic (Diamond-Blackfan) anemia." J Clin Invest 61(2): 489-498.

Ng, C. L., D. G. Waterman, et al. (2009). "Conformational flexibility and molecular interactions of an archaeal homologue of the Shwachman-Bodian-Diamond syndrome protein." BMC Struct Biol 9: 32.

Nicolis, E., A. Bonizzato, et al. (2005). "Identification of novel mutations in patients with Shwachman-Diamond syndrome." Hum Mutat 25(4): 410.

Nierhaus, K. H. (1991). "The assembly of prokaryotic ribosomes." Biochimie 73(6): 739-755.

Nissan, T. A., J. Bassler, et al. (2002). "60S pre-ribosome formation viewed from assembly in the nucleolus until export to the cytoplasm." EMBO J 21(20): 5539-5547.

Nissen, P., J. Hansen, et al. (2000). "The structural basis of ribosome activity in peptide bond synthesis." Science 289(5481): 920-930.

Nitta, I., T. Ueda, et al. (1998). "Possible involvement of Escherichia coli 23S ribosomal RNA in peptide bond formation." RNA 4(3): 257-267.

O'Mahony, D. J., W. Q. Xie, et al. (1992). "Differential phosphorylation and localization of the transcription factor UBF in vivo in response to serum deprivation. In vitro dephosphorylation of UBF reduces its transactivation properties." J Biol Chem 267(1): 35-38.

Ohene-Abuakwa, Y., K. A. Orfali, et al. (2005). "Two-phase culture in Diamond Blackfan anemia: localization of erythroid defect." Blood 105(2): 838-846.

Ohtake, Y. and R. B. Wickner (1995). "Yeast virus propagation depends critically on free 60S ribosomal subunit concentration." Mol Cell Biol 15(5): 2772-2781.

Okuwaki, M., M. Tsujimoto, et al. (2002). "The RNA binding activity of a ribosome biogenesis factor, nucleophosmin/B23, is modulated by phosphorylation with a cell cycle-dependent kinase and by association with its subtype." Mol Biol Cell 13(6): 2016-2030.

Orelio, C. and T. W. Kuijpers (2009). "Shwachman-Diamond syndrome neutrophils have altered chemoattractant-induced F-actin polymerization and polarization characteristics." Haematologica 94(3): 409-413.

Pelletier, G., V. Y. Stefanovsky, et al. (2000). "Competitive recruitment of CBP and Rb-HDAC regulates UBF acetylation and ribosomal transcription." Mol Cell 6(5): 1059-1066.

Peng, W. T., M. D. Robinson, et al. (2003). "A panoramic view of yeast noncoding RNA processing." Cell 113(7): 919-933.

Perdahl, E. B., B. L. Naprstek, et al. (1994). "Erythroid Failure in Diamond-Blackfan Anemia Is Characterized by Apoptosis." Blood 83(3): 645-650.

Perry, R. P. and D. E. Kelley (1970). "Inhibition of RNA synthesis by actinomycin D: characteristic dose-response of different RNA species." J Cell Physiol 76(2): 127-139.

Pestov, D. G., Z. Strezoska, et al. (2001). "Evidence of p53-dependent cross-talk between ribosome biogenesis and the cell cycle: effects of nucleolar protein Bop1 on G(1)/S transition." Mol Cell Biol 21(13): 4246-4255.

Rawls, A. S., A. D. Gregory, et al. (2007). "Lentiviral-mediated RNAi inhibition of Sbds in murine hematopoietic progenitors impairs their hematopoietic potential." Blood 110(7): 2414-2422.

Repo, H., E. Savilahti, et al. (1987). "Aberrant phagocyte function in Shwachman syndrome." Clin Exp Immunol 69(1): 204-212.

Robert, F., D. K. Pokholok, et al. (2004). "Global position and recruitment of HATs and HDACs in the yeast genome." Mol Cell 16(2): 199-209.

Rotenberg, M. O., M. Moritz, et al. (1988). "Depletion of Saccharomyces cerevisiae ribosomal protein L16 causes a decrease in 60S ribosomal subunits and formation of half-mer polyribosomes." Genes Dev 2(2): 160-172.

Ruggero, D. and P. P. Pandolfi (2003). "Does the ribosome translate cancer?" Nat Rev Cancer 3(3): 179-192.

Rujkijyanont, P., K. Watanabe, et al. (2008). "SBDS-deficient cells undergo accelerated apoptosis through the Fas-pathway." Haematologica 93(3): 363-371.

Ruutu, P., E. Savilahti, et al. (1984). "Constant defect in neutrophil locomotion but with age decreasing susceptibility to infection in Shwachman syndrome." Clin Exp Immunol 57(1): 249-255.

Saunders, E. F., G. Gall, et al. (1979). "Granulopoiesis in Shwachman's syndrome (pancreatic insufficiency and bone marrow dysfunction)." Pediatrics 64(4): 515-519.

Savchenko, A., N. Krogan, et al. (2005). "The Shwachman-Bodian-Diamond syndrome protein family is involved in RNA metabolism." J Biol Chem 280(19): 19213-19220.

Savilahti, E. and J. Rapola (1984). "Frequent myocardial lesions in Shwachman's syndrome. Eight fatal cases among 16 Finnish patients." Acta Paediatr Scand 73(5): 642-651.

Schluenzen, F., A. Tocilj, et al. (2000). "Structure of functionally activated small ribosomal subunit at 3.3 angstroms resolution." Cell 102(5): 615-623.

Senger, B., D. L. Lafontaine, et al. (2001). "The nucle(ol)ar Tif6p and Efl1p are required for a late cytoplasmic step of ribosome synthesis." Mol Cell 8(6): 1363-1373.

Shammas, C., T. F. Menne, et al. (2005). "Structural and mutational analysis of the SBDS protein family. Insight into the leukemia-associated Shwachman-Diamond Syndrome." J Biol Chem 280(19): 19221-19229.

Shimamura, A. (2006). "Inherited bone marrow failure syndromes: molecular features." Hematology Am Soc Hematol Educ Program: 63-71.

Shimamura, A. (2006). "Shwachman-Diamond syndrome." <u>Semin Hematol</u> **43**(3): 178-188.

Shwachman, H., L. K. Diamond, et al. (1964). "The Syndrome of Pancreatic Insufficiency and Bone Marrow Dysfunction." <u>J Pediatr</u> **65**: 645-663.

Si, K. and U. Maitra (1999). "The Saccharomyces cerevisiae homologue of mammalian translation initiation factor 6 does not function as a translation initiation factor." <u>Mol Cell Biol</u> **19**(2): 1416-1426.

Smith, O. P., I. M. Hann, et al. (1996). "Haematological abnormalities in Shwachman-Diamond syndrome." <u>Br J Haematol</u> **94**(2): 279-284.

Srivastava, A. K. and D. Schlessinger (1990). "Mechanism and regulation of bacterial ribosomal RNA processing." <u>Annu Rev Microbiol</u> **44**: 105-129.

Steitz, T. A. (2008). "A structural understanding of the dynamic ribosome machine." <u>Nat Rev Mol Cell Biol</u> **9**(3): 242-253.

Stepanovic, V., D. Wessels, et al. (2004). "The chemotaxis defect of Shwachman-Diamond Syndrome leukocytes." <u>Cell Motil Cytoskeleton</u> **57**(3): 158-174.

Stolovich, M., H. Tang, et al. (2002). "Transduction of growth or mitogenic signals into translational activation of TOP mRNAs is fully reliant on the phosphatidylinositol 3-kinase-mediated pathway but requires neither S6K1 nor rpS6 phosphorylation." <u>Mol Cell Biol</u> **22**(23): 8101-8113.

Suda, T., H. Mizoguchi, et al. (1982). "Hemopoietic colony-forming cells in Shwachman's syndrome." <u>Am J Pediatr Hematol Oncol</u> **4**(2): 129-133.

Sugimoto, M., M. L. Kuo, et al. (2003). "Nucleolar Arf tumor suppressor inhibits ribosomal RNA processing." <u>Mol Cell</u> **11**(2): 415-424.

Sun, X. X., M. S. Dai, et al. (2007). "5-fluorouracil activation of p53 involves an MDM2-ribosomal protein interaction." <u>J Biol Chem</u> **282**(11): 8052-8059.

Tang, H., E. Hornstein, et al. (2001). "Amino acid-induced translation of TOP mRNAs is fully dependent on phosphatidylinositol 3-kinase-mediated signaling, is partially inhibited by rapamycin, and is independent of S6K1 and rpS6 phosphorylation." <u>Mol Cell Biol</u> **21**(24): 8671-8683.

Thiagalingam, S., K. H. Cheng, et al. (2003). "Histone deacetylases: unique players in shaping the epigenetic histone code." <u>Ann N Y Acad Sci</u> **983**: 84-100.

Thomas, F. and U. Kutay (2003). "Biogenesis and nuclear export of ribosomal subunits in higher eukaryotes depend on the CRM1 export pathway." J Cell Sci 116(Pt 12): 2409-2419.

Thomas, G. (1986). "Translational control of mRNA expression during the early mitogenic response in Swiss mouse 3T3 cells: identification of specific proteins." J Cell Biol 103(6 Pt 1): 2137-2144.

Tran, A. D., T. P. Marmo, et al. (2007). "HDAC6 deacetylation of tubulin modulates dynamics of cellular adhesions." J Cell Sci 120(Pt 8): 1469-1479.

Trapman, J., J. Retel, et al. (1975). "Ribosomal precursor particles from yeast." Exp Cell Res 90(1): 95-104.

Traub, P. and M. Nomura (1968). "Structure and function of E. coli ribosomes. V. Reconstitution of functionally active 30S ribosomal particles from RNA and proteins." Proc Natl Acad Sci U S A 59(3): 777-784.

Tsai, P. H., S. Arkin, et al. (1989). "An Intrinsic Progenitor Defect in Diamond-Blackfan Anemia." British Journal of Haematology 73(1): 112-120.

Udem, S. A., K. Kaufman, et al. (1971). "Small ribosomal ribonucleic acid species of Saccharomyces cerevisiae." J Bacteriol 105(1): 101-106.

Udem, S. A. and J. R. Warner (1972). "Ribosomal RNA synthesis in Saccharomyces cerevisiae." J Mol Biol 65(2): 227-242.

Uechi, T., Y. Nakajima, et al. (2008). "Deficiency of ribosomal protein S19 during early embryogenesis leads to reduction of erythrocytes in a zebrafish model of Diamond-Blackfan anemia." Hum Mol Genet 17(20): 3204-3211.

Venema, J. and D. Tollervey (1999). "Ribosome synthesis in Saccharomyces cerevisiae." Annu Rev Genet 33: 261-311.

Venkatasubramani, N. and A. N. Mayer (2008). "A zebrafish model for the Shwachman-Diamond syndrome (SDS)." Pediatr Res 63(4): 348-352.

Vlachos, A., S. Ball, et al. (2008). "Diagnosing and treating Diamond Blackfan anaemia: results of an international clinical consensus conference." Br J Haematol 142(6): 859-876.

Vlachos, A., N. Federman, et al. (2001). "Hematopoietic stem cell transplantation for Diamond Blackfan anemia: a report from the Diamond Blackfan Anemia Registry." Bone Marrow Transplant 27(4): 381-386.

Voit, R., A. Kuhn, et al. (1995). "Activation of mammalian ribosomal gene transcription requires phosphorylation of the nucleolar transcription factor UBF." Nucleic Acids Res **23**(14): 2593-2599.

Voit, R., K. Schafer, et al. (1997). "Mechanism of repression of RNA polymerase I transcription by the retinoblastoma protein." Mol Cell Biol **17**(8): 4230-4237.

Voit, R., A. Schnapp, et al. (1992). "The nucleolar transcription factor mUBF is phosphorylated by casein kinase II in the C-terminal hyperacidic tail which is essential for transactivation." EMBO J **11**(6): 2211-2218.

Wessels, D., T. Srikantha, et al. (2006). "The Shwachman-Bodian-Diamond syndrome gene encodes an RNA-binding protein that localizes to the pseudopod of Dictyostelium amoebae during chemotaxis." J Cell Sci **119**(Pt 2): 370-379.

Wickner, R. B. (1996). "Double-stranded RNA viruses of Saccharomyces cerevisiae." Microbiol Rev **60**(1): 250-265.

Widner, W. R., Y. Matsumoto, et al. (1991). "Is 20S RNA naked?" Mol Cell Biol **11**(5): 2905-2908.

Wolffe, A. P. (1998). "Packaging principle: How DNA methylation and histone acetylation control the transcriptional activity of chromatin." Journal of Experimental Zoology **282**(1-2): 239-244.

Woloszynek, J. R., R. J. Rothbaum, et al. (2004). "Mutations of the SBDS gene are present in most patients with Shwachman-Diamond syndrome." Blood **104**(12): 3588-3590.

Woods, W. G., W. Krivit, et al. (1981). "Aplastic anemia associated with the Shwachman syndrome. In vivo and in vitro observations." Am J Pediatr Hematol Oncol **3**(4): 347-351.

Wu, L. F., T. R. Hughes, et al. (2002). "Large-scale prediction of Saccharomyces cerevisiae gene function using overlapping transcriptional clusters." Nat Genet **31**(3): 255-265.

Yang, X. J. and E. Seto (2003). "Collaborative spirit of histone deacetylases in regulating chromatin structure and gene expression." Curr Opin Genet Dev **13**(2): 143-153.

Yang, X. J. and E. Seto (2008). "The Rpd3/Hda1 family of lysine deacetylases: from bacteria and yeast to mice and men." Nat Rev Mol Cell Biol **9**(3): 206-218.

Yuan, X., Y. Zhou, et al. (2005). "Genetic inactivation of the transcription factor TIF-IA leads to nucleolar disruption, cell cycle arrest, and p53-mediated apoptosis." Mol Cell **19**(1): 77-87.

Zaid, H., S. Abu-Hamad, et al. (2005). "The voltage-dependent anion channel-1 modulates apoptotic cell death." Cell Death Differ **12**(7): 751-760.

Zanchin, N. I., P. Roberts, et al. (1997). "Saccharomyces cerevisiae Nip7p is required for efficient 60S ribosome subunit biogenesis." Mol Cell Biol **17**(9): 5001-5015.

Zhai, W. and L. Comai (2000). "Repression of RNA polymerase I transcription by the tumor suppressor p53." Mol Cell Biol **20**(16): 5930-5938.

Zhang, J., P. Harnpicharnchai, et al. (2007). "Assembly factors Rpf2 and Rrs1 recruit 5S rRNA and ribosomal proteins rpL5 and rpL11 into nascent ribosomes." Genes Dev **21**(20): 2580-2592.

Zhang, S., M. Shi, et al. (2006). "Loss of the mouse ortholog of the shwachman-diamond syndrome gene (Sbds) results in early embryonic lethality." Mol Cell Biol **26**(17): 6656-6663.

Zhang, X., Z. Yuan, et al. (2007). "HDAC6 modulates cell motility by altering the acetylation level of cortactin." Mol Cell **27**(2): 197-213.

Zhang, Y., N. Li, et al. (2003). "HDAC-6 interacts with and deacetylates tubulin and microtubules in vivo." EMBO J **22**(5): 1168-1179.

Zhang, Y., G. W. Wolf, et al. (2003). "Ribosomal protein L11 negatively regulates oncoprotein MDM2 and mediates a p53-dependent ribosomal-stress checkpoint pathway." Mol Cell Biol **23**(23): 8902-8912.

APPENDIX I

Introduction

Initial Remarks

Some experimental results acquired throughout the course of my dissertation work, which provided additional contrasting molecular features between the yeast models of DBA and SDS, were omitted from the main body of presented work. This was chiefly due to changes in research aims and/or experimental focus. As a result, some studies and supporting experiments were not completed or were deemed unnecessary for inclusion into dissertation chapters for reasons that it would potentially distract from this work's intended line of reasoning. Despite this, some of the experiments and resulting data not included in the main body of this dissertation contributed to the conclusions of the work presented here and therefore are shown in the appendix. Below, these data will be explained in the context of the previous work described.

Review of DBA and SDS Clinical Features

Shwachman-Diamond syndrome and Diamond-Blackfan anemia are members of a rare group of genetic disorders classified as inherited bone marrow failure syndromes (IBMFS) with clinical presentations most notably involving hematological abnormalities and generalized growth delays. Both diseases (manifest in early infancy) present with heterogeneous clinical phenotypes involving a wide range of congenital anomalies and predisposition to cancer. Although SDS and DBA share certain overarching features, they differ immensely in their clinical manifestations. SDS patients exhibit multisystem abnormalities which include intermittent or persistent neutropenia, skeletal abnormalities (i.e. metaphyseal dysostosis), and exocrine pancreatic insufficiency. Moreover,

123

retrospective studies of SDS patients reveal a high propensity for malignant transformation into myelodysplastic syndrome and acute myeloid leukemia (25-33% of patients) (Alter 2007; Coccia, Ruggiero et al. 2007). Conversely, DBA patients present with an erythroid hypoplasia (anemia) and display variable congenital anomalies including abnormal or triphalangeal thumbs, craniofacial anomalies, and cleft palate. DBA patients exhibit an overall lower incidence of cancer (0.5-6.6% of patients) and have a predisposition to solid tumors (i.e. osteosarcoma) in addition to hematopoietic malignancies (Alter 2007; Vlachos, Ball et al. 2008).

Overview of Disease Etiology

Given that DBA and SDS exhibit distinct clinical phenotypes, it is intriguing to find that the molecular bases for both diseases converge on a common target – the ribosome. Several genes are mutated in DBA, all of which encode structural components of the ribosome. Moreover, both small and large subunit proteins have been described in the literature, many of which have been shown to be required for biogenesis of their respective subunit. For example, early studies in yeast indicated that *RPS19*, the first gene identified as mutated in DBA, is required for the maturation of 40S ribosomal subunits. Yeast cells deficient in *RPS19* have a marked reduction in the steady-state level of 40S ribosomal subunits and compromised protein synthetic capacity (Liu and Ellis 2006). Moreover, siRNA knockdown of *RPS19* in human cell lines (TF-1 and HeLa) provide additional support to its already suggested role in 40S subunit biogenesis (Choesmel, Bacqueville et al. 2007; Flygare, Aspesi et al. 2007). These data provide substantial evidence to implicate DBA as a disorder resulting from a failure to produce

124

adequate quantities of ribosomes. Given that *RPS19* is required for the maturation of 40S

subunits, questions now remain as to how haploinsufficiency for an essential ribosomal

protein results in a DBA phenotype characterized by defective differentiation of pro-

erythroblasts and pro-apoptotic hematopoiesis. While a number of affected genes

encoding ribosomal proteins have been implicated in DBA, only one gene has been found

to be mutated in SDS, *SBDS*. The *SBDS* gene, though not a structural component of the

ribosome, associates with 60S ribosomal subunits (Ganapathi, Austin et al. 2007). Its

true function, to date, is still not completely clear, though, considerable evidence from

both yeast and mammalian based studies implicate *SBDS* in 60S ribosomal subunit

biogenesis (Menne, Goyenechea et al. 2007; Ball, Zhang et al. 2009; Moore IV, Farrar et

al. 2009). Indeed these data suggest that both DBA and SDS converge on deficiencies in

ribosome synthesis and/or function in their disease pathophysiology, but specifically how

these ribosome based defects lead to the common and distinct clinical phenotypes among

these two disorders have yet to be determined.

Nucleolar Stress Signaling in DBA

Recent studies in the DBA field led to the discovery of a signaling pathway that

could potentially bridge the gap between the failure to synthesize adequate amounts of

ribosomes and the pro-apoptotic phenotype of erythroid progenitors in DBA patients.

This nucleolar stress signaling pathway is thought to proceed via direct interactions of

unassembled ribosomal proteins with proteins moderating cell cycle progression and

apoptosis. It is believed that when ribosome synthesis is disrupted, these proteins

become free to act as molecular messengers to activate pathways (MDM2) leading to the

stabilization and activation of p53. The role of p53 in the context of this pathway has been documented in a zebrafish model of DBA (Danilova, Sakamoto et al. 2008). To date, three large ribosomal proteins (Rpl5, Rpl11, and Rpl23) have been shown to activate p53 by acting directly on MDM2 (Dai and Lu 2004; Dai, Zeng et al. 2004). While appealing, this model does not explain how other disorders linked to ribosome biogenesis have clinical phenotypes distinct from DBA. SDS has been reported to be connected to defects in 60S subunit biogenesis and, as my data suggests, may induce nucleolar stress as well. However, DBA and SDS clinical features are distinct and thus nucleolar stress signaling alone would not likely be sufficient to explain these observed clinical differences. In chapter II, I turned to yeast models of these two disorders to mechanistically dissect how these ribosome-based syndromes affected both ribosome formation and function in an effort to elucidate common and distinct pathways leading to clinical divergence. My results reveal that both models differ in terms of their effects on subunit assembly and stability, and their potential for subsequent induction of nucleolar stress.

Translational Alterations

In this dissertation's work, I exploited yeast deletion strains of the orthologs of those human genes identified to affect the 60S subunit in DBA and SDS, *RPL33A* and *SDO1*, respectively. Each disease model shows defects in 60S subunit maturation, but with distinct underlying mechanisms. In the DBA model, 60S subunit maturation is disrupted at a relatively early stage with abortive complexes subject to rapid degradation. In contrast, subunit maturation in the SDS model is affected at a later step, giving rise to

126

relatively stable pre-60S particles that are notably retained in the nucleus. Moreover, with respect to the SDS model, we revealed that Sdo1 functions in 60S subunit maturation via modulating histone deacetylase activities. These studies have elucidated differing mechanisms between the two models by which the translational machinery is affected, albeit both demonstrating 60S subunit deficits. The differences between the yeast DBA and SDS models have implications for signaling mechanisms linking abortive ribosome assembly to cell fate decisions and may contribute to the divergent clinical presentations of DBA and SDS. Despite this, I believe that the differences in clinical phenotypes between SDS and DBA may also result from their diverse effects on the translation of varying cellular mRNAs. Early studies supporting this notion demonstrated that alterations in polypeptide chain initiation components could alter, in a predictable manner, the relative translation of certain mRNAs (Lodish 1974). Here I show some data that demonstrates the yeast DBA and SDS models, which have unique ribosome based defects, to have differing affects on translational output.

SDS and Apoptosis

Increased apoptosis has been implicated as a central pathogenic mechanism in both DBA and SDS. However, little is known concerning disease specific cellular mechanisms leading to apoptosis and more importantly, reasons for hematopoietic lineage specificity. Nucleolar stress has been implicated in DBA where ribosome assembly is clearly affected, and could be a contributing factor in SDS as well. However, others have demonstrated increased expression of Fas antigen and hyperactivation of the Fas signaling pathway in SDS hematopoietic progenitors (Dror and Freedman 2001).

This extrinsic pathway may contribute to the faulty proliferative properties and pro-apoptotic phenotype of SDS hematopoietic progenitors; however, it does not address the basis for the hematopoietic lineage specificity associated with the disease whereas the major hematologic defect in SDS is neutropenia. Thus, questions linger as to whether this observation is due to neutrophil progenitors undergoing apoptosis prior to complete maturation or due to the activation of additional apoptotic signaling pathways. My preliminary studies have shown the SDS yeast model exhibits a significant increase in the mitochondrial porin protein termed Por1. The human ortholog of the gene encoding this protein is *VDAC1*, a voltage-dependent anion channel that is a subunit of the mitochondrial polyprotein channel called the permeability transition pore (PTP). Interestingly, the PTP is implicated in mediating the release of apoptogenic intermediates such as cytochrome c from the intermembrane space, which appears to be a central event in the initiation of the cascade leading to programmed cell death (Zaid, Abu-Hamad et al. 2005). Previous studies have shown increased *VDAC1* expression correlates with increased sensitization of human hematopoietic cells to various extracellular stimuli leading to apoptosis (Liu, Ishikawa et al. 2006). The yeast SDS model introduces the potential involvement of intrinsic mitochondrial pathways leading to apoptosis in SDS pathogenesis.

Supplemental Results

The Influence of SDO1 and RPL33A Deletion on the 20S Replicon

The work presented in chapter II revealed unique effects of *SDO1* and *RPL33A* deletion on the translational machinery of cells. The goal was to determine whether these

mechanisms were sufficiently distinct to account for the different clinical phenotypes. One way I addressed this issue was by examining how these different mechanisms influenced translation in each model.

Both yeast disease models displayed a sub-40S peak in their polysome profiles that was present in much reduced amounts in their corresponding wild-type strains. This peak corresponds to a yeast endogenous single-stranded RNA virus, termed the 20S replicon or 20S RNA. The 20S RNA is a noninfectious virus found in most laboratory strains of the yeast *Saccharomyces cerevisiae* and encodes a protein (91 kDa), which non-covalently associates with the RNA and is responsible for its replication (Widner, Matsumoto et al. 1991; Garcia-Cuellar, Esteban et al. 1997). The 20S RNA lacks both a 5' cap and a poly (A) tail, and the host antiviral system maintains a low copy number of the 20S replicon via a high rate of turnover of the 20S RNA and by inefficient translation of the 20S RNA encoded polymerase. Mutations in a number of yeast genes affect the copy number of the 20S replicon, and interestingly, a number of these involved mutations in genes encoding proteins of the 60S subunit; mutations in these genes result in decreased 20S replicon copy number (Ohtake and Wickner 1995). In contrast to these earlier studies, my results demonstrated the copy number of the 20S replicon to increase in both Δ*RPL33A* and Δ*SDO1* strains compared to their respective wild-types (Figure S1).
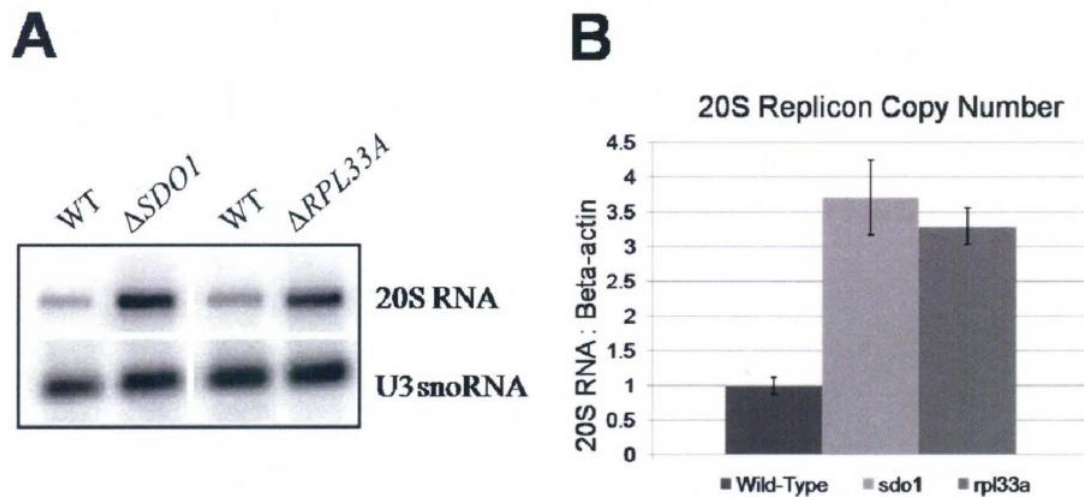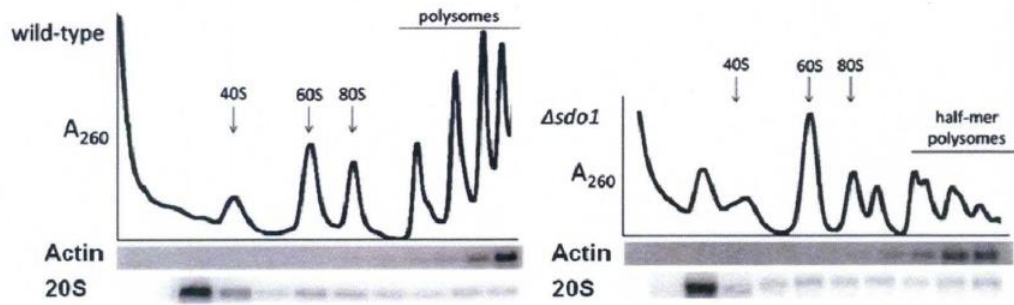
Figure S1. **Deletion of *SDO1* or *RPL33A* results in an increase in the 20S replicon copy number.** (A) Northern blot analyses of 20S RNA or U3 snoRNA derived from Δ*SDO1*, Δ*RPL33A*, or isogenic wild-types strains. Total RNA was isolated from aforementioned yeast strains, resolved on 1.5% formaldehyde-agarose gels, transferred to nylon membranes, and hybridized with oligonucleotides (specific to 20S RNA or U3 snoRNA) labeled at their 5′ ends with ^{32}[P]. (B) Bar graph denoting 20S replicon copy number in Δ*SDO1*, Δ*RPL33A*, and isogenic wild-type strains, which are reported as ratios of 20S RNA:β-actin mRNA. Error bars representing standard error of the mean (SEM) are present.

In figure S1, the 20S replicon copy number is quantified for both yeast deletion strains. These data reveal the copy number of this virus is greatly enhanced in the disease models compared to their respective wild-types. Moreover, the magnitude of induction appears greater in the SDS model than that of the DBA model, though this is not statistically significant and is likely the result of low sample numbers. I demonstrated that both disease models possess greater copy numbers of 20S RNA compared to isogenic wild-types, and as a result, I sought to determine if this observation was a consequence of altered translation of the 20S replicon-encoded polymerase. I did so by comparing the relative distribution of the 20S replicon in fractionated polysomes from mutant versus wild-type cells. A different abundant cellular message, β-actin, was used as a control (Figure S2).
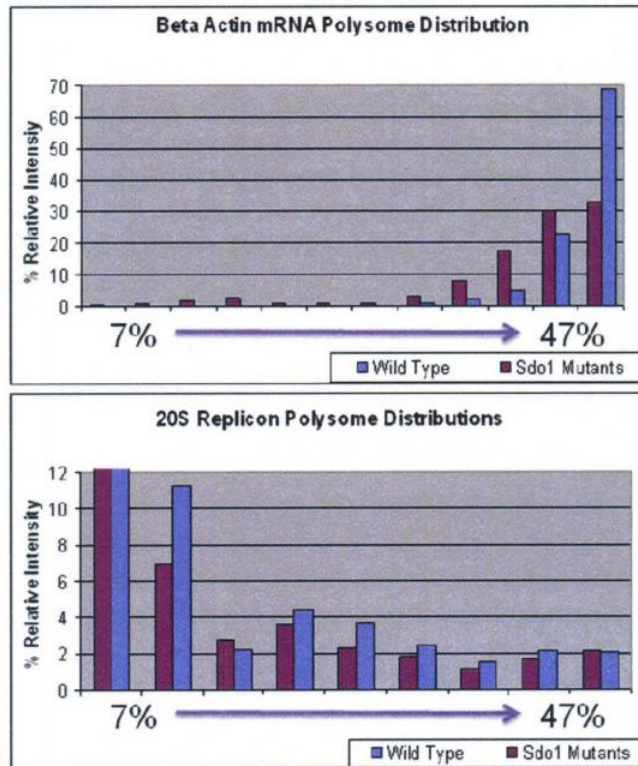
The data in figure S2 show that the distributions of 20S replicon in those fractions representing the polysome region remained relatively unchanged in the SDS model compared to the wild-type. Conversely, the polysome distributions of actin mRNA shifted to fractions containing smaller polysomes in the SDS model relative to the wild-type. The data on the distribution of the actin mRNA was consistent with the general decrease in translation observed in ΔSDO1 polysome profiles. As previously mentioned, the distribution of the 20S replicon RNA did not change between the wild-type and the ΔSDO1 strain. This indicates that the 20S replicon RNA competes more efficiently than other cellular messages for the limiting translational machinery in the ΔSDO1 strain and thus, its translation could be enhanced relative to the bulk mRNA. I had planned to address this same question in the yeast DBA model using the same methodology described above, however this was not pursued due to adjustments in research focus.

A

wild-type

A₂₆₀

40S 60S 80S polysomes

Actin

20S

Δsdo1

A₂₆₀

40S 60S 80S

half-mer polysomes

Actin

20S

B

Beta Actin mRNA Polysome Distribution

% Relative Intensity

7% ➞ 47%

■ Wild Type   ■ Sdo1 Mutants

20S Replicon Polysome Distributions

% Relative Intensity

7% ➞ 47%

■ Wild Type   ■ Sdo1 Mutants

<u>Figure S2.</u> **The 20S replicon RNA competes more efficiently than other cellular messages for the limiting translational machinery in the *ΔSDO1* strain.** **(A)** Distribution of 20S replicon and β-actin in fractionated polysomes from wild-type (left) and *ΔSDO1* (right) strains. Northern blot analysis of RNA recovered from fractionated polysomes profiles are depicted below, which utilized radiolabeled oligonucleotide probes specific to β-actin or 20S replicon. **(B)** Quantification of the distributions of 20S replicon (bottom panel) and β-actin (top panel) from fractionated polysomes of both wild-type (blue bars) and *ΔSDO1* (red bars) strains. Y-axis denotes % relative intensity of Northern blot signals quantified from individual fractions. X-axis denotes individual fractions and relative sucrose gradient concentrations (%).

## Broad Analysis of Translational Output of Yeast DBA and SDS Models

The increase in the copy number of the 20S replicon appeared to be a response to general translational stress that does not distinguish between the two disease models. For this reason, I carried out a more broadly based analysis of translational output in the DBA and SDS yeast models in an effort to identify proteins that are selective to either of these specific models. Yeast strains were pulse labeled with $[^{35}S]$-methionine and newly synthesized proteins were resolved by both one and two-dimensional gel electrophoresis (Figure S3). A number of proteins in the SDS-PAGE gel were reduced and enhanced in the two mutants relative to their respective wild-types. Interestingly, an unknown protein with an approximate molecular weight of 30 kDa was greatly enhanced in the $\Delta SDO1$ strain relative to wild-type using conventional one-dimensional SDS-PAGE gel analysis (Figure S3, Panel A). Further analysis of this protein was performed by two-dimensional gel analysis of normalized total protein extracts isolated from the $\Delta SDO1$ and corresponding isogenic wild-type yeast strains (Figure S3, Panel B). The enhanced expression of the 30 kDa protein in the $\Delta SDO1$ yeast strain was apparent by both autoradiography (Figure S3) and Colloidal Coomassie Blue staining. MALDI-TOF mass spectroscopic analysis of the excised 30 kDa protein from 2D gel analysis identified this protein to be the post-transcriptionally regulated protein known as Por1 (a mitochondrial voltage-dependent anion channel).
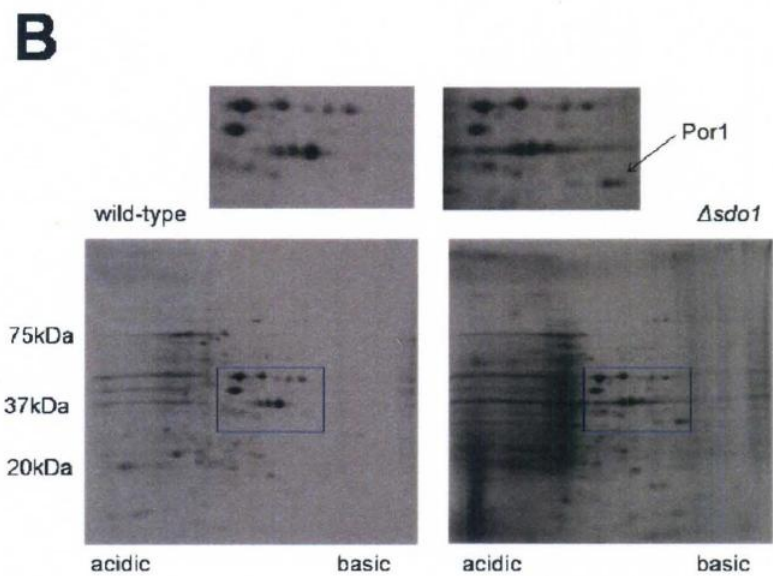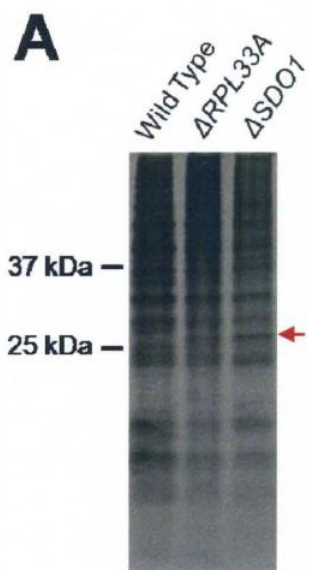
Figure S3. **Yeast DBA and SDS models have differential effects on translational output.** (A) Autoradiograph of S^{35}-labeled newly synthesized proteins resolved on single dimension SDS-PAGE gels. Wild-type, $\Delta RPL33A$, or $\Delta SDO1$ strains were incubated for 30 minutes with [^{35}S]-methionine, total protein isolated (Yaffe-Schatz method), and resolved using a standard 12% SDS-PAGE gel. A red arrow highlights an unknown protein band at ~30 kDa in the $\Delta SDO1$ strain. (B) Autoradiograph of S^{35}-labeled newly synthesized proteins resolved using 2-dimensional gel electrophoresis. Wild-type (left panels) or $\Delta SDO1$ (right panels) strains were incubated for 30 minutes with [^{35}S]-methionine, cells mechanically lysed with glass beads, and total protein extracts finally resolved by 2D gel electrophoresis. Proteins underwent isoelectric focusing on immobilized pH gradients that ranged from pH 3-10. The second dimension was resolved via a 4-12% gradient polyacrylamide gel. Molecular masses for size standards are shown to the left. Regions enclosed by the boxes are expanded above each gel. The spot labeled Por1 was excised and identified via MALDI-TOF mass spectroscopy.

*Mechanisms of POR1's Enhanced Expression in Yeast DBA and SDS Models*

As two-dimensional gel analysis qualitatively revealed differences in the abundance of Por1 protein among the SDS and DBA yeast models, I subsequently used western analysis to analyze the relative quantities of Por1 in both disease models. Western blots showed this protein to be more abundant in mutant cells (DBA and SDS yeast models) compared to their respective wild-type controls, but appeared to differ greatly in quantity between the two disease models (Figure S4); Por1 was induced to a much greater extent in the SDS strain than in the DBA strain. I next wanted to determine whether the enhanced expression of Por1 was a consequence of differences in transcription or translation. Northern blotting revealed similar increases in *POR1* and β-actin cellular messages in mutants compared to respective wild-type strains suggesting that the observed selective increase in Por1 protein in the SDS model was mediated at the post-transcriptional level (Figure S4).
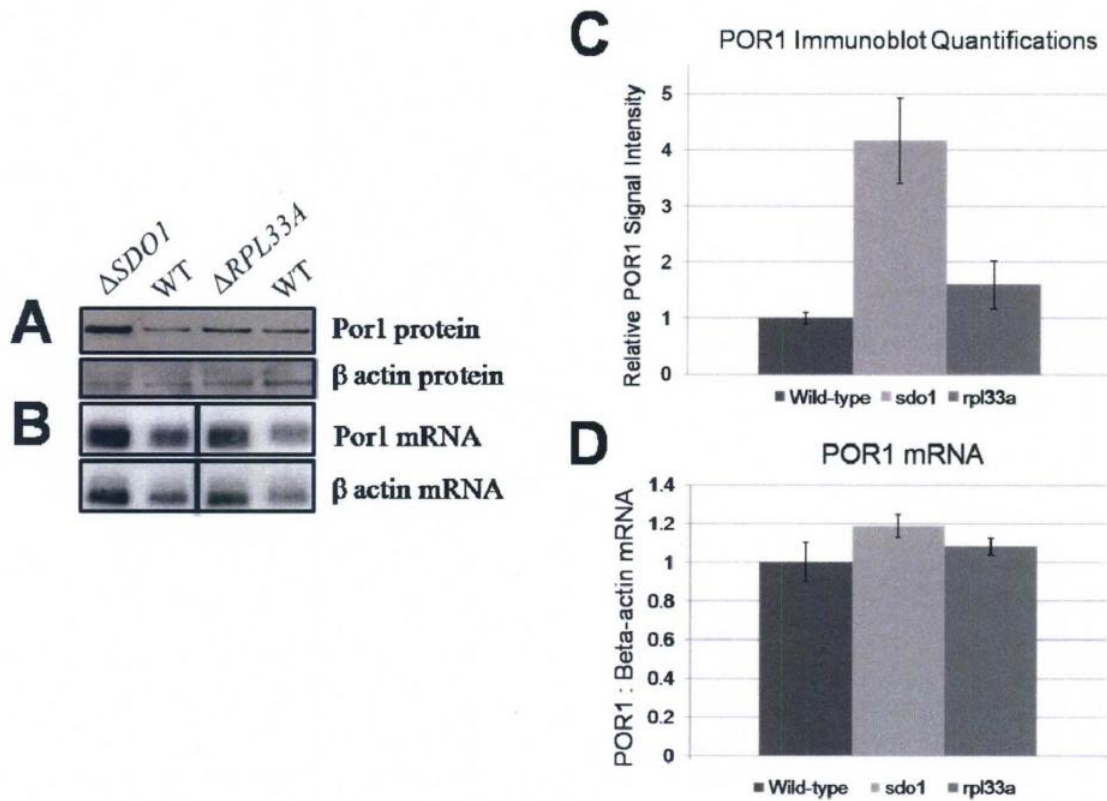
Figure S4. **Selective induction of the Por1 protein in the Δ*SDO1* yeast strain.** (A) Immunoblot of whole cell extracts from wild-type, Δ*RPL33A*, and Δ*SDO1* strains. Blots were probed with anti-sera raised to either Por1 or β-actin. (B) Total RNA was isolated from the strains listed and hybridized with radiolabeled oligonucleotide probes specific to *POR1* or β-actin mRNA. Quantification of (C) Por1 immunoblots (reported as relative signal intensity) and (D) *POR1* mRNA Northern blots (reported as ratios of signal intensity of *POR1*:β-actin mRNA) from wild-type, Δ*RPL33A*, and Δ*SDO1* yeast strains. Error bars representing standard error of the mean (SEM) are present in bar graphs.

To determine if the enhanced expression of Por1 corresponded to enhanced translational efficiency of the *POR1* message in the yeast disease models, I examined the relative distribution of the *POR1* mRNA in fractionated polysomes from mutant versus wild-type cells. I began these studies on the yeast SDS model and its related wild-type (Figure S5). As was expected, the actin mRNA shifted from larger to smaller polysomes in the Δ*SDO1* strain compared to the wild-type strain, consistent with the general translational stress observed in the SDS model. Moreover, an unexpected shift of the *POR1* message from larger to smaller polysomes was observed in the SDS model compared to wild-type, similar to what was observed for the β-actin control. Thus, at the present, the translation of *POR1* mRNA does not appear to be enhanced in the ΔSDO1 strain. This observation needs to be confirmed, and if so, may suggest an effect of the *SDO1* mutation on Por1 protein stability. Concerning these observations, I have not repeated these experiments in either disease model nor pursued additional methods to address the mechanisms leading to their enhanced expression of the Por1 protein, as this projects research focus changed directions.
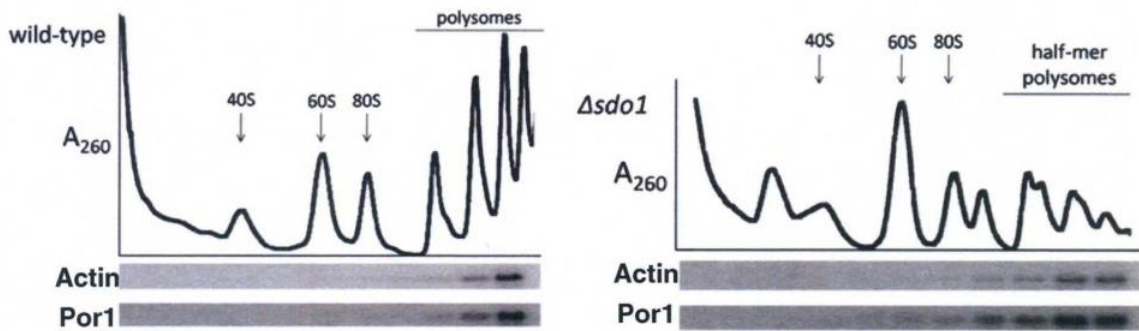
<u>Figure S5.</u> **Distributions of *POR1* mRNA and actin in fractionated polysomes.**
Polysome profiles corresponding to wild-type (left) and Δ*SDO1* (right) yeast strains are
shown. Polysomes were fractionated, RNA collected, and Northern analysis performed
(depicted below absorbance tracings) using radiolabeled oligonucleotide probes specific
to β-actin or *POR1* mRNA.

Conclusions

Northern blot analyses of both DBA and SDS yeast models revealed quantitative differences in the 20S replicon copy number compared to wild-types, though differences between the two disease models were not statistically significant. Examination of the distribution of the 20S RNA in fractionated polysomes from the SDS model revealed that 20S RNA competes much more efficiently in translation in comparison to the β-actin control, whereas β-actin shifted to smaller polysomes and the 20S replicon remained unaffected.

Por1 immunoblots confirmed its enhanced expression in both disease models compared to wild-types, however it was much higher in the yeast SDS model. I anticipate these increases to correspond to enhanced translational efficiency of the *POR1* message. Preliminary results concerning the distribution of *POR1* message in polysome fractions, obtained from the SDS model, did not support the notion of its enhanced translation efficiency; however, these experiments require replication in an effort to tackle this disparity. I predict both models will demonstrate increased translational efficiency of this cellular message, with greater efficiency in the SDS model than in the DBA model. Northern blot analyses show the relative quantities of *POR1* message to not differ among disease models and related wild-types suggesting that this is not a result of enhanced transcription of *POR1*. Por1 protein stability was not investigated and thus could be a contributing factor to its enhanced expression in the *SDO1* deletion strain. Based on these results, I hypothesize *VDAC1* to be a possible contributor to the pro-apoptotic phenotype observed in SDS. The data shown in this dissertation exposed distinct mechanisms relating to how DBA and SDS yeast models impact the translational

apparatus of cells. Further, the supplemental data expands on these observations to demonstrate that both models have differential affects on the translational output of cells, which could be an additional factor that contributes to the clinical divergence in DBA and SDS.

APPENDIX II

LIST OF ABBREVIATIONS AND SYMBOLS

[Methyl-^{3}H]-methionine	Tritiated-methyl methionine
20S Replicon or 20S RNA	A yeast endogenous single-stranded RNA virus
5'-TOP	5' terminal oligopyrimidine
5S-L5-L11 ternary subcomplex	A complex containing 5S rRNA and Rpl5 and Rpl11 ribosomal proteins
A_{254}	Absorbance at a wavelength of 254 nanometers
AML	Acute myelogenous leukemia
ARF	Alternative reading frame tumor suppressor
ARX1	Yeast pre-60S shuttling factor
B23/NPM	Nucleophosmin
BFU-E	Erythroid burst-forming units
CFU-E	Erythroid colony-forming units
CFU-GM	Granulocyte-monocyte colony-forming units
CHH	Cartilage-hair hypoplasia
DAPI	4',6-diamidino-2-phenylindole
DBA	Diamond-Blackfan anemia
DBAR	Diamond-Blackfan Anemia Registry
DC	Dyskeratosis congenita
DEPC	Diethyl pyrocarbonate
eADA	Erythrocyte adenosine deaminase activity
ECL	Enhanced chemiluminescence

144

EFL1	Yeast cytoplasmic GTPase involved in biogenesis of the 60S ribosome
ERG6	Yeast delta(24)-sterol C-methyltransferase (ergosterol biosynthetic pathway)
ETS	External transcribed spacer
GFP	Green fluorescent protein
HDA1	Yeast class II histone deacetylase
HDAC	Histone deacetylase
IBMFS	Inherited bone marrow failure syndromes
IEF	Isoelectric focusing
IgG	Immunoglobulin G
ITS1	Internal transcribed spacer 1
ITS2	Internal transcribed spacer 2
MALDI-TOF mass spectroscopy	Matrix-assisted laser desorption/ionization mass spectroscopy
MDM2	Murine double minute oncogene
MDS	Myelodysplastic syndrome
mRNA	Messenger RNA
Mut	Mutant
NES	Nuclear export signal
NHLBI	National Heart, Lung, and Blood Institute
NMD3	Yeast protein involved in 60S ribosomal subunit nuclear export (Crm1p-dependent adapter protein)
p53	p53 tumor suppressor
PDR5	Yeast plasma membrane ATP-binding cassette (ABC) transporter

PI3K	Phosphotidyl inositol 3-kinase
Pol I	DNA polymerase I
Pol II	DNA polymerase II
Pol III	DNA polymerase III
pre-rRNA	Pre-ribosomal RNA
PTM	Posttranslational modification
PTP	Permeability transition pore
RB	Retinoblastoma
rDNA	Ribosomal DNA
RNP	Ribonucleoprotein
RP	Ribosomal protein
RPD3	Yeast class I histone deacetylase
RPM	Revolutions per minute
rRNA	Ribosomal RNA
SBDS	Gene mutated in Shwachman-Diamond syndrome
SBDSP	*SBDS* paralogous pseudogene
SDO1	Yeast ortholog of the human SBDS protein; responsible for Shwachman-Diamond syndrome
SDS	Shwachman-Diamond syndrome
SDS-PAGE	Sodium dodecyl sulfate polyacrylamide gel electrophoresis
SEM	Standard error of the mean
snoRNA	Small nucleolar RNA

snoRNP	Small nucleolar ribonucleoprotein
SNQ2	Yeast plasma membrane ATP-binding cassette (ABC) transporter
TAP	Tandem affinity purification
TIF6	Yeast translation initiation factor 6 (constituent of 66S pre-ribosomal particles)
TSA	Trichostatin A
UBF	Upstream binding factor
w/v	weight/volume
WT	Wild-type
XPO1/CRM1	Yeast karyopherin, involved in export of proteins, RNAs, and ribosomal subunits from the nucleus
$\gamma\text{-}^{32}[P]\text{-ATP}$	Radiolabeled gamma-phosphate of adenosine triphosphate

CURRICULUM VITAE

JOSEPH BRADY MOORE IV
1001 CHARLES STREET, LOUISVILLE, KY 40204
JBMOOR01@LOUISVILLE.EDU

PERSONAL INFORMATION

Date of Birth: **May 26, 1981**
Place of Birth: **Louisville, KY**
Citizenship: **United States**
Marital Status: **Single**

EDUCATION

University of Louisville, School of Medicine, Louisville, KY
Ph.D. Biochemistry and Molecular Biology   2005 - 2010

University of Louisville, School of Medicine, Louisville, KY
M.S. Biochemistry and Molecular Biology (Awarded in 2009)   2005 - 2007

University of Louisville, Louisville, KY
B.S. Chemistry with a Concentration in Biochemistry   2000 - 2005

RESEARCH EXPERIENCE

University of Louisville, Department of Biochemistry and Molecular Biology
Predoctoral Research   2005 - 2010

Dissertation Project: "RIBOSOME MATURATION IN YEAST MODELS OF
DIAMOND-BLACKFAN ANEMIA AND SHWACHMAN-DIAMOND SYNDROME"

Research Focus: My dissertation was focused on Shwachman-Diamond syndrome
and Diamond-Blackfan anemia, two inherited bone marrow failure syndromes
where defects in ribosome synthesis underlie disease pathophysiology. My
approach was to use yeast models of both diseases to explore mechanisms
by which ribosome synthesis was affected using the 60S ribosomal subunit as
a common molecular target. My studies revealed that 60S subunit biogenesis
was affected by distinct mechanisms in the two disease models and that these
differences may provide the molecular underpinnings for the distinct clinical
presentations observed in DBA and SDS patients. Further, concerning the yeast
SDS model, our objective was to analyze the function of Sdo1 in 60S subunit
maturation from the perspective of its potential role as a regulator of protein
acetylation. This work has established a molecular foundation for the potential
use of histone deacetylase inhibitors as a treatment for Shwachman-Diamond
syndrome (SDS).

Techniques/Methodology: Gene cloning/manipulation, one and two-dimensional
protein separation techniques, cell-tissue culture (adherent/non-adherent cells),

yeast genetics, transformations/transfections, polysome analyses, and standard biochemistry techniques (i.e. Northern, Southern, and Western blots). I also have extensive experience with radioisotopic labeling of proteins, DNA, and RNA.

University of Louisville, Department of Biochemistry and Molecular Biology
Undergraduate Research Program   **2004 - 2005**

<u>Research Focus:</u> Characterization of the human collagen binding domain of matrix metalloproteinase-2 (MMP-2).

<u>Techniques/Methodology:</u> Affinity chromatography, gene cloning, fluorescence spectroscropy, MALDI-TOF mass spectroscropy, circular dichroism spectroscopy, and standard protein separation techniques.

Microbac Laboratories Inc., Louisville, KY
Analytical Chemist   **2003 - 2004**

<u>Services/Procedures Performed:</u> Analyzed various biological, soil, water, and unknown samples for trace metals using inductively coupled plasma atomic emission spectroscopy. In addition, I analyzed effluent waste samples for total dissolved solids and mercury content.

HONORS

- Outstanding Graduate Talk, 2008 Southeastern Regional Yeast Meeting **2008**
- Dean's list (6 Awards)   **2000-2005**
- Academic Achievement Award, House of Representatives of the Commonwealth of Kentucky
- Academic Achievement Award, United States Achievement Academy

GRANTS/SUPPORT

Project title: **A Yeast Screen for Shwachman Diamond Syndrome Therapeutics** **2008**
Role: Principal Investigator
Source of support: Shwachman Diamond Project
Award amount: $40,773 (1/2/2008-12/31/2008)

SCIENTIFIC PUBLICATIONS IN PEER-REVIEWED JOURNALS

Guo J, Garraido-Lecca A, **Moore IV JB**, Knight C, Wong T, Sneed B, Blackwell J, Gruber C, Bertuch A, Fu H, Dingledine R, Shimamura A, Ellis SR, de Figueiredo P, and Huang JN: The Shwachman Diamond Syndrome Protein is an Endogenous Inhibitor of Cellular Histone Deacetylase Activities. *Submitted for publication and currently under revision. Cell* 2010

Moore IV JB, Farrar JE, Arceci RJ, Liu JM, and Ellis SR: Distinct Ribosome Maturation Defects in Yeast Models of Diamond-Blackfan anemia and Shwachman-Diamond syndrome. *Haematologica.* 2010; 95:57-64. doi:10.3324/haematol.2009.012450

ABSTRACTS PRESENTED: INTERNATIONAL AND REGIONAL SCIENTIFIC SESSIONS

Cold Spring Harbor, NY
12th Biannual International Meeting on Yeast Cell Biology   **2009**
Abstract title: Sdo1p regulation of histone deacetylase activity in yeast
Guo J, Garrido-Lecca A, **Moore IV JB**, Knight C, Wong T, Sneed B, Blackwell J, Gruber C, Bertuch A, Fu H, Dingledine R, Shimamura A, Ellis SR, de Figueiredo P, and Huang JN

San Francisco, CA
50th American Society of Hematology Annual Meeting and Exposition   **2008**
Abstract title: Yeast Models of Diamond Blackfan Anemia and Shwachman Diamond Syndrome Differ in Their Effect on the Synthesis and Function of Ribosomal Subunits
Ellis SR, **Moore IV JB**, Liu JM, Arceci RJ, and Farrar JE

Gatlinburg, TN
Southeastern Regional Yeast Meeting   **2008**
Abstract title: Shwachman Diamond Syndrome and Diamond Blackfan Anemia: 60S Ribosomal Subunit Defects Leading to Distinct Features in Clinical Presentation
Moore IV JB and Ellis SR

INVITED PRESENTATIONS

Bellarmine University, Louisville, KY
Guest Speaker   **2007**
Title: Shwachman Diamond Syndrome: Defects in Ribosomal Subunit Joining

HOBBIES AND INTERESTS

- Volunteer firefighter (North Oldham Fire Department)
- Motorcyclist (Road and Track)
- Guitarist
- Automotive repair and car restoration